DISSERTATION

Titel der Dissertation

Synthetic Materials Designed by Molecular Imprinting for Developing Chemical Sensors for Oil Degradation, Metals Ions and PAHs

angestrebter akademischer Grad

Doktor der Naturwissenschaften (Dr. rer. nat.)

Verfasser:	M.Sc. Adnan Mujahid
Matrikel-Nummer:	0649445
Dissertationsgebiet (lt. Studienblatt):	Doktoratsstudium der Naturwissenschaften (Chemie)
Betreuerin / Betreuer:	O. Univ.-Prof. Mag. Dr. Franz Dickert

Wien, 1. February 2010

Preface

This work is done in the work-group of Chemical Sensors and Optical Molecular Spectroscopy from February 2007 till now under the supervision of O. Univ. Prof. Dr. Franz Ludwig Dickert at the Institute of Analytical Chemistry, University of Vienna, Währingerstraße 38, 1090-Vienna, Austria.

To

My Parents

Acknowledgements

I offer my humble and heartfelt gratitude to my laudable research advisor, *O. Univ. Prof. Dr. Franz Ludwig Dickert,* for his unswerving support and guidance. He always provided me with new ideas and feedback throughout my research work. I extend my appreciation to him for many valuable and motivating discussions on theoretical and practical aspects of the development of sensitive materials for chemical sensors.

I ought to submit thanks to *Ao. Univ. Prof. Mag. Dr. Peter A. Lieberzeit* for supervising my first steps in the field of chemical sensors and for his continued assistance afterwards. He has always been there to help, whether it was an academic or a beaurocratic matter.

I'm obliged to the Higher Education Commission (HEC) of Pakistan for the grant of scholarship to pursue PhD studies in Austria. I'm grateful to the Austrian Exchange Service (OeAD) for regulating the scholarship installments and for helping me in admission, visa and insurance processes.

There are so many people, whom I always wanted to thank for their helpful and caring attitude, yet I could not do so properly. I'm still unable to mention the names of all those; but I hope, they will understand that I never overlooked any of them. Many thanks are due to my *friends* in Vienna for their cheerful company and assistance. I owe to submit thanks to my *friends* and *family members* in Pakistan for their sincere wishes and prayers.

I am at a loss of words to express the gratitude towards *my father, my mother, my brothers* and *my sister.* It was hard living far away from them; but their lifelong love, continuous encouragement, truthful prayers and belief in my abilities made me stronger and I always felt their presence by my side.

Table of Contents

Chemical Sensors

1.1 Introduction

A device which measures a physical or chemical quantity in real time conditions and converts this information into an appropriate digital or analogue form is considered as a sensor. Chemical sensor carries information about the chemical property and physical sensor provides data about physical parameters of the analyte, some other definitions for chemical sensors are also available in the literature[1,2]. An ideal sensor should only be sensitive towards a particular property of analyte mixture in the system; it should not show any interaction to any other property of the system, more precisely sensitivity and selectivity are pronounced features of an excellent sensor. Normally sensors are designed for a specific analyte in a mixture in certain working conditions, but it is not due that a sensor should insensitive to unspecific analyte. A typical chemical sensor[3] has three major parts; one is the chemical sensitive layer, second is transducer and third is a data processing unit. Chemical sensitive layer changes its properties when it is exposed to analyte environment; the degree of change is detected by transducer which converts it into a measureable physical quantity and data processing unit process this information. The basic idea behind development of a chemical sensor is to produce small, handy devices which are capable for recognition of chemical changes taking place in the system.

1.2 Chemical Sensors in Modern World

During the last few decades there has come a great revolution in almost every field of industrial developments, which has become very important for the life, but on the other hand industrial waste has also become a big potential hazard to our environment. Different gases exhausted from our power plants and from auto mobiles, like nitric oxide, sulfur dioxide and heavy metal's oxides are very

dangerous for living beings. The incomplete oxidation of automotive engine oil produces numerous hydrocarbons and aromatic compounds which are thrown out to environment without any treatment. Chloro flouro hydrocarbons like freon are destroying the protective layer of ozone which is a global hazard.

In order to make a healthy atmosphere, emission of these dangerous gases and vapours in to environment has to be minimized. Desulfurization and denitrification of power plants already turned out to be a substantial success. Because of this increase in environmental pollution corresponding increase in demand of analytical tools for the rapid and easy detection of pollutants has also increased in the same way.

There are two different approaches to solve this global issue, one is to miniaturize the already existing analytical instruments like high performance liquid chromatography (HPLC), mass spectrometry (MS) and inductively coupled plasma (ICP), and other is to develop chemical sensors.
Chemical sensors have many advantages over the first strategy as they are small and cheap devices by means of which even a layman is able to handle it and miniaturization is already far advanced. Therefore, chemical sensors established themselves as an important part of analytical chemistry and have much wide applications than classical instruments. As due to their size, robustness, simplicity and ability to function in complex analyte mixtures make them superior than other analytical instruments. The other important thing about them is that they can be employed for online monitoring where the other instruments cannot perform effectively.

Recent developments in the field of chemical sensors attract the scientists to ponder on this branch of analytical chemistry. As in the modern world there is a growing demand for rapid detection and identification of biological and environmental threats, industrial process control, medical diagnosis, food preservation and pharmaceutical drug analysis with high accuracy and

sensitivity. Such highly reliable detection systems with low cost are needed to meet the challenges of 21st century.

1.3 Basic Principle of Chemical Sensor

There are three main components of sensor systems which are as follows.

- ➢ Chemical sensitive layer
- ➢ Transducer
- ➢ Data processing unit

A chemical sensitive layer is developed to determine a particular analyte; this layer has special characteristics that it changes its properties e.g. optical absorbance, when it is exposed to the sample mixtures in a certain working conditions. An ideal chemical layer shows no response towards unspecific analyte and it should not change the fundamental properties of analyte.These
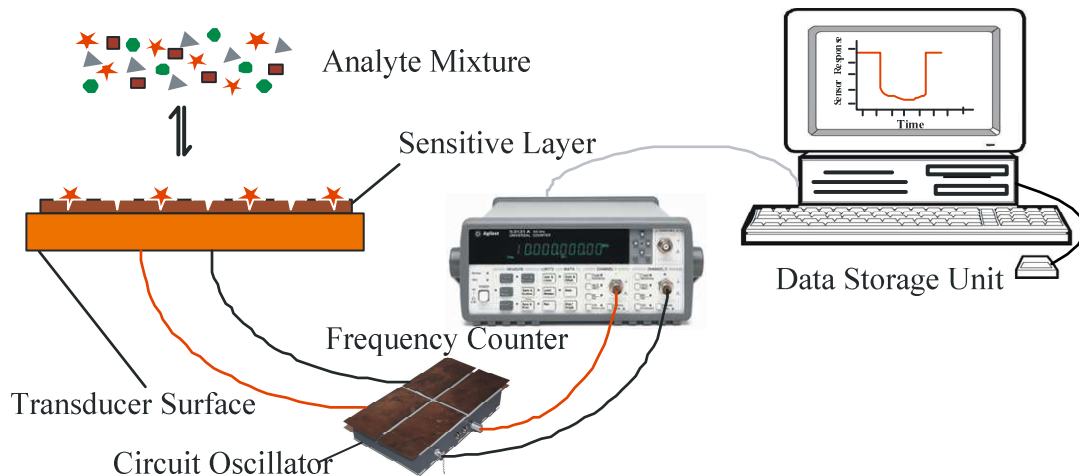
Figure 1: Schematic Set-up of a Chemical Sensor

changes in properties are recorded by a transducer which converts this information to data processing unit, and data processing unit process it and shows in a suitable form.

1.4 Design of Chemical Sensor

As we know that a chemical sensor has three main parts, one is sensitive layer, second is transducer and third is data processing unit. How to approach these three units to design a chemical sensor is very important.

1.4.1 Sensitive layer

Recognition ability of a sensitive layer is a key aspect of sensor device. This layer has to respond selectively to analyte avoiding other interactions with unwanted substances, and to change one of its properties which are detected. Considering the mass sensitive sensing the one strategy is to design a layer that shows host-guest interactions[4] with target molecule. Strong binding lead to high sensitivity and selectivity but if the binding with analyte is covalent then it is not easy to release the molecule after entrapment. So for the reversibility of device other phenomena like π-π and dipolar interactions can be considered.

To develop a biosensor enzyme-substrate binding, ligand receptor binding and immunological interactions are used. These biological materials can prove very useful as recognition elements for bio sensors. Such natural antibodies can be replaced by synthetic ones to overcome the inherent limitations in chemical, thermal and mechanical stability.

Another strategy to design a sensitive layer is *Molecular Imprinting*. Recognition abilities for chemical sensing are produced within a polymeric material. In this technique the pre-polymerized mixture e.g. monomers and the template mixture is polymerized under certain reaction conditions. After polymerization the template or analyte molecule is surrounded by self organized polymer chains, which is removed from polymer by washing or evaporation without disturbing polymer configuration. The removal of template leaves behind a cavity in polymer which acts as recognition site for chemical sensing.

This technique for generating synthetic antibodies is very useful to develop sensitive and selective sites for re-inclusion of analyte in a complex mixture. By increasing the number of interacting sites in imprinted polymer, the sensitivity is also increased. So for optimal sensitivity, maximum possible interacting sites can be generated by adjusting the polymer template ratio.

1.4.2 Transducer

A device that converts the chemical response in to electrical signal energy from one form to another is supposed to be transducer e.g. electrochemical transducers. Different types of devices are used as transducers in the field of chemical sensing, as they convert chemical information into electrical data. They can be classified according to the type of electrical signal or their signal processing principle. Transducers[5] can be subdivided in to the following main types.

1.4.2.1 Electrochemical Transducers

I) *Potentiometric devices*

These devices explain the relationship between the concentration of the analyte and the electric potential (*emf*). Difference in the potential between a working electrode and a reference electrode is measured due to change in analyte's concentration. The *emf* is directly proportional to the logarithm of analyte activity of the analyte. An early development of such device is the glass electrode for pH measurement. Most widely used Potentiometric device is the Lambda probe[6], which is made of ZrO_2/Y_2O_3. Most common application of Lambda probe is in automobile vehicles where the concentration of oxygen is determined in stoichiometric way in internal combustion engines for the required oxygen fuel ratio.

II) *Amperometric devices*

These devices are also known as Voltammetric devices as in this case a change in current is measured due to an electrochemical reaction. When a certain potential is applied to an electro active substance, it undergoes to a redox reaction and in that process a change in current is observed which is linked with analyte concentration, because the peak current is directly proportional to the concentration of electro active substance. The serious problem with these devices is that when potential is applied the electrode material is consumed during the reaction. But the sensor cost is comparatively low because these devices are employed for discardable one-way systems.

III)   *Conductometric devices*

Many reactions take place due to the change in the composition of the material. In conductometric devices these changes lead to change in conductivity of the systems which is measured electrically. The best example of these sensors is Taguchi or Figaro sensor which was first commercially available in 1968[7], for monitoring of gases produced during combustion. SnO_2 is used as sensing element in Figaro sensor; it is doped with a noble metal like Pt. When this metal oxide crystal is heated at a certain temperature it absorbs the oxygen from atmosphere on its surface. The donor electrons from the crystal are transferred to the oxygen, this leads to a change in the surface resistance as the positive charge is produced due to the transfer of electrons. Reduced or combustible gases react with this oxygen present on the surface of the device and decrease its concentration on surface and at the same time the conductivity of the material is increased due to an increase in concentration of electrons.

IV) *Field Effect Devices*

Principally there are two types of electronic devices, one is active and other is passive. Active devices produce high current comparably by using low voltage, in other words they act as amplifiers. Field effect devices have both sorts of

components; the best example is *Field effect Transistor* (FET). Most commonly used FET is metal oxide semiconductor field effect transistor which has significant importance in the construction of modern inter digital circuits.

1.4.2.2 Optical Transducers

Unlike the previous devices, the chemical information is not converted directly into an electronic quantity in optical transducers. They change their optical properties upon interaction with analyte; this change may be in absorption, reflection or fluorescence. Light emitting diode (LED) is an excellent example of optical sensing where the wavelength extended from ultraviolet (UV) to near infrared (NIR) region. Optical sensors can be categorized in two ways, first in which the analyte directly affects the optical behavior of the system i.e. plain fiber sensors and the second one in which a dye interact with the analyte and from this interaction the change in the optical properties of that dye is measured i.e. indicator –mediated optical sensors.

Surface Plasmon resonance (SPR) also falls under the class of optical sensors. In this technique electromagnetic waves interact with metal surface as the angle of reflectance directly depends upon angle of incident. At a particular angle of incident these waves produce very sensitive oscillations in thin films on metal surface which leads to change in reflectivity of light. These effects can be used for development of a chemical sensor by applying a suitable chemically sensitive layer on metal surface.

1.4.2.3 Mass Sensitive Devices

These are piezoelectric materials which change their mechanical properties on applying an electric field. When a quartz sheet made of Lithium tantalate is cut at a specific angle subjected to an alternating current, some mechanical oscillations are produced both on surface and the bulk. It had been observed by Sauerbrey[8] in 1959 that the resonance frequency of this quartz sheet directly

depends on the mass deposit on it. So the change in mass on quartz surface causes a change in its resonance frequency which makes these material highly sensitive balances. As the mass is a fundamental property of any analyte, by applying a suitable sensitive coating material on it, they can be used excellent chemical sensors. Mass sensitive devices are most important class of chemical sensors and they will be discussed in detail in next chapter.

These above devices can be summarized in the following way in figure 2.
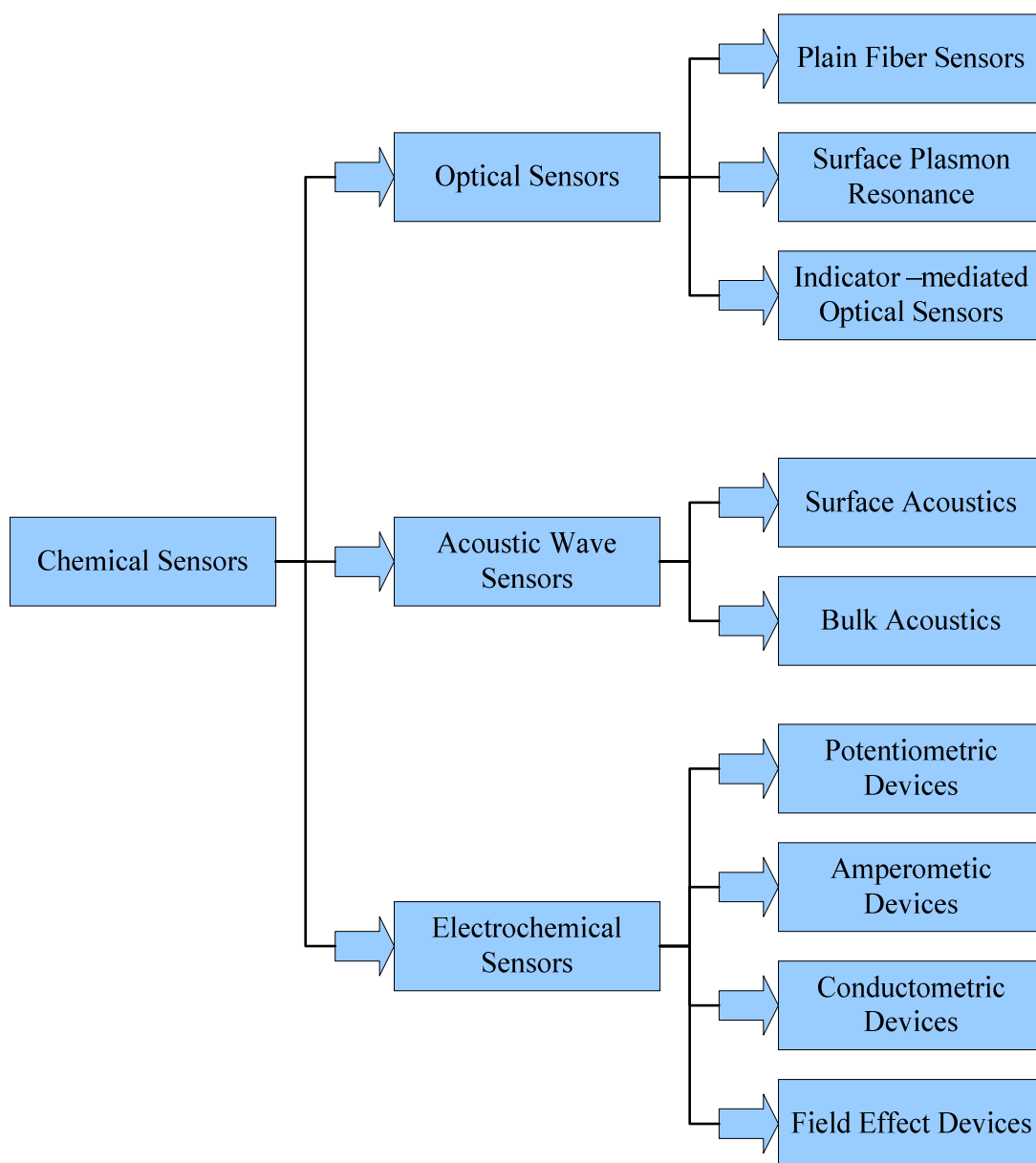
Figure 2: Classification of Chemical Sensors

1.5 Sensor Characteristics

A lot of studies had already been done on sensors characteristics but while developing a chemical sensor certain parameters and conditions need to be defined. They have been discussed as under one by one.

1.5.1 Sensitivity

Sensitivity of device shows that how large is the signal obtained from measurement of a physical quantity. A highly sensitive system responds more efficiently to minute concentrations and gives more information about the analyte. In case of chemical sensors, more sensitive systems generate signals to lower concentrations of analyte in comparison to others. The sensitivity of a chemical sensor depends upon the type of transducer and the nature of chemical layer.

1.5.2 Linearity

The relationship between sensor response and the measured physical quantity in a certain range can be explained by linearity. It gives us information about the degree of deviation from the ideal curve in analytical measurements. Considering Beer Lambert's law in which absorption of a substance is directly proportional to its concentration provided path length is constant, it means doubling the concentration of the substance would result double the absorption, ibut it is true only at low concentrations or unless the intermolecular forces are not operating. When the intermolecular forces start working then the absorption concentration relationship is no more linear and the measured curve departs from the ideal line.

1.5.3 Selectivity

One of the most important features of chemical sensors is the selectivity; an ideal selective sensor shows response only when there is change in the behavior of target specie. It should not give any signal to unwanted substances provided the other physical parameters constant. In case of chemical sensors, a selective layer is designed for sensing of a certain analyte which shows a pattern of sensitivity towards a similar class of substance and from this sensitivity pattern the degree of selectivity is known.

1.5.4 Response Time

It is the time taken by the sensitive device to change an output signal due to the corresponding change in input value, because sensors don't change the output state instantly. In other words it is the time required to develop a new stable state within the tolerance band of correct value from its previous state.

1.5.5 Accuracy and Precision

Accuracy refers as the degree of closeness of a measured value to the actual correct value, while the ability of a system to give consistently reproduced values is called precision regardless how close or far is the exact value. The concept of precision is associated with the degree of reproducibility or repeatability of measurement data. An ideal sensor system gives accurate and precise results when measurements are made in different times. But in actual practice this does not happen and the real time measurement data is distributed in some order comparing to the correct actual value.

1.5.6 Noise

In the field of chemical sensors any disturbance that can reduce the clarity of a signal is called noise. It is an unwanted signal that corrupts the actual signal or more precisely we can say data without any meaning is noise. It could be

random or persistent in the measurement and could have different origins, for example electric fluctuations or variations in the environment in which measurement is going on. Ideal sensors have low noise level so that it does not influence the measured data. When dealing with a system having high sensor response, then the original signal can be distinguished from noise but when the sensor response is too low then it is very difficult to pick original signal or to eliminate noise from it. So the signal to noise(S/N) ratio have to be decide in both sort of measurements qualitative and quantitative as well. In analytical chemistry for qualitative analysis the (S/N) should be at least 3 as mentioned by international union of pure and applied chemistry (IUPAC) while for quantitative analysis it should be around 20. Higher (S/N) values are the measure of quality of a chemical sensor.

1.5.7 Hysteresis

It is the property of a sensor device to follow the changes made by input parameters, no matter in what directions these changes have been made. The term Hysteresis is derived from a Greek word whose meaning is deficiency or lagging behind. There are different examples of Hysteresis, for example magnetic hysteresis, elastic hysteresis and thermal hysteresis. Most simple example to illustrate hysteresis is if the temperature of an incubator is set at 80°C turns on when the temperature reaches 78°C and turns off at 82°C, the hysteresis is the range from 78°C to 82°C.

1.5.8 Range

A group of values from a minimum to a maximum is called the range of that system. The range of a device is the minimum and maximum values of applied parameters that can be measured, for example, a thermal sensor records the temperature of a certain atmosphere from -10°C to +10°C. The positive and

negative ranges may equal or not, but the sensor behavior should be linear in the defined range.

1.5.9 Resolution

The *resolution* of a sensor is the smallest detectable incremental change of input parameter it can detected in output signal of the measurement. Mostly in a instrument the least significant digit on display will fluctuate, indicating that changes of that magnitude are only just resolved. The resolution is related to the precision with which the measurement is made. For example, a scanning probe (a fine tip near a surface collects an electron tunneling current) can resolve atoms and molecules.

1.6 Conclusion

Chemical sensors is one of the growing branch of modern analytical science due to their wide spread applications in different areas especially environmental analysis. They possess significant advantages over the classical instruments which makes them easily operatable by non-professionally trained personnel. This chapter gives an overview to understand the basic concept of chemical sensors and explain their design, classification, characteristics and their significance in modern world.

Acoustic Wave Mass Sensitive Devices

2.1 Introduction

Acoustic wave or mass sensitive devices are very advantageous in the field of chemical sensing and has gained a lot of interest during last years. These devices have wide applications in biosensors and environmental monitoring. The applicability of these sensors is universally wide as they detect or sense the change in mass which is a fundamental property of all analytes. The change in mass cause by the analytes is detected due to the corresponding change in the frequency of acoustic devices. Basically an acoustic device is of two types, first is Surface acoustic wave (SAW) and second is Bulk acoustic wave (BAW). These devices can be employed as a sensing element in both gas and liquid phases. In SAW devices adsorption takes place which is a surface phenomena while absorption is in BAW. A suitable chemically sensitive layer is coated on their surface which selectively incorporates the analyte leading to a change in their fundamental frequency of the device. Acoustic wave devices can be best understood under the heading of Piezoelectricity.

2.2 Concept of Piezoelectricity

When a dielectric crystal or eclectically non conducting material is subjected to applied mechanical stress, it generates an electric potential in response, the effect is known as Piezoelectricity and the material is called Piezoelectric. This behaviour was first discovered in 1880[9] by the brothers Pierre Curie and Jacques Curie. The common examples of these substances are ceramic materials, quartz crystals and Rochelle salt. When some stress is applied in a certain dimension on such materials then it goes under mechanical deformation. Actually the applied stress polarizes the material in such a way that it slightly

separates the centres of positive and negative charges creating a dipole as explained in the following figure 3.
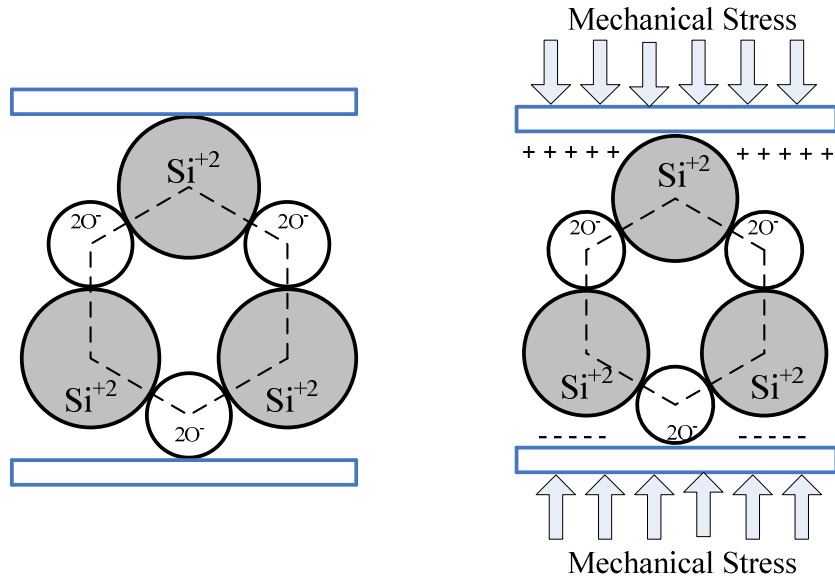
Figure 3: Explanation of Piezoelectric effect

The reverse of this phenomenon is known as *Converse Piezoelectric* effect and at first it was not experimentally confirmed. After one year in 1881 Gabriel Lippmann proved this effect mathematically by employing basic thermodynamic principles while later on the reversibility of the effect was proved experimentally. In Converse Piezoelectric effect, the applied electric field across surface of the material causes mechanical distortion in it. So applying a high frequency alternating current to a piezoelectric material, an ultrasonic wave of same frequency can be generated.

Piezoelectricity and Converse Piezoelectricity phenomena both have useful applications for generating the high power and voltage source, sensors and actuators and frequency standards as well.

2.2.1 Piezoelectric Materials

Piezoelectric materials can be classified in two categories, natural occurring materials and synthetic materials. Some natural sources of these materials are

Cane sugar, Rochelle salt, Berlinite (AlPO$_4$) and Quartz, while interestingly Bones also shows piezoelectric behaviour due to apatite crystals.

Synthetic materials are of various types which cover the crystalline, ceramic and polymers as well. Crystalline materials include Gallium orthophosphate (GaPO$_4$) and Langasite (La$_3$Ga$_5$SiO$_{14}$) both are similar to natural occurring quartz crystal.

The synthetic ceramic materials contain Barium titantate (BaTiO$_3$), Lead titanate (PbTiO$_3$), Lead zirconate titanate (Pb(ZrTi)O$_3$), Lithium niobate (LiNbO$_3$) and Lithium tantalate (LiTaO$_3$).

Polyvinylidene fluoride (PVDF) is an excellent material that possesses many times higher piezoelectricity than quartz where long molecular chains attract or repel each other due to applied electric potential.

The selection of material largely depends upon the nature of its application, e.g. Gallium orthophosphate has high temperature coefficient than quartz and can be employed in working environment having temperature up to 900°C.

2.3 Surface Acoustic Wave (SAW) Devices

As from name it is clear that these are devices in which oscillation phenomena is confined to the surface of the material. They have wide applications as narrow band-width frequency filters, oscillators and resonators in commercial and scientific field. In 1885, Lord Rayleigh discovered the surface acoustic wave phenomena and explained their mode of propagation in his classic paper[10]. Surface acoustic waves have both longitudinal and shear component that can couple with the surface of material and propagate non-dispersively. Coupling of these components have an effect on velocity and amplitude of the waves which makes SAW devices a promising tool to sense the mass and the other mechanical properties of the medium.

Principally SAW devices made of piezoelectric materials; in case of quartz they are ST-cut on which inter digital transducer (IDT) comb electrodes are fabricated. When an electric field is applied across these electrodes, particles

present on the surface of the crystal are displaced from their position and a Rayleigh wave is generated, which travel from one electrode to the other along
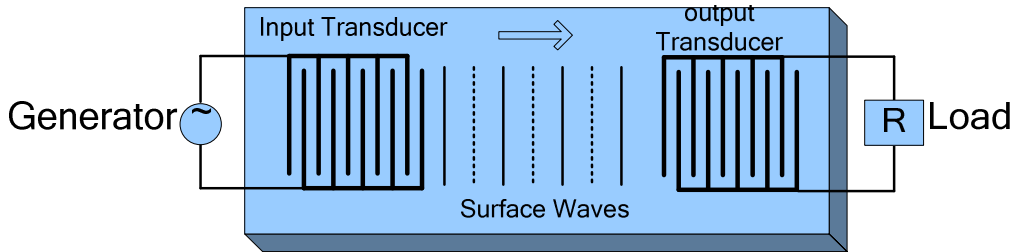

Figure 4: A typical surface acoustic wave resonator

the surface and create potential difference which is measured electrically. A typical SAW device has been shown in figure 4.

The distance between the centres of equally polarized electrodes determines the wavelength while dimension of the comb electrode structure determines the resonance frequency of the SAW devices. Typically SAW can be operated in the frequency ranges up to 2.5 GHz but reported analytical applications is 1GHz that shows remarkably enhanced sensitivity in comparison to QMB.

The excessive damping of these devices restricts their use in liquid phase but this drawback can be overcome by using shear wave resonators[11]. The vertical shear wave component can be altered to shear horizontal component by adjusting the angle of cutting which reduces the damping significantly and make the device useable in liquid phase as well.

2.4 Bulk Acoustic Wave (BAW) Devices

Quartz crystal microbalance (QMB) is best known simplest example of (BAW) device resonating in Trans Shear Mode (TSM). Originally TSM was used to measure the rate of metal deposition in vacuum systems where it was used in an oscillator circuit.

The TSM sensor is commonly referred to At-cut quartz crystal microbalance having circular gold electrodes designed on both sides as shown in figure 5. By

applying a certain frequency to electrodes excitation of shear mechanical resonance takes place. This allows the surface materials in contact with quartz to interact mechanically disturbing the resonant frequency and damping. Deposition of mass on quartz surface produces a shift in resonance frequency which can be detected by oscillator circuit joined with frequency counter.
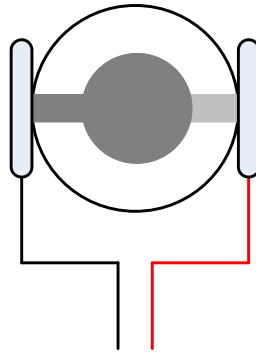

Figure 5: A 10MHz AT-cut quartz crystal having gold electrodes designed on both sides.

The resonant frequency and the oscillation magnitude in the liquid phase depend upon the visco elastic behavior of the medium. Chemical sensors consist of TSM resonators having sensitive and selective surface layers. Analytes in the liquid or vapor phase are sorbed onto or into the coating, changing the film mass or perturbing the film visco elastic properties.

2.5 CLASSIFICATION OF ACOUSTIC DEVICES

Acoustic wave devices can be classified according to the nature of wave propagation mode. These waves are distinguished principally by their velocities and displacement directions; many combinations are possible, depending on the substrate material. Table 1 shows a brief classification of different acoustic devices. This classification explain the type of the device, suitable working medium, dimensions of the material, typical frequency determining factor, operational range and most importantly their mass sensitivity capability. This table helps us to pick and choose right device for right application.

Acoustic Devices	Bulk Acoustic Devices	Surface Acoustic Devices	
Device type	QCM	SAW	STW
Working Medium	Gas, Liquid	Gas	Gas, Liquid
Particle Displacement	Transverse	Transverse Parallel	Transverse
Plate Thickness	$\lambda/2$	$\gg\lambda$	$\gg\lambda$
Frequency Determining Factor	Plate thickness	IDT Spacing	IDT Spacing
Operational Range	5-20 MHz	0.3-1.8GHz	0.3-30GHz
Mass Sensitivity (Hz/ng)	0.0095 (for 10 MHz)	0.2 (for 158 MHz)	0.18 (for 250MHz)

Table 1: Basic classification of Acoustic wave devices

2.6 QCM as Mass Sensitive Device

2.6.1 Introduction and Basic Theory[12]

Quartz Crystal Microbalance (QCM) is a piezoelectric material having affixed electrodes on both sides of the quartz plate as already shown in figure 5.It

is highly mass sensitive device capable of measuring mass changes in the nano-gram range. High mechanical stability, low temperature dependence and low damping make this material extremely useful for mass sensitive measurements.
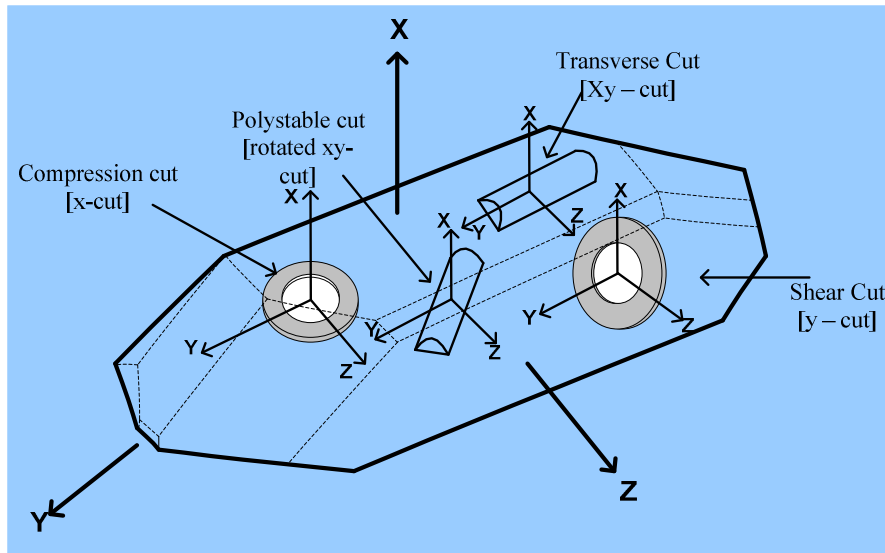
Figure 6: Morphology of a quartz crystal according to wave propagation mode.

Figure 6 explain the morphology of a quartz substrate with respect to different cutting modes.

In order to achieve the desired properties, the quartz crystal plate should be cut to a specific orientation with respect to the crystal axes. These include the AT- and BT cuts as shown in the following figure 7.
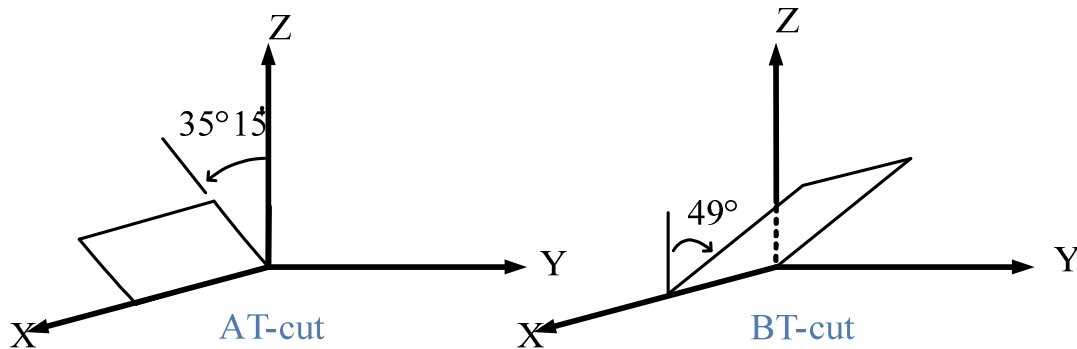

Figure 7: AT-cut and BT-cut angles for a quartz crystal.

AT-cut quartz crystal can easily be manufactured on commercial scale and is most widely used crystal for mass sensitive measurements, but it has certain limitations concerning high and low temperature. In extreme temperature conditions the crystal structure is easily disrupted by the internal stress. These internal stress points produce some undesired frequency shifts during measurements which reduce the accuracy. Quartz crystal performs resonance oscillations when it is bring in to the circuit oscillator where the mechanical and the electrical oscillations are close to the fundamental frequency of the crystal. An equivalent circuit model can be designed for QCM which is helpful to calculate the resonant frequency and quality factor (Q) or dissipation (D) i.e. mass accumulation on the quartz surface and the visco elastic nature of the deposited layers. This equivalence circuit model is shown in figure 8.
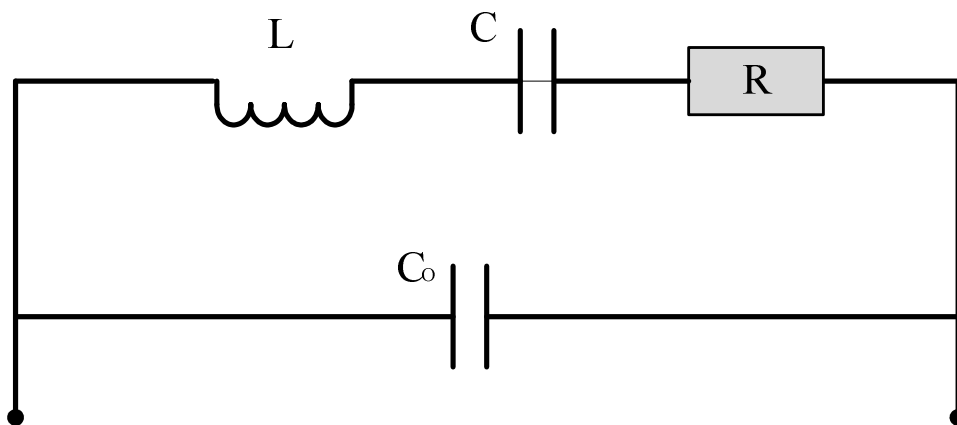
Figure 8: An equivalence circuit for QCM.

The oscillations of QCM can be compared to the above circuit in which mechanically vibrating mass is considered as inductance L, the capacitance C represents the elastic behaviour of the resonator, R shows the damping losses during mechanical vibrations and C_0 stands for the capacity between two electrodes on QCM. The ratio of applied electrical voltage and the electricity flowing through the quartz crystal gives the value of impedance. The inverse of this impedance is called admittance. The impedance value gives all the

30

information about the vibrating quartz crystal and is helpful in understanding the nature of the deposited layer. For example, frequency and quality of resonance (Q) or damping losses can be calculated. Moreover, different harmonics and the distorted resonance curves can also be determined.

The fundamental frequency of the quartz is determined mainly by the thickness of the sheet. The characteristic frequency of piezoelectric crystals is given by the following relationship.

$$f = \frac{C}{2d} \quad \text{or} \quad f = \frac{N}{d}$$

Where C is velocity of sound in quartz, d is the thickness of the quartz sheet while for typical AT-cut crystal N is 1670 kHz·mm. Some other parameters like chemical structure of the crystal, shape and mass can also affect the fundamental frequency. Commercially available QCMs have the fundamental frequencies up to 50MHz but at this point the crystal plates become too thin to be mechanically stable. Commonly used QCMs have the frequency range 10-20MHz in sensor applications. Figure 9 shows explain the principal of wave propagation in 10MHz AT-cut quartz having sensitive layers over gold electrodes.
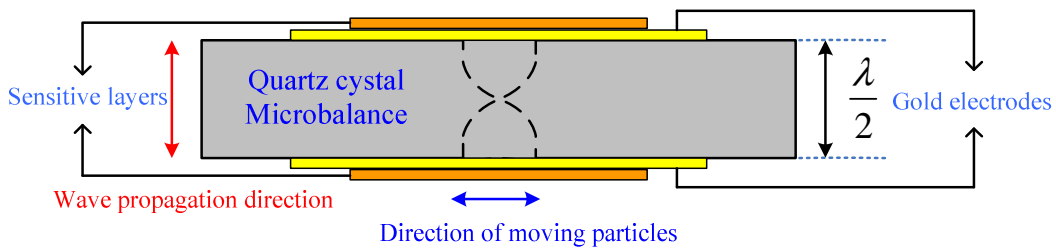

Figure 9: QCM designing and wave propagation mode.

The oscillation frequency of QCM is influenced by the shear modulus of the crystal and some other physical properties of the working medium which include density or viscosity of the gas or liquid phase. Mass accumulation on quartz

surface changes its resonant frequency. This relationship of mass deposition to the resonant frequency was first introduced by Sauerbrey[13] in 1959, which is as follows.

$$\Delta f = -f_o{}^2 \frac{2}{A_{cr}\left(\rho_m C_q\right)^{1/2}} \Delta m \qquad (2.1)$$

Where,

Δf = Frequency change

f_o = Resonant frequency

Δm = Change in mass

A_{cr} = Active Piezoelectric area of quartz (usually electrode area)

C_q = Shear modulus of quartz crystal

ρ_m = Density of Quartz

This equation clearly indicates that the change in resonant frequency is directly related to the mass deposited on crystal surface. The above relationship was derived for the systems working in gas phase. While going to the liquid phase, certain parameters have to be considered, among the viscosity and density are most important. For that purpose above equation is modified and its new form is as follows.

$$\Delta f = -f_o{}^2 \frac{2}{\left(\rho_m C_q\right)^{1/2}} \sqrt{\frac{\rho_l \eta_l}{4\pi f_o}} \qquad (2.2)$$

Where (η_l) and (ρ_l) are viscosity and the density of the liquid phase respectively. While performing the mass sensitive measurements in the liquid phase a frequency shift is observed. For 10MHz quartz the theoretically expected

frequency shift is about 2 to 4 kHz. This value may be different from the observed value due to the difference in the surface and bulk values of viscosity and density. In liquids the damping losses for QCM are quite high and depend upon the visco elastic behavior of the deposited layer and the nature of the liquid medium as well.

QCM resonates in different modes of vibration like symmetric, anti symmetric and twist mode; these modes can easily be correlated by phase shift. All information about quartz during oscillations can be understood from resonance spectra as shown in figure 10.
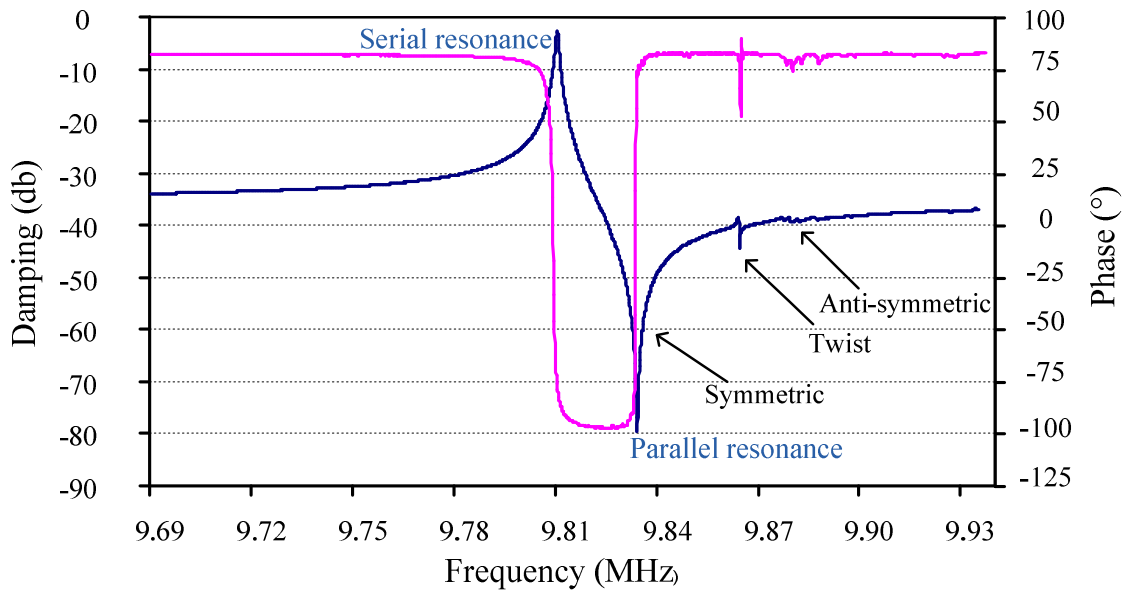
Figure 10: A typical damping (blue) and phase (pink) spectra of a 10MHz QCM

This damping spectrum is for 10MHz quartz having gold electrode over the QCM surface. The serial and parallel resonance frequencies can be calculated by using following equations respectively.

$$f_s = \frac{1}{2\pi\sqrt{LC}}\,\Delta m \qquad \text{and} \qquad f_p = \frac{1}{2\pi\sqrt{LC}}\sqrt{1 + \frac{C}{C_o}} \qquad (2.3)$$

33

2.6.2 QCM in the Field of Chemical Sensing

Several strategies can be purposed to sense an analyte in a complex mixture by using different sensing techniques but Quartz Crystal Microbalance (QCM) is the best choice among all considering its several advantages in the many regards over others in both gaseous and liquid phase. During recent years a number of reviews[14] and articles are reported that explain the applications and technical issues involving QCM use. Their capability for online monitoring in complex mixtures makes these a distinct tool in the domain of analytical chemistry. The early developments in QCM application were just to sense the mass change in gas phase, which includes the humidity sensor, detection of volatile organic compounds[15,16], monitoring of environmental pollutants and gas phase chromatography detectors[17]. Previously, single analyte was measured at one time but now days by designing a suitable sensor array several different analytes can be measured on a single array with higher degree of sensitivity and selectivity that further miniaturizes the mass sensitive devices.

In the decade of 1980, an advanced liquid phase QCM devices were developed that measures the change in the frequency which could be related to the density and viscosity of the solution having high degree of damping. These QCM devices provide an interesting way to sense the mass of the analyte in complex mixtures and characterize the visco elastic properties while operating in liquid phase. The behaviour of the bound interfacial mass to the surface and properties of that medium can be investigated in a better way. Even in opaque solutions where some classical instruments fails the efficiency of QCM devices is not disturbed. These devices are capable to sensitively measure the changing in mass associated with liquid-solid interfacial phenomena and to characterize the energy dissipation due to the visco elastic behaviour of the deposited mass on the metal electrode surface of QCM. These devices have been accepted as a powerful tool to monitor adsorption processes at interfaces in different physical, chemical and biological research areas.

Since the discovery of QCM devices, they have found enormous applications[12] in areas of food chemistry, environmental and clinical analysis. The inherent ability of these devices to monitor different processes in real time makes these superior over other techniques. A brief description about QCM applications in different areas can be presented in following manner in figure 11.
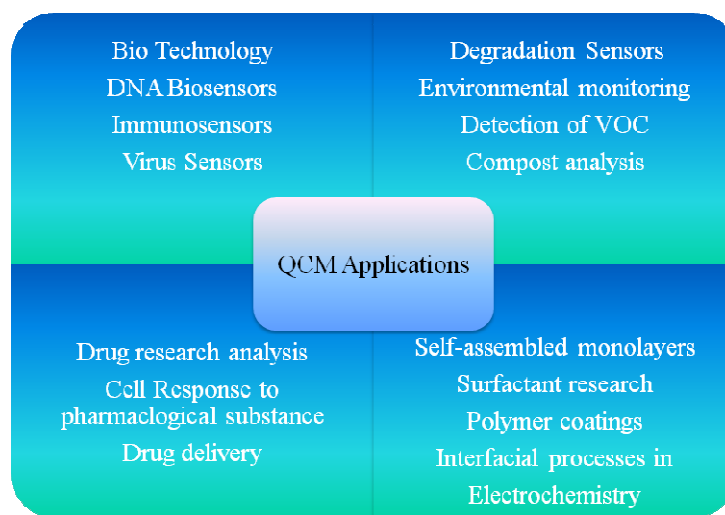
Figure 11: Applications of QCM in different fields.

2.7 Conclusion and Future Directions

These mass sensitive devices have proven themselves a handy tool for the monitoring of clinical and environmental processes. The re-usability of these sensor systems is the one of the most important feature which is gaining the considerable attention of all the scientists around the world. This technique is relatively cheap and easy in terms of its use in gaseous and liquid phase especially in harsh environments. The most exciting feature of these devices is to perform measurements without any specific labeling or any pre treatment of the analyte mixture. The synthesis of a chemically sensitive layer is a major issue which binds the analyte selectively. On the other hand these acoustic wave devices can be integrated wirelessly. So, applying a suitable coating material on

integrated wireless acoustic wave devices can open new horizons in the field of chemical sensors.

Advanced Synthetic Materials for Analysis of Degradation Products

Various types of lubricants are used in automobile vehicles, heavy industrial machinery, and power generating engines. These lubricants reduce the internal friction during operation and increase the life time of the engine but with the passage of time they undergo different degradation phases. In order to make these lubricants more effective a variety of additives are added depending upon type of combustion engine and their end use. These additives serve different jobs like reduction in corrosion, viscosity modification, surfactants and many more. Beside this some basic ingredients are also added such as sulfonate and salicylate salts of calcium in order to neutralize nitrogen and sulphur containing acidic products, produced during fuel combustion of diesel and gasoline engines.

3.1 Classical Engine Oil Parameters

The classical engine oil parameter such as total base number (TBN) or the total acid number (TAN)[18] representing the total basic and acidic compounds respectively, are very important in terms of quality of lubricant. These values have considerable importance during manufacturing processing of lubricants and also predicting their expiry. In fact from these values it is easy to decide about quality of engine oil during fuel combustion, oxidation of oil takes place which yields acidic products, these acidic products are neutralize by the basic additives present in oil. So as long as the basic additives are present in oil they will react towards acidic products. With the passage of time the basic products are going down and acidic products are going up due to oxidation phenomena. This substantial increase in acidic products over a certain value can cause serious corrosion in the piston and other parts. The acidic products are directly linked with oxidation of the engine oil, in fact it represent the degree of oxidation, so

greater the oxidation higher is the acidic products. It is necessary to control these acidic products and more importantly to know the exact life time of engine oil so that when it actually needs to replace. Because an early replacement of the oil would be costly on consumer side and on the other hand a delayed exit of degraded oil can cause severe damage to engine wear. So a continuous monitoring of these oxidation processes is required which enable us to make a quick decision about its replacement, as in case of automobile vehicles the deriving behaviour is not same all the way.

3.2 Literature Review and Previous Work

In order to analyze these acidic products different strategies are employed in literature[19,20,21,22] including both physical and chemical techniques. One recently used physical method for the analysis of degraded oil is Fourier transform infra red (FTIR) spectroscopy[23], in which different characteristics of used engine oil is investigated and the obtained data is compared with other methods in field test. Another spectrophotometric detection method is reported which involves the examination of acid buffers and indicators. In this method a change in absorbance of indicator is measured during acid base buffer solutions. There are some other physical methods which rely on characteristic properties of engine oil; these include a change in viscosity or conductivity[24] of the lubricant. Another path is followed by making a correlation of degraded engine oil parameters with data obtained from classical voltammetric or amperometric measurements.

But these methods do not provide enough information about the molecular recognition systems[25,26] and are not compatible with harsh environments especially in high temperature conditions. Molecular Imprinting[27] is highly suitable and more advantageous technique to generate highly sophisticated molecular recognition sites leading to a favourable interaction towards a defined target analyte. Capric acid imprinted sol-gel layers[28] have proven themselves as a

highly sensitive material for the selective incorporation of degraded base oil additives. These layers are rigid, robust and sensitive enough to perform efficiently. But these layers do not possess large surface area and do not provide better diffusion path ways moreover they lose their sensing capabilities at elevated temperatures. This problem has been overcome by introducing nano particles in place of sol-gel layers. The idea behind invention of nano particles for mass sensitive measurements was to increase interaction sites for the analyte on transducer surface, which leads to an enhanced sensor response. Literature shows that these imprinted nano materials are more sensitive, as they have more number of interaction sites offering more acidic products for selective incorporation. Imprinted TiO_2 nano particles[29] proven themselves a highly efficient tool for engine oil degradation measurements as compared to thin sol-gels. They have higher sensitivity by a factor of two; moreover they can bear high temperature environment which is most significant feature of these synthetic materials. This sensitivity was highly associated with the size of particles. Particles having smaller size shows higher sensor signal than those having greater size. Improved sensitivity and high temperature resistivity justified selection of these materials for online monitoring and process control applications. But going over the temperature range of 250ºC, these nano particles lose their mechanical properties and sensitivity goes down surprisingly. This may due to the collapse of cavities, created artificially in those materials.

3.3 Basic Strategy

Going down to the group IVB in periodic table zirconium is located, which has almost similar properties like titanium but possess some extra temperature durability and resistance towards corrosion. Some other inherent mechanical and thermal characteristics of zirconium suggest that this element could prove more effective in substitution of titanium. So, the strategy is to replace titania with zirconia and generate similar cavities for selective re-inclusion of acidic products to make it better sensitive material at much higher temperatures.

The first section of this chapter gives an overview about making of quartz crystal microbalance having desired electrode design and focus about the synthesis of molecular imprinted nanoparticles of ZrO_2, their characterization by atomic force microscopy (AFM), and mass sensitive measurements with used automotive engine oil. Some mass sensitive measurements are also correlated with Infra red spectroscopic data. The second section of the chapter follows a similar sort of protocol to examine the combined effect of Titania and Zirconia. Finally a comparison is being made among the individual and joint significance of these especially designed materials, which helps in their selection in desired conditions.

Section 1

3.4 Sensor Design and Set up

Before advancing towards the synthetic steps of the nano particles a brief introduction of the sensor design and setup has been described in the coming sections.

3.4.1 Screen Manufacturing and Gold Printing on QCM

An optical lithographic procedure is followed for silk screen manufacturing to cast the desired electrode image on QCM. For this purpose silk cloth of 21µm mesh size is tightly glued on a metallic frame. A very fine film of a UV sensitive polymer (Azocol Poly plus S of KIWO) is coated on silk and kept under dark for half an hour. The electrode design is printed in black color on a transparent sheet which is fixed in UV chamber. Now sieve is placed on this image in such a way that the design should be in centre of the frame and then UV light is exposed for 30 seconds. The image appeared on the sieve after washing with warm water. The sieve used for the manufacturing of QCM for both mass and electric sides in oil analysis is shown in the figure 12.
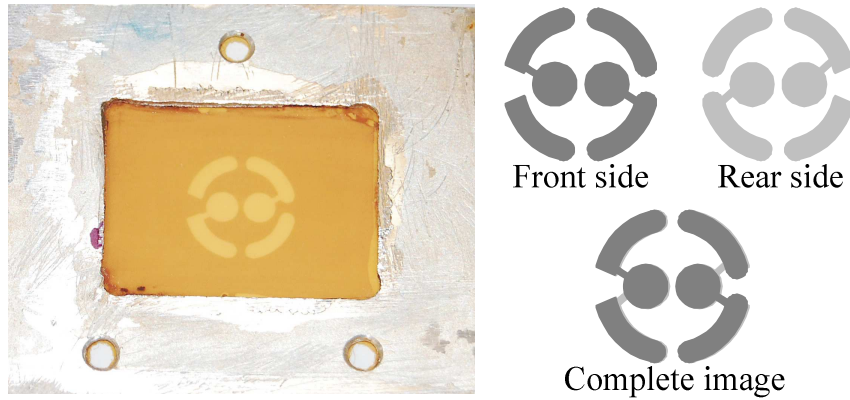
Figure 12: Sieve design for dual electrode QCM. The impression from front and the rear ends are also highlighted.

For screen printing, QCMs of fundamental frequency of 10MHz were purchased from Zheijiang quartz crystal electric company, China. At first quartz wafer is put onto a Teflon block and the sieve frame is placed over it as shown in the figure. To keep the QCM alignment fix the Teflon block is connected to a vacuum pump. Now the gold paste from is spread over the sieve with the help of a sharp edge rubber to make it smooth and uniform. A fine image of this electrode shape has been stamped on QCM wafer which is then placed into an
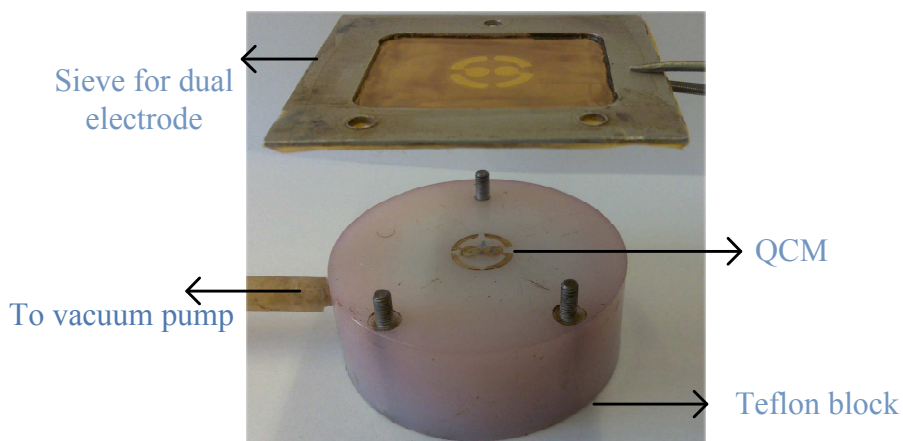

Figure 13: Representation of screen printing procedure.

oven at 400⁰C for 3 to 4 hours to evaporate the organic residues. Similar process is followed for back side of the QCM. The important thing is that the temperature

and heating time should not be increased otherwise the quartz might shifted to another phase which can influence the fundamental resonance frequency.

3.4.2 Electronic Circuits

Electrical connections of above prepared QCM are made by a DC power supply and a circuit oscillator which is coupled with Agilent frequency counter. An input DC voltage of 12V is applied to the oscillator which is connected from one part to the measuring cell and from other to frequency counter. A typical oscillator circuit diagram is shown in the following figure 14. The frequency counter is connected to a computer via GPIB USB cable. Any change in frequency is recorded by the software installed on computer.

Figure 14: Oscillator circuit diagram for 10MHz for QCM.

3.4.3 Cell Design

In liquid phase where the viscosity effects are more pronounced than gas phase, measurements become more tedious especially in the case of oil which can influence the analysis. So the problem can be solved by increasing temperature of the measuring cell. The temperature proposed during the measurement is about 80ºC. For this purpose a water bath is used which can

maintain the desired temperature of the cell. To withstand at such a high temperature a special brass cell is designed which is connected to water bath through special pipelines. A typical brass cell is shown in the following figure.
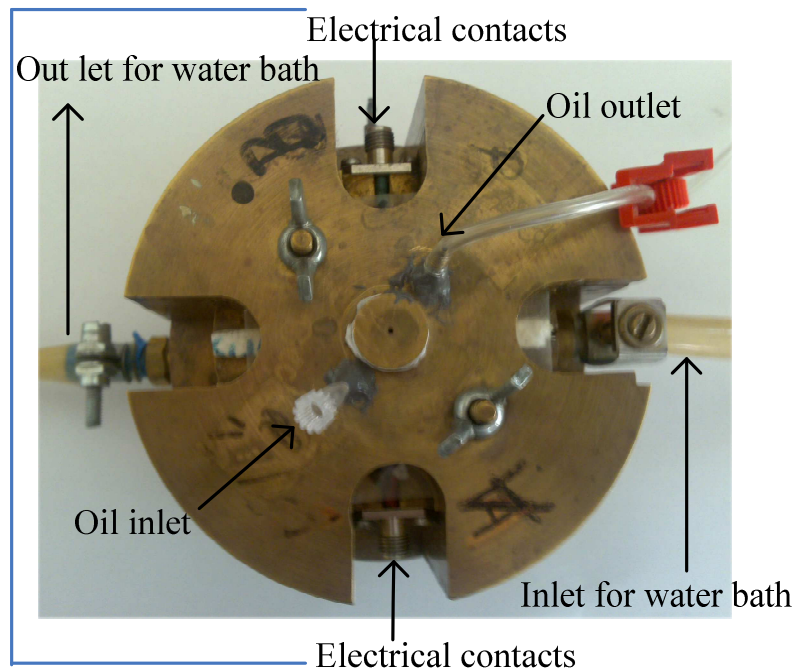

Figure 15: Brass cell used for oil measurements. Different arrows show direction of inlet and outlet for oil samples and electrical contacts.

3.4.4 Layer Material Coating

The layer material is coated exactly over the electrode surface with the help of a spin coater. QCM is fixed on the spin coater using a plastic tape which covers the whole quartz expect the electrode area that has to be coat. After fixing QCM, spin coater is turned on and a very small quantity typically in µL of coating solution is dropped on electrode by a micro pipette. The drop spread all over the electrode surface and form a very thin and fine film. The rpm and spinning time can be adjusted according to requirements to obtain desired layer height.

3.5 Experimental Section

3.5.1 Materials and Chemicals

All the chemicals and reagents used for the synthesis of nanoparticles were purchased from Sigma Aldrich in highest purity.

3.5.2 Synthesis of Molecularly Imprinted Zirconia Nanoparticles

Molecularly imprinted nanoparticles for detection of engine oil degradation were synthesized by hydrolysis reaction of ammonium hydroxide and zirconium propoxide using capric acid as template. Equimoler quantities of zirconium propoxide and capric acid i.e. 327mg and 172mg respectively were dissolved in 1000µL of iso-propanol separately and the mixture was sonicated for 15 minutes to make a clear and homogenous solution. To initiate the hydrolysis reaction ammonium hydroxide was added slowly on constant stirring to this mixture until precipitation stops. This mixture is kept under constant stirring for 15 minutes. After that mixture was transferred into a vial and centrifuged at 4000rpm for 10minutes. Supernatant liquid was decanted off while the remaining matter was washed with water and acetone respectively, and later on dried in oven at 60°C. These dried particles were finely grinded and sonicated with 0.1N HCl for 10 minutes to neutralize the traces of ammonium hydroxide. Now washed these nanoparticles in a same manner with water and acetone respectively and dried in oven.

3.5.3 Synthesis of Non-Imprinted Titania Sol-Gel

Non-imprinted titania sol-gel layers were prepared from condensation reaction of titanium propoxide. In order to prepare these sol-gel layers 67µL of tetrabutyl orthotitanate Ti $(OBu)_4$ is dissolved in 970µL of iso-propanol, to carry out condensation, 10µL of $TiCl_4$ was added to above matrix. This mixture was

heated on 60°C for 1hour on continuous stirring to complete polymerization. This layer performs two functions, first it is used as reference to the imprinted nano particles compensating the viscosity effects of used engine oil during mass sensitive measurements and secondly it immobilized nano particles on gold surface.

3.6 AFM studies

Atomic force microscopic (AFM) studies provide an excellent way to investigate the distribution of zirconia nanoparticles and imprinting effects. AFM consist of an extremely fine tip fixed on a cantilever spring that is moved mechanically over the sample surface. When cantilever tip is brought near to the sample surface, attractive or repulsive forces operate resulting from their interactions. The information collected from these attractive or repulsive forces are monitored from a laser attached to the back side of the cantilever and from this information image of the sample surface is produced. In this surface study AFM from Veeco digital instruments company is used as shown in figure 16.

To prepare an AFM sample a glass piece of 5×5 mm is coated with

Digital Instruments NanoScope
scan size   5.000   µm
scan rate   0.9864 Hz
Number of samples   512
Image Data   Height
Data scale   50.00 nm
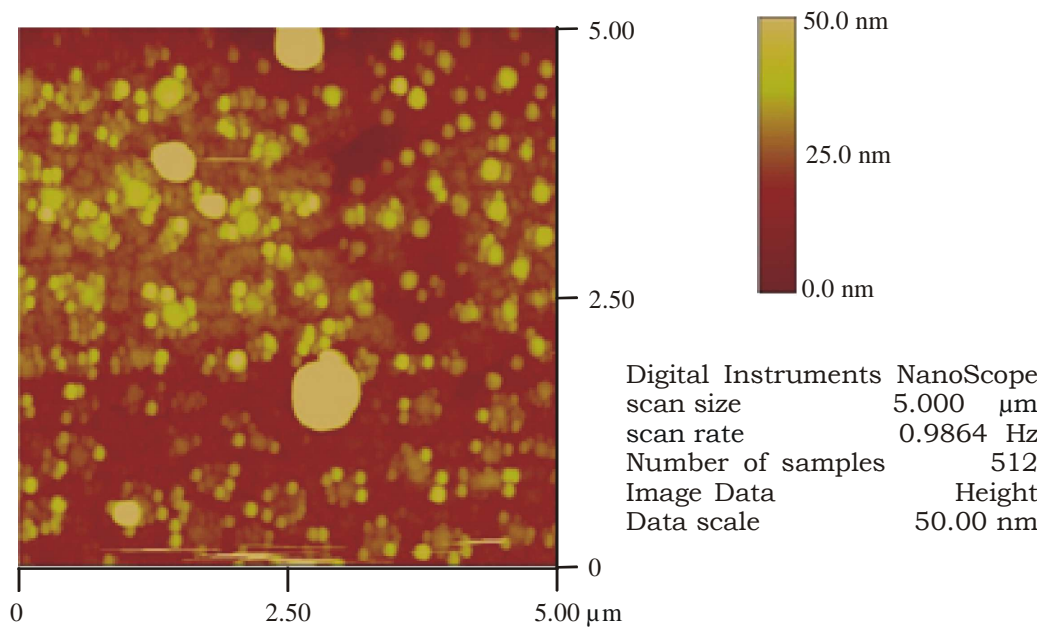
Figure 16: Imprinted zirconia nano particles at a scale of 5 µm.

nanoparticles solution and heated in an oven at 110ºC for 2 hrs. The height image obtained is presented as follows. This image shows a very fine distribution of zirconia nanoparticles having size of 100nm to 200nm approximately on a scale of 5µm.

3.7 Coatings on QCM for Mass Sensitive Measurements

For coating nanoparticles on quartz electrode, 5mg of previously dried zirconia nano particles were mixed with 500µL of iso-propanol to make a homogenous and uniform suspension, 100µL of non-imprinted titania sol-gel were also added which served as gluing agent. On one electrode, 5µL of this suspension is coated on a spin coater at a speed of 3000rpm for one minute, while the other electrode was coated with non-imprinted sol-gel material which considered as reference under the same protocol. Before coating the second electrode the layer formed on first electrode should be dried and then covered with some material to avoid any interference during other electrode's coating. This quartz is heated in oven at 110°C for two hours; frequencies of both electrodes before coating and after heating were noted in order to calculate the layer heights.

This coated QCM was placed in the measuring cell like a sandwich between the O rings. As the quartz is very fragile so these O rings saves it from breaking in the metallic body of the cell. The temperature was maintained at about 80ºC to minimize the viscosity effects of degraded oil. The cell is now flush through n-heptane which not only removes the template from the imprinted channel but also act as the base line solvent during the measurements. After some time when a stable base line was achieved n-heptane was drained off and 200µL sample of 83 hours used engine oil was introduced into the cell. A sudden change in the frequencies of the both channel was recorded on LAB VIEW software installed on the computer. The difference appears after subtracting the frequency change in imprinted channel to the change in reference channel is called the net sensor response which is shown in the figure 17.
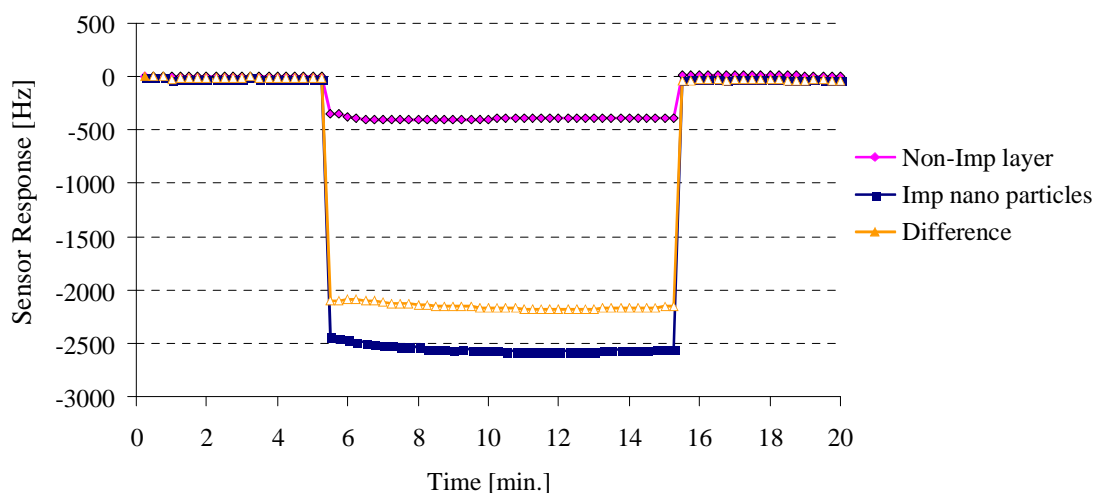
Figure 17: Sensor response of imprinted ZrO_2 nanoparticles of 83 hours used oil at 80°C.

These imprinted nanoparticles shows highly appreciable sensor response towards the 83 hours used engine oil as compare to the reference channel on which a titania sol gel layer was coated.

3.8 Selection of Zirconia Nanoparticles

Zirconium is well reputed transition element in periodic table due to its corrosion resistive properties. The idea of replacing titania nanoparticles with zirconia is to improve the thermal stability and durability of the sensor material that can show significant sensor response at higher temperatures. To examine the behavior of zirconia, their sensor response at elevated temperatures have been recorded and then compared to the previous work on titania. Moreover the surface studies have also been carried out to observe the changing in the particle size and their distribution with respect to different temperatures.

3.8.1 Mass Sensitive Measurements at Elevated Temperatures

A set of eight different QCMs have been prepared and heated in the range of 110°C to 400°C in a similar manner as explain in the section 3.7 to perform mass

sensitive measurements. The layer height of all the QCMs have been calculated from the frequency difference [Δf (1kHz) = 40nm] before and after coating of the nanoparticles.
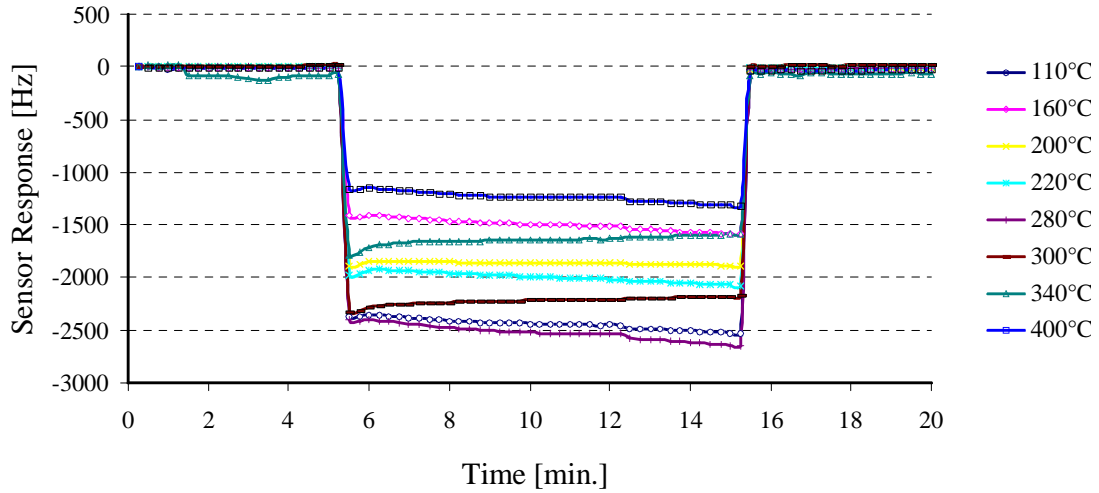

Figure 18: Sensor response of zirconia nanoparticles on eight different QCMs heated from110ºC to 400ºC to 83 hours used oil measured at 80°C.

Mass sensitive measurements recorded at higher temperatures produce a full picture to understand the behaviour of the sensing material in different environments. As the degradation processes takes place at higher temperatures so, it is very important to know that how the coated nanoparticles will behave at elevated temperature. Comparatively at low temperature i.e. 110ºC the sensor response was quite nice in the case of titania and same was observed for zirconia between 200ºC to 400ºC. A special trend was followed which has been shown in the figure 19. The graph can be explained in two ways first in terms of increasing sensor response with increasing temperature i.e. from 200ºC to 280ºC and secondly in terms of decreasing sensor response with increasing temperature. In fact in first part sensitivity is directly proportional to the temperature where as in the second part it is inversely proportional.
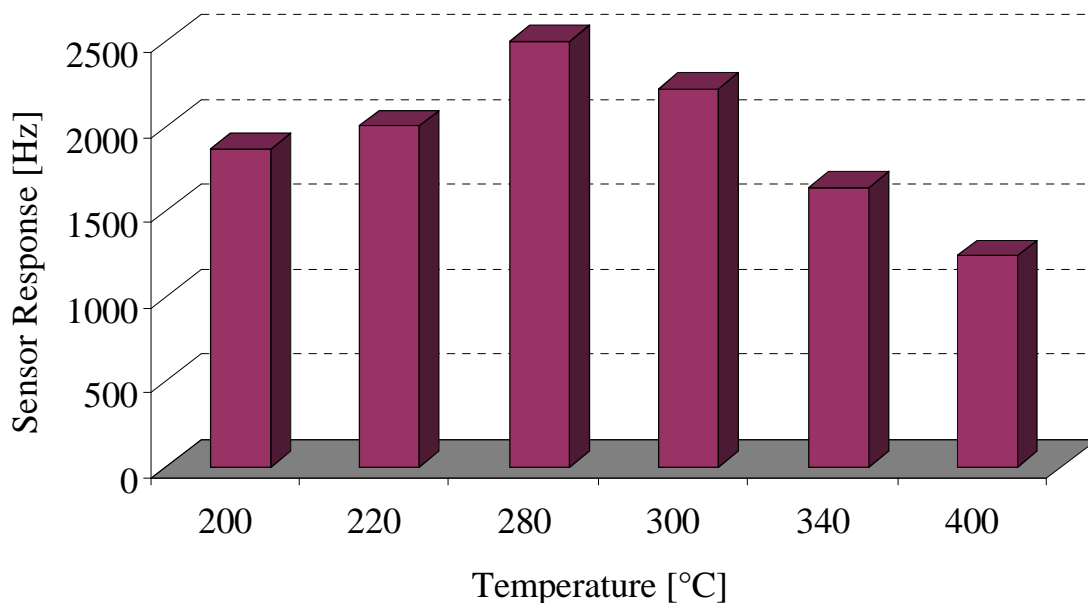
Figure 19: Sensor response of zirconia nanoparticles heated in the range of 200ºC to 400ºC to 83 hours used oil at 80°C.

Considering the first part there is a consistent increment in sensor signal till 280ºC which can be explained in terms of phase transformation[30] of zirconia nanoparticles. It has been reported that heating at about 500K (227ºC) or over initiates the process of phase transformations to tetragonal structures. This might change the dimensions of nanoparticles providing a better surface area for sensing of acidic products. In the second part of the graph sensor response is diminishing with temperature enhancement which clearly suggests destruction in numbers of molecularly imprinted sites for re-inclusion of acidic products due to losing control of nanoparticles over their positions.

3.9 Surface Studies at Different Temperatures

Nanoparticles have been coated from the same solution of the QCM coating on four different glass slides and heated at different temperature range from 110ºC to 400ºC. Their AFM images have been captured and shown in the following figures starting from 110ºC, 200ºC, 300ºC and 400ºC at the scale of 10µm respectively to understand the surface behaviour of zirconia. The AFM image of glass slide heated at 110ºC shows a very fine distribution of nano particles.

At 110 ºC
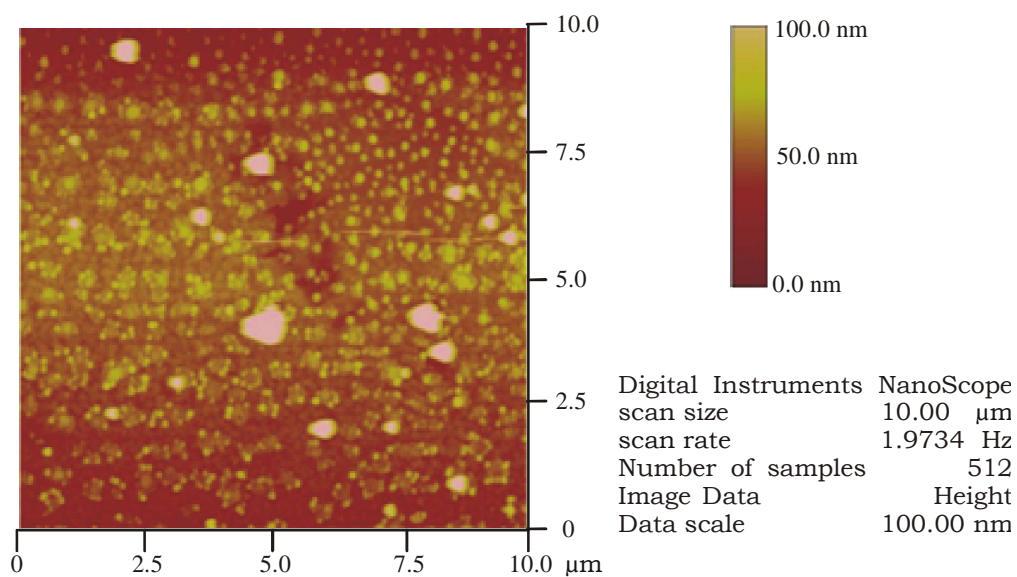
Figure 20: AFM image of imprinted nanoparticles heated at 110 ºC.

At 200 ºC
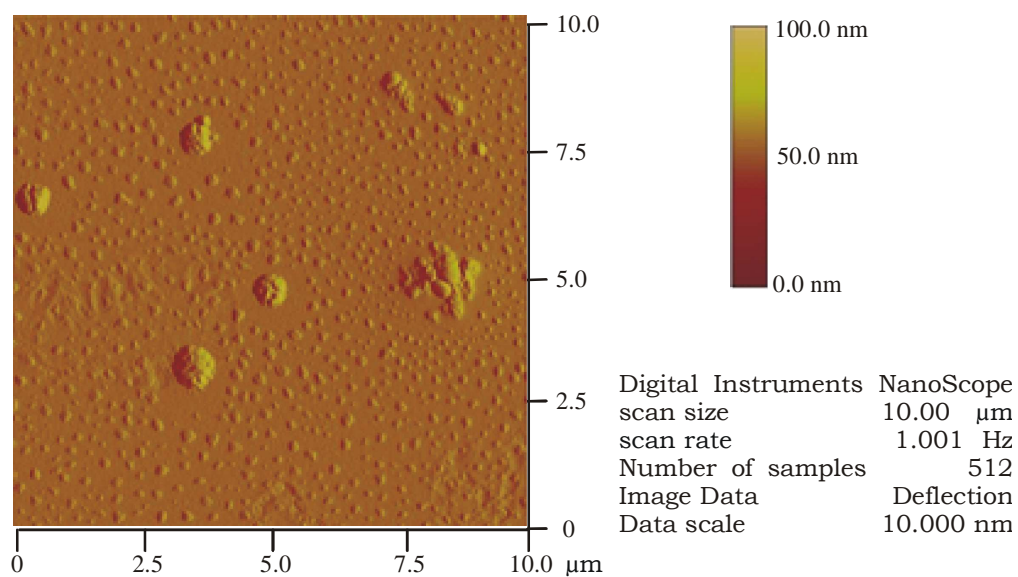
Figure 21: AFM image of imprinted nanoparticles heated at 200 ºC.
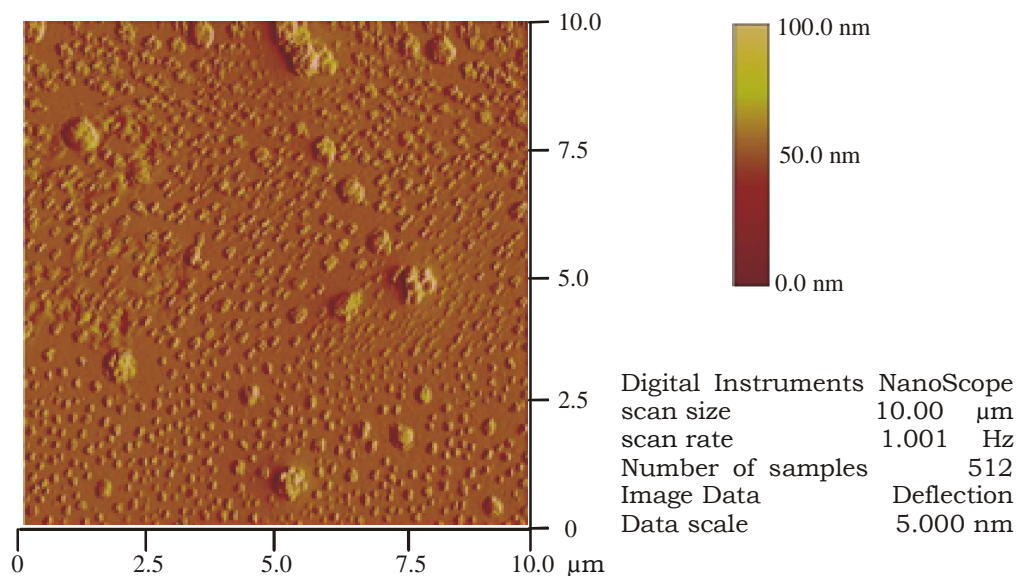
At 300℃

Figure 22: AFM image of imprinted nanoparticles heated at 300 ℃.
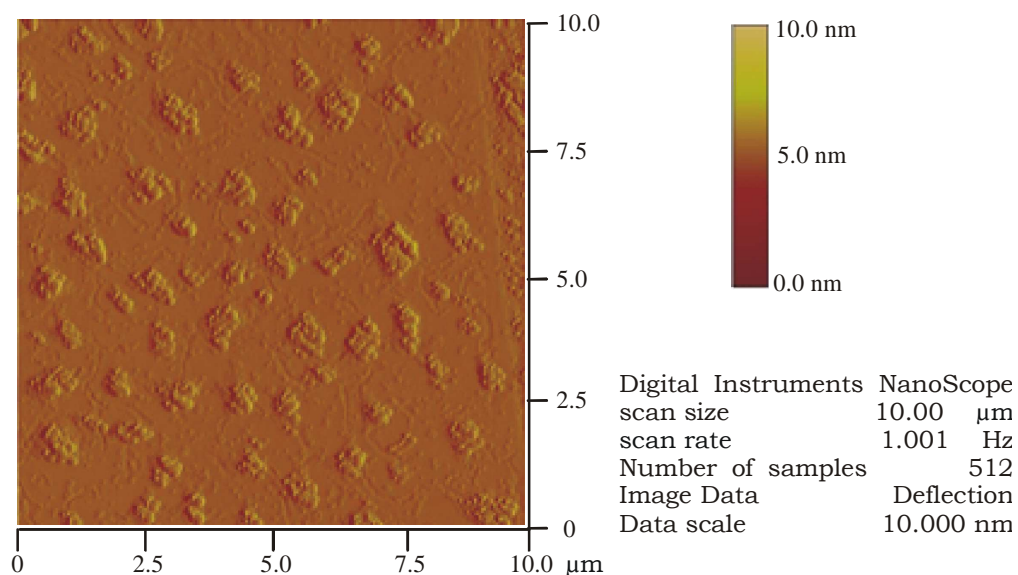
At 400℃

Figure 23: AFM image of imprinted nanoparticles heated at 400 ℃.

The number of interaction sites are proportional to sensor response of the system as greater the acidic products interaction with the surface of nanoparticles greater will be the effect. But at 200 ℃ distance between particles starts increasing at slow pace. This trend continues till 400 ℃ where the distance between nano particles becomes maximum and they start agglomeration which results a major loss in the sensitivity of the sensor material. But unexpected behaviour of this material was around 300℃ where the sensor response was highest. The reason of this surprising behaviour has been explained above that deals with phase transformation of nanoparticles in this temperature range, which changed the crystal phase as well as the dimensions of nanoparticles that provides slightly better diffusion pathways to the acidic products.

3.10 Correlation of the IR Data with the Sensor Response

The age of the degraded engine oil can be measured in two ways, firstly to find out total time that has been spent by oil sample when the engine was running and secondly recording the difference of metre readings (in terms of kilometres) from first to the next change of engine oil. First method gives the life of used oil in terms of time (hours) while second gives in terms of mileage (Km) of an automotive car. Here some mass sensitive measurements have been performed with different samples of a Punto car and Punto Grande diesel oil samples and the reversibility of the sensor signal has been presented in the figure 24.

The graph shows a gradual increase in sensor response with the growing age of used oil samples. The sensor response was higher to that sample of oil which had covers longest mileage and was lowest to shortest mileage. The QCM sensor response of degraded engine oil can be explained with the help of Infra red spectroscopy.

As the long carbon chains present in the fresh oil undergoes several degradation phases with the passage of time and ultimately converted in to carboxylic acid

which increase the overall concentration of carbonyl group in the oil sample. Greater the intensity of the carbonyl group older the life of the oil sample. The
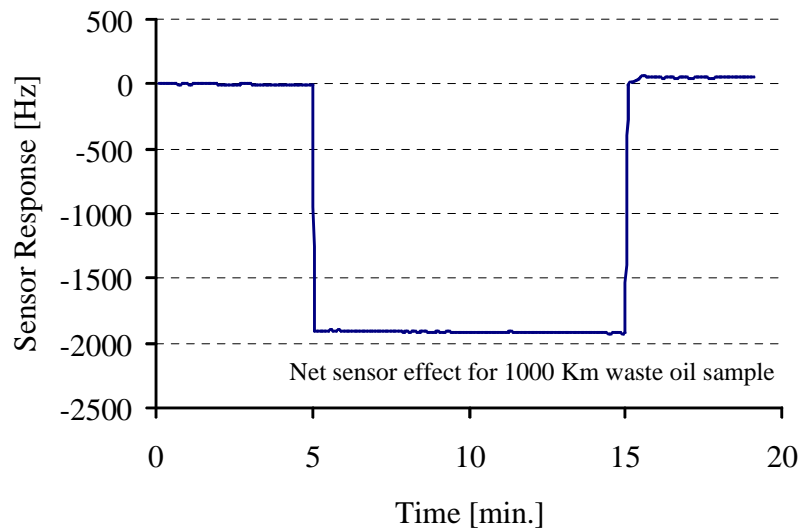

Figure 24: Net sensor response of 1000 km used oil samples from *Punto Grande.*

maximum absorption curve for carbonyl group appears at about 1746cm^{-1}. By drawing a base line to this absorption peak the exact IR intensity of that particular sample can be calculated as shown in the following graph.
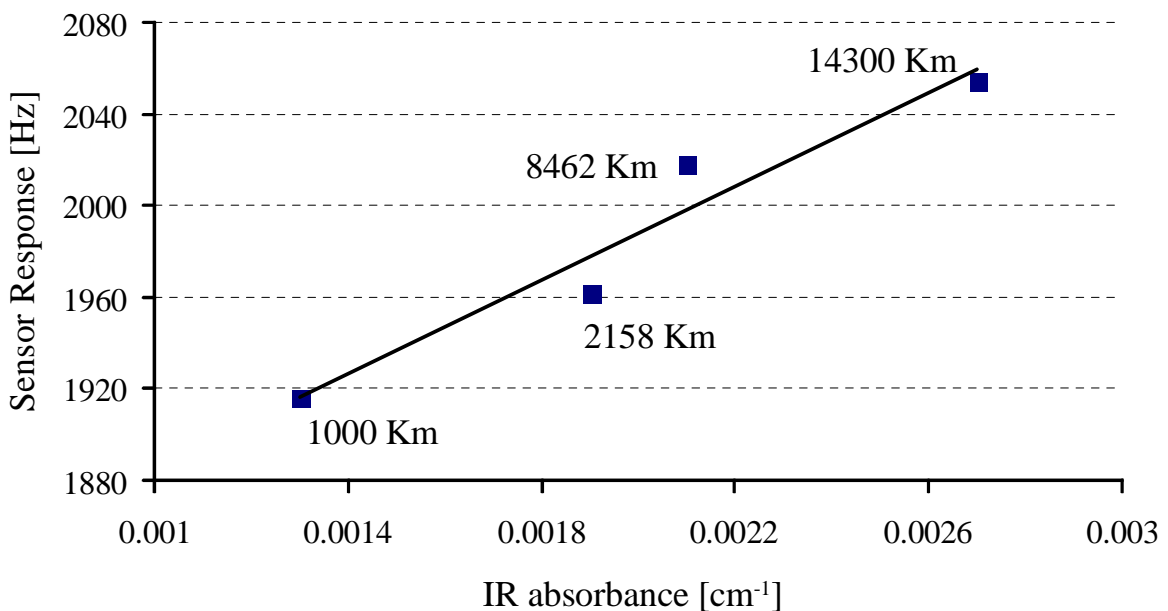

Figure 25: Correlation of IR absorbance *'Punto Grande'* motor oils and their respective sensor responses.

The correlation between sensor responses of QCM with IR data of degraded engine oil samples has been illustrated in the above graph. This result worked as a bridge between two different dimensions of used oil samples where increasing engine oil life corresponds to an increase in IR intensity and the sensor response of mass sensitive devices.

Section 2

3.11 Synthesis of Mixed Composite Titania and Zirconia Nanoparticles

In order to prepare mixed imprinted nanoparticles of titania and zirconia, 327 mg of zirconium propoxide and 172 mg of capric acid (template) were dissolved in 500 µL of iso-propanol separately then mixed these two solutions and sonicated at least for 15minutes to make a clear matrix, named as **A**. On the other hand mixture of 170 mg of titanium tetra chloride and 172 mg of same template e.g. capric acid each in 500 µL of iso-propanol, mixed and heated at 60 °C for 30minutes, named as **B**. Now **A** and **B** were mixed in a 10 mL beaker with constant stirring and drop wise addition of 25% NH_4OH until precipitation was stopped. Stirring was maintained up to 15 minutes allowing the mixture to complete the reaction. Make sure that there was no further precipitation on adding a drop of NH_4OH, stop the stirring and centrifuge the solution on 4000 rpm for 10 minutes. Carefully decant the supernatant liquid, and wash the precipitates first with acetone to remove the un-reacted organic matter and then add 0.1N HCl to neutralize the excessively added NH_4OH in reaction mixture. Filter the precipitates and wash with de-ionized water, final washing was done with acetone and then dried in oven at 60 °C.

3.12 Surface Studies

Before doing mass sensitive measurements of above prepared composite material their surface studies has been performed on AFM. Similar process followed for

preparation of coating solution on glass slides as explained in section 3.6. The AFM images were taken in different modes especially in 3-D plot to examine the nature of the material which helped us to understand the size, distribution and the imprinting cavities generated for acidic products. Previous studies were carried out focusing on individual character of titanium and zirconium but this will provide a combined view of both these materials.


Digital Instruments NanoScope
Scan size   10.00 µm
Scan rate   0.9864 Hz
Number of samples   512
Image Data   Deflection
Data scale   20.00 nm

Z = 20.000 nm/div

view angle
light angle

0 °

X 2.000 µm/div
Z 20.000 nm/div

30-07-2007ti_zr_160c_10.004_5
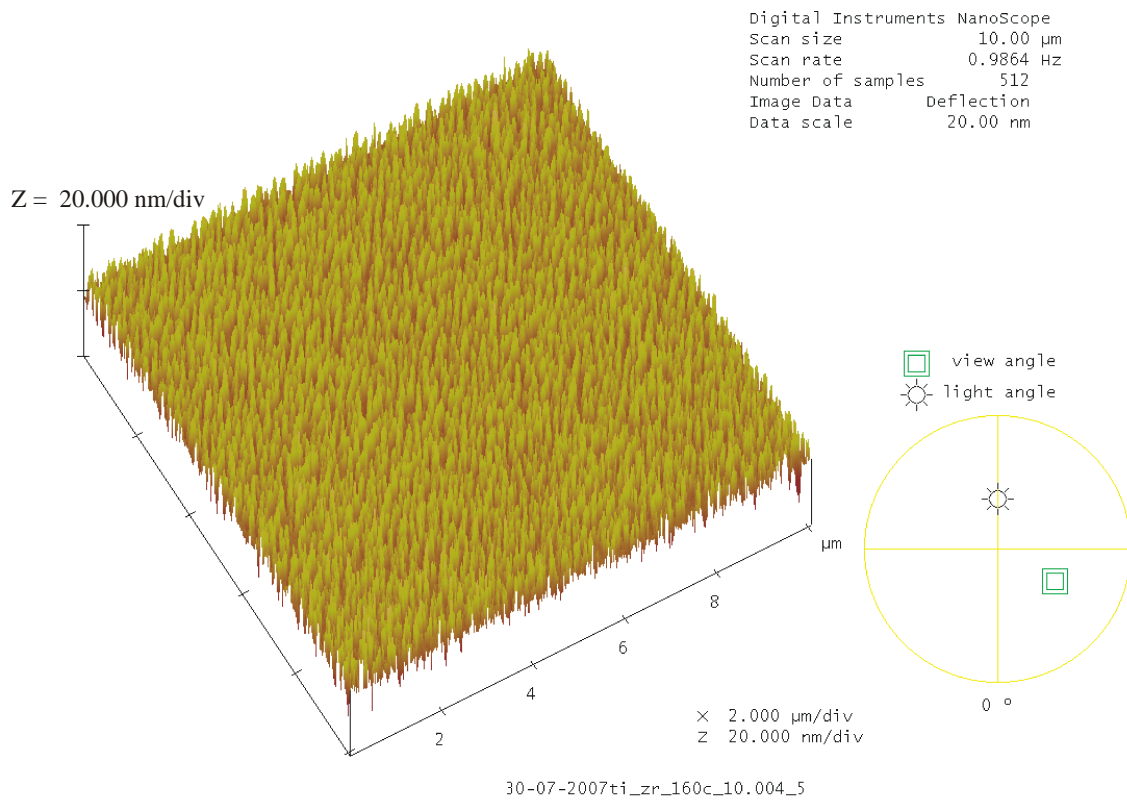
Figure 26: A 3D view of the surface of imprinted titania_zirconia nano particles heated at 110 °C.

This 3-D surface image on a scale of 10 µm of composite material shows a regular pattern of imprinting sites developed between nanoparticles. It is beauty of synthetic procedure that the size of nanoparticles of two different elements is very much identical to each other which facilitate the generation of cavities in an organized way.

3.13 Mass Sensitive Measurements

The mixed nanoparticles were coated on dual electrode quartz crystal microbalance to perform mass sensitive measurement following the same protocol of pure zirconia. Coating solution was prepared by dispersing 5mg of nanoparticles in 500µL of iso-propanol along with 200 µL of previously prepared non-Imprinted titania sol-gel. 5 µL of this uniform dispersion was coated on one electrode while the other was coated with titania sol-gel for reference. This QCM was heated at 110 ºC for 2 hours in oven and mass sensitive measurements were performed with different samples of used engine oil i.e. 40, 83, 123 and 166 hours are presented in the following graph.
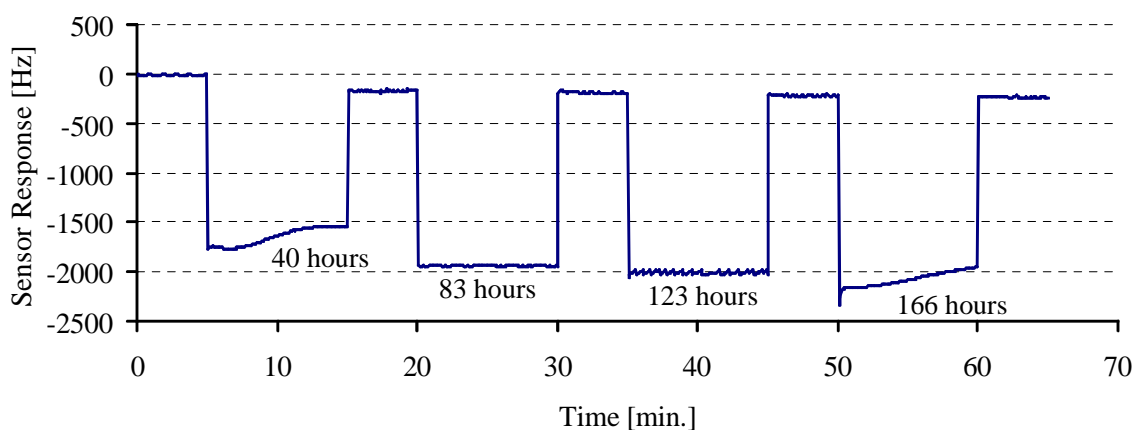

Figure 27: Sensor response of imprinted titania_zirconia nano particles to different used engine oil samples (hours) at 80 ºC.

The sensitivity pattern is quite good towards different used engine oil samples having different ages based on time (hours) spent in running engine. Concerning the life of used engine oil based on mileage (Km), some mass sensitive measurements have also been performed and their result is explained in figure 28. In both curves one thing is very obvious that the sensor response of this material is linear over a wide range of different samples. This linearity help

56

us in drawing a curve in which sensor response is plotted against life of the oil
i.e. mileage covered from first change to the next. All the oil samples tested on
the same QCM should belong to the same engine. The results obtained are shown
in figure 29.
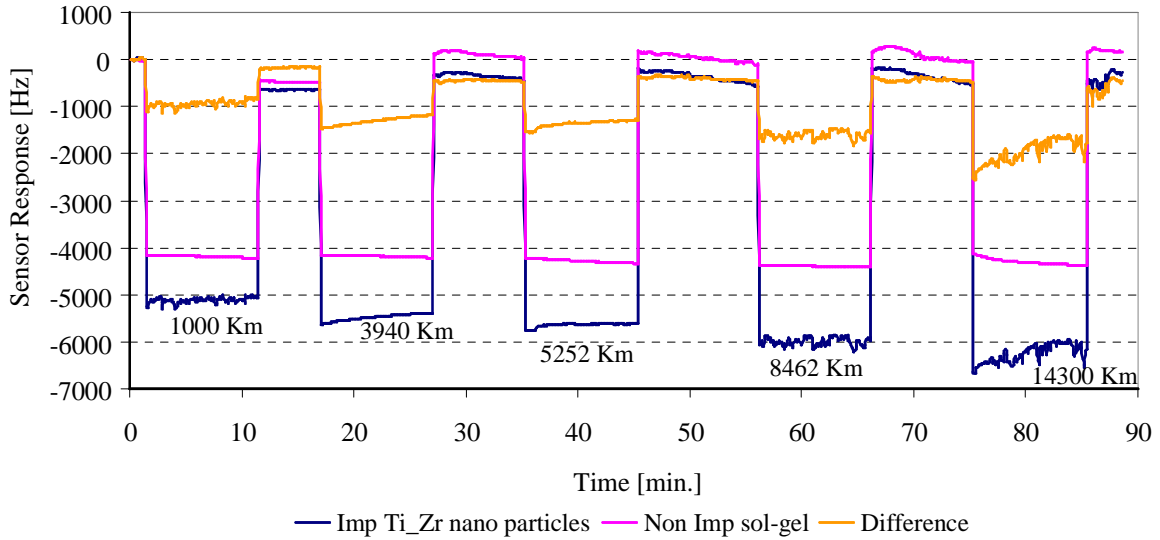
Figure 28: Sensor response of imprinted titania_zirconia nano particles to different used
engine oil samples (Km) at 80 ⁰C.
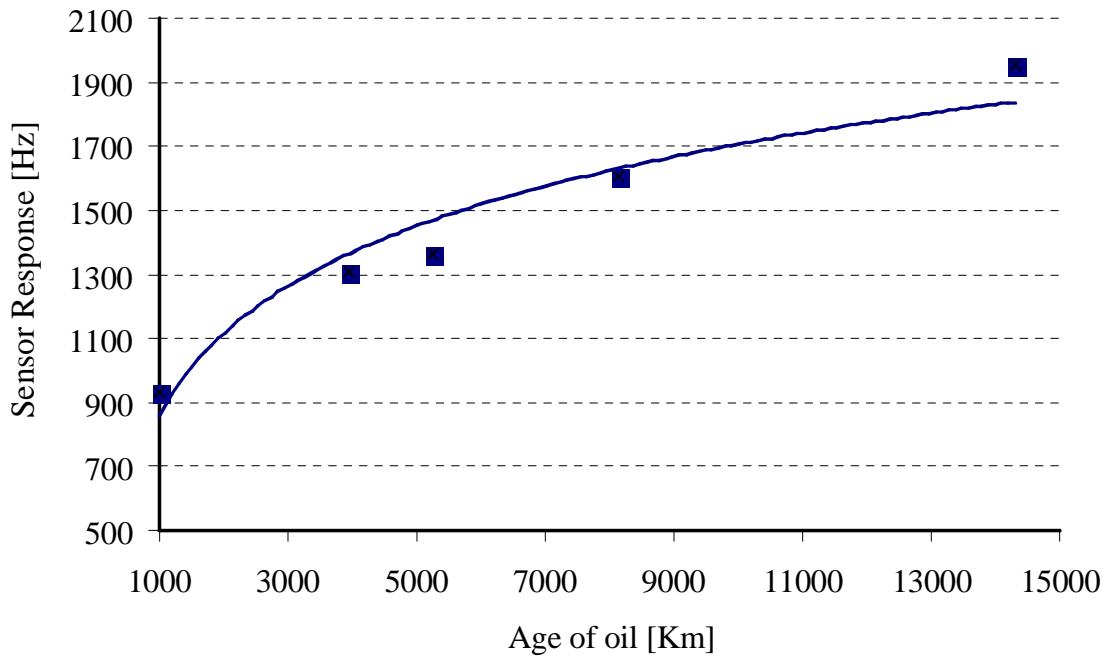
Figure 29: Sensor response of imprinted titania _zirconia nano particles plotted against
age of the oil.

In a similar way six different QCMs have been coated and were heated at different temperatures starting from 110°sC to 400°C in oven for 2 hours. Sensor responses obtained from mass sensitive measurements for all QCMs heated at different temperatures are presented in figure 30.
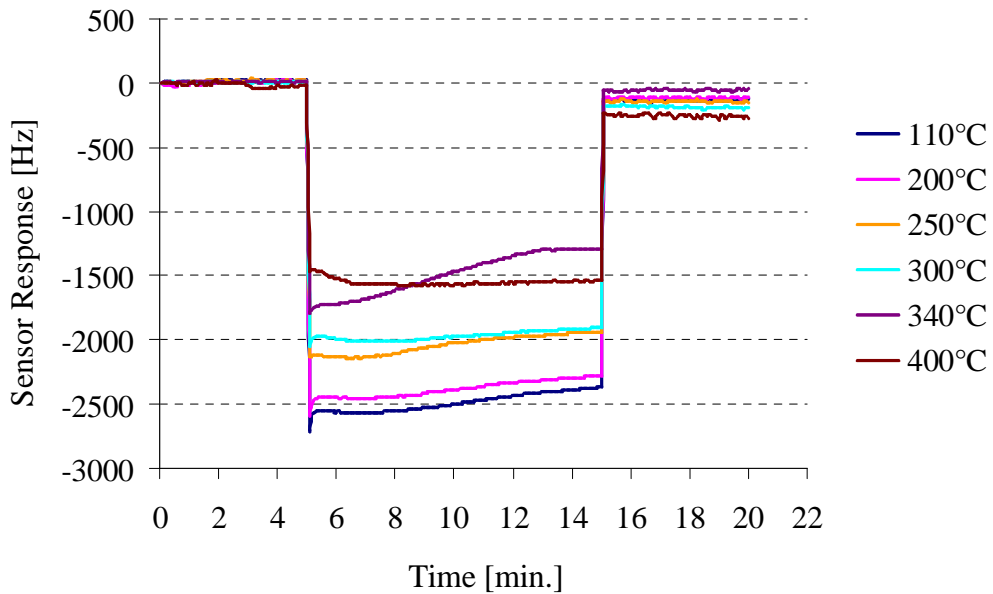

Figure 30: Net sensor effect of mass sensitive measurements performed to 83 hour used engine oil with imprinted nano particles heated at different temperatures.

This graph gives information about the sensor response as function of time to
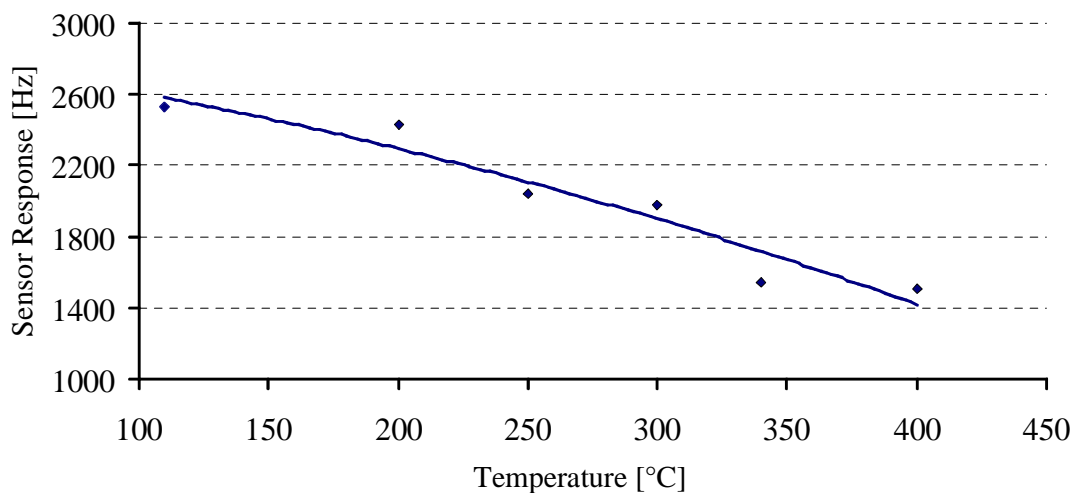
Figure 31: Effect of temperature on sensor response of imprinted titania_zirconia nano particles.

different QCMs heated at different temperatures. This relationship can be better understood in terms of changing sensor response due to temperature where frequency change [Δf] is plotted against the function of temperature [$°C$].

3.14 Particles Size and Distribution

Sensitivity of the nanoparticles is greatly associated with particle size of the material and its distribution on the surface. It has already been assesed that the particles having smaller size are more sensitive than those of larger size. Because smaller size particles provide greater surface for interactions to degraded products or in other words they have more accessible sites in comparison to larger ones under same scale. Sintering or heating of nano particles at elevated temperatures strongly influences their size and distribution. A 3-D image of this composite material heated at 110 ℃ has already been shown in the figure describing the imprinting sites for acidic products. Nano particles were heated at 110 ℃, 200 ℃, 300 ℃, and 400 ℃ and their deflection images on the scale of 10 µm have been captured as shown in the following figures respectively.

At 160 ℃

Digital Instruments NanoScope
scan size   10.00   µm
scan rate   0.9864 Hz
Number of samples   512
Image Data   Deflection
Data scale   20.000 nm
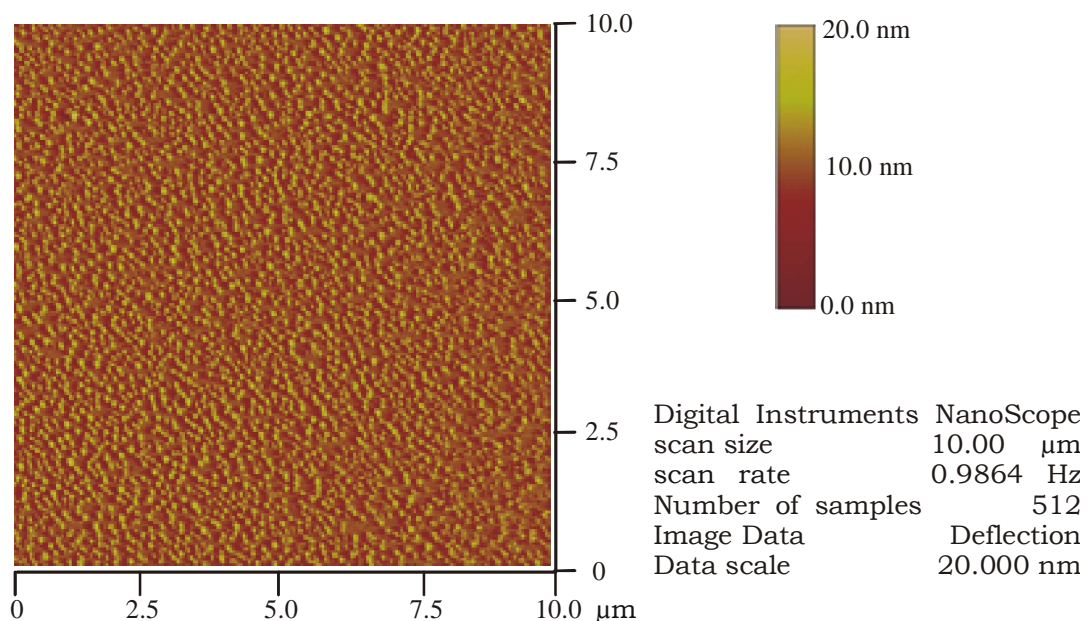
Figure 32: AFM image of imprinted titania zirconia nanoparticles heated at 160 ℃.

At 200 ℃

10.0 nm

5.0 nm

0.0 nm

Digital Instruments NanoScope
scan size   10.00   μm
scan rate   0.9864 Hz
Number of samples   512
Image Data   Deflection
Data scale   10.000 nm
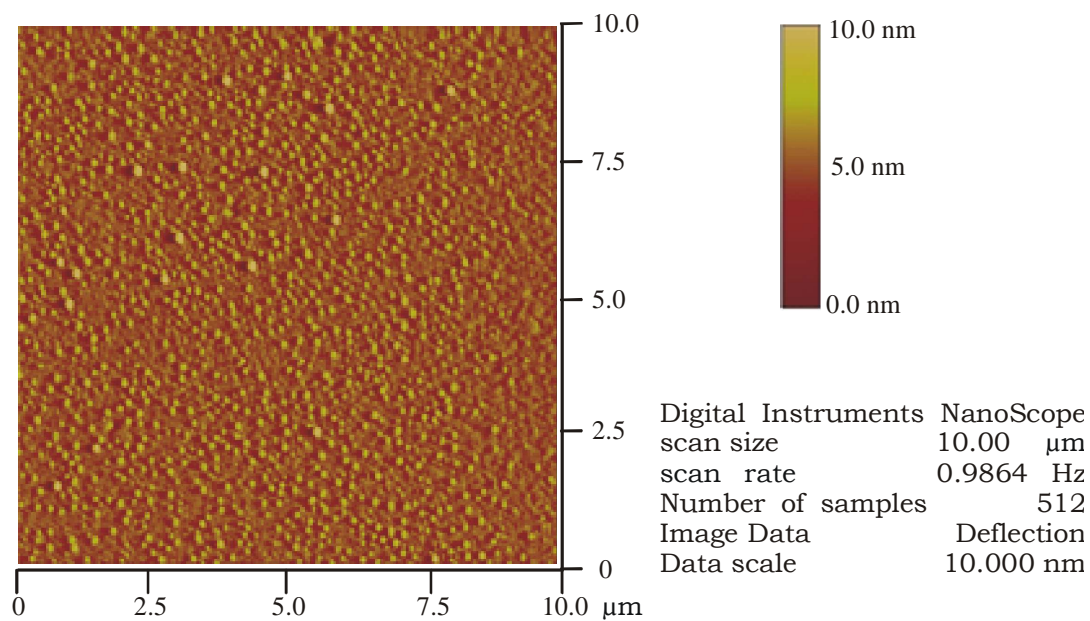
Figure 33: AFM image of imprinted titania_zirconia nanoparticles heated at 200 ℃.

At 300 ℃

50.0 nm

25.0 nm

0.0 nm

Digital Instruments NanoScope
scan size   10.00   μm
scan rate   0.9864 Hz
Number of samples   512
Image Data   Deflection
Data scale   50.000 nm
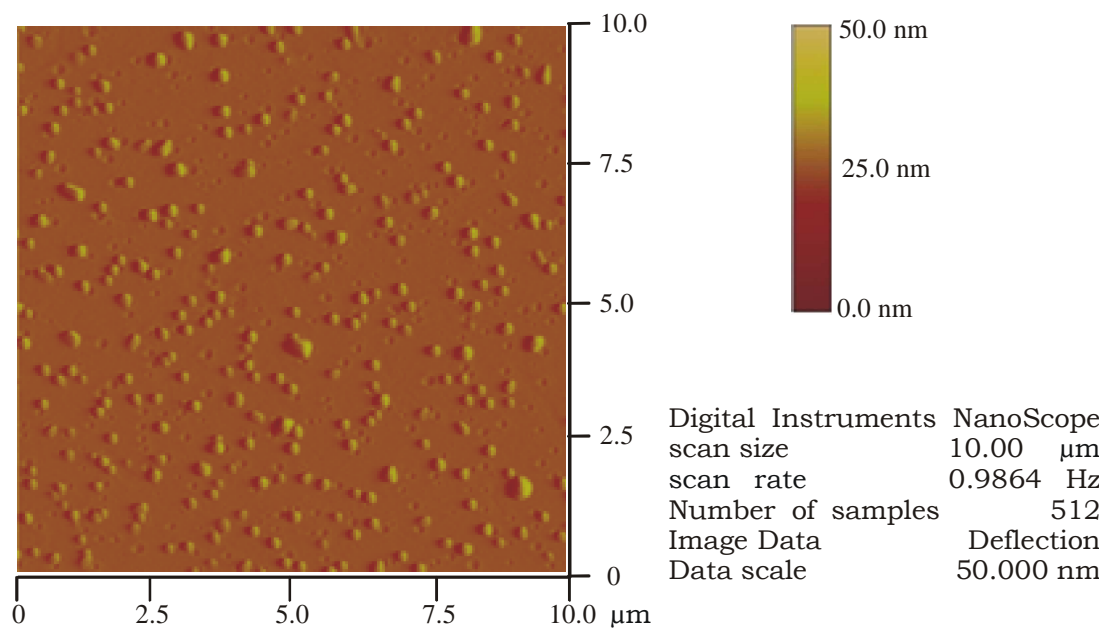
Figure 34: AFM image of imprinted titania_zirconia nanoparticles heated at 300 ℃.

At 400 ºC
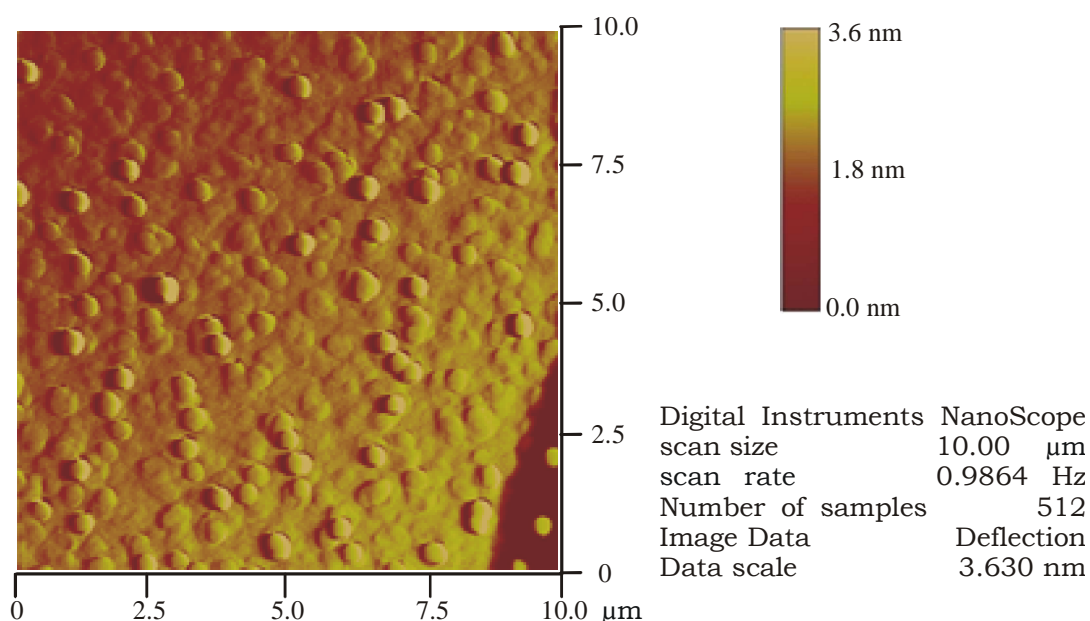

Figure 35: AFM image of imprinted titania_zirconia nanoparticles heated at 400 ºC.

At temperature of 110º C the distribution of nanoparticles was very fine and maximum numbers of sites were available for re-inclusion of degraded products. This has also been proven from the results of mass sensitive measurements where the sensor response of a QCM heated at 110 ºC is highest. Going above at 200 ºC the size of the particles increases and this make the sensor signal slightly down. Further heating up to 300 ºC compel the particles further close which decreases the sensor signal substantially. In fact the idea of introducing titania with zirconia is to develop an innovative material having different centres of mass that can bear extreme temperatures without immediate collapsing. Sintering at 400 ºC strongly influence size of the particles resulting a comparatively small sensor effect. AFM images of nanoparticles heated at different temperatures reveals that the particle size and their distribution gradually changes with changing temperature. The nanoparticles blend of titania and zirconia in specific proportions can lead to the development of highly useful sensitive coating materials that can be used according to their trade mark features in different

working environments. The relationship between average sizes of the particles and QCM sensor response at four different temperatures can be explain by the following curve.
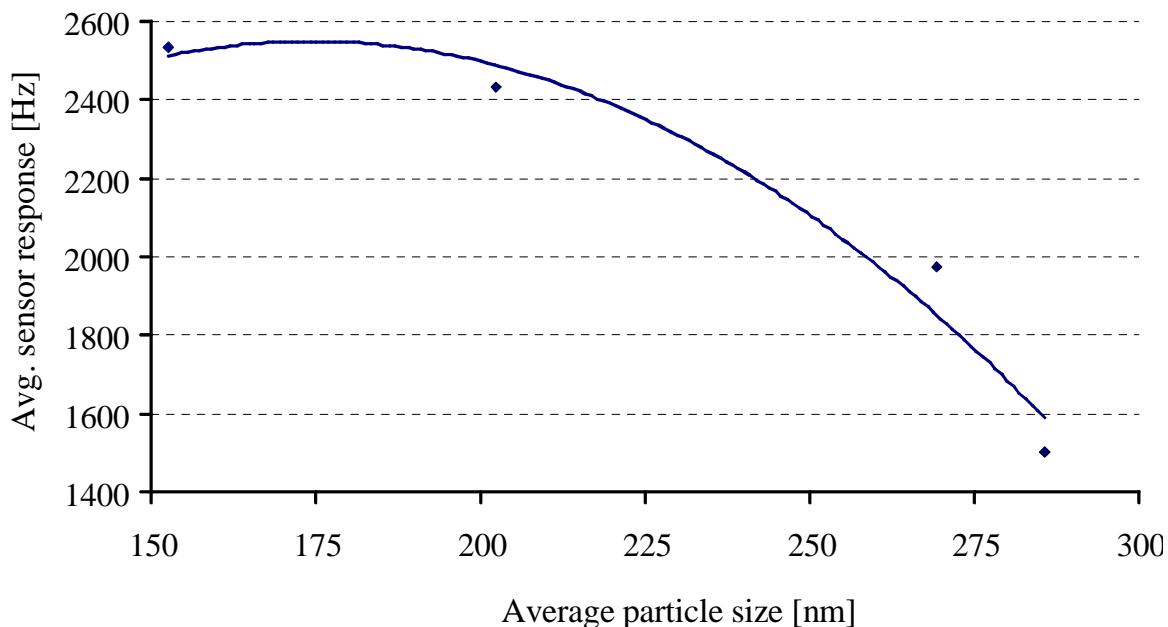

Figure 36: Explanation of the relationship between sensor response and average particle size.

AFM studies and the above graph clarified that the increasing temperature changes the morphology of particles forcing them to come closer to each other destroying the artificially designed imprinting sites which ultimately decreases sensor response.

3.15 Comparison of Sensitivity at Different Temperatures

The individual performance of imprinted titania nanoparticles and of zirconia at higher temperatures had already been studied. In previous investigations, titania proves itself as a promising material concerning the sensitivity at lower temperatures working ranges i.e.160 °C. But at a temperature of about 400°C the sensitivity goes down by a factor of 5 and the material loses its imprinting properties. In the case of zirconia the sensor response is not as high as in case of

titania but is still excellent at lower temperatures. The remarkable feature of this material is that it shows much higher sensitivity than titania at 400°C.

The degradation processes takes place at higher temperatures. Especially in the case of engine oil where the temperature is too high, a very sensitive and rigid sensing material is desired which can work through complex sample of oil efficiently and can withstand at high temperature working environments without losing the original functionality. Combining high sensitivity of titania and high temperature durability of zirconia a novel material is developed possessing both features.

Figure 37 shows a substantial decline in sensitivity with increasing temperature but the important thing is that the sensor response at elevated temperature about 400 ℃ is much higher than the titania or zirconia's individual effects. A sensitivity comparison can be made among the individual and combined strength of these sensor materials at five different temperatures i.e. 110 ℃, 200 ℃, 340 ℃ and 400 ℃ which give us a full picture.
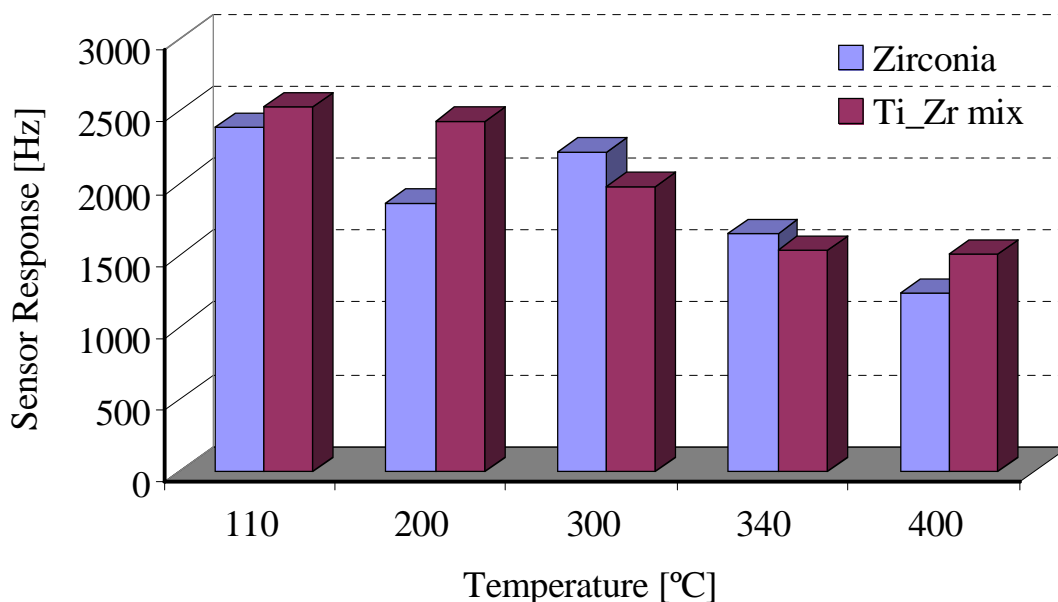

Figure 37: Sensitivity comparison of two different materials at different temperatures.

3.16 Conclusion

Previous studies suggest that imprinted titania nanoparticles are very effective at lower temperatures in regard of engine oil analysis. But in comparison titania imprinted zirconia nanoparticles shows high thermal resistivity at extreme temperatures which makes it prominent in material designing for monitoring of degradation processes. The artificially synthesized composite material of titania and zirconia contains both capabilities of sensitivity and high temperature durability that has been proven by mass sensitive and AFM studies. The selection of the material becomes much easier according to its application.

Selective Polymer Coatings for Sensing of Divalent Metal Ions

4.1 Introduction

Metal ions play vital role in several biological and ecological processes. In various biological processes such as drug designing, smooth functioning of RNA, binding with different proteins to form complex structures[31] and especially in enzyme regulations[32] they are highly essential. Their excess or deficiency can lead to serious problems in different living systems. Concerning ecological aspect these are equally important. In normal surface or drinking water the concentration of heavy metals[33] is normally in µg/L to ng/L range but in industrial waste water this range could be 1000 fold higher. Consequently the health risks are also increased in a similar manner.

The quantitative detection[34] of metal ions is very important in different applications such as, environmental monitoring, developmental biology and waste water management. The continous operation of combustion engine tends to add some metal traces in engine oil samples as due to friction presnet among the metalic parts of engine wear. This continous addition of metals from engine parts also affect the quality of oil. Due to the noxious health effects of metal ions and especially the increasing impact of heavy metals on drinking water, there is a growing demand for their highly sensitive and selective detection. The already established methods are atomic absorption spectrometry[35], inductively coupled plasma spectrometry[36], anodic stripping voltammetry[37,38], X-ray fluorescence spectrometry[39], micro probes[40] and high performance liquid chromatography[41]. All these techniques are very expensive and some of them require sample pre-treatment and analyte pre-concentration steps. Therefore a rapid, cost effective and uncomplicated detection system is needed with suitable sensitivity and

selectivity which can easily be operated by non-professionally trained personnel avoiding the exposure of heavy metals. QCM based mass sensitive devices are simple, in-expansive, with high resolution and require minimal sample volume for analysis. If these devices are coated with suitable polymeric recognition material, they would become powerful sensing engine. The practical approach to this concept is delivered by molecular imprinting[42] where specific recognition sites are generated in a very sophisticated manner. In principal there are two types of molecular imprinting first covalent imprinting and second is non-covalent. The first type of molecular imprinting is considered as pre-organized approach in which reversible covalent bonds are formed between monomer and template prior to polymerization. It was first developed by Wulff and Sarhan[43]. The second type was introduced by Mosbach[44] in which pre arrangement between monomer and template is formed by some non-covalent interactions. Both techniques have their own significance in the field of molecular recognition. Our focus is on non-covalent molecular imprinting due to its versatility in material designing of various analytes for their sensitive and selective detection. This idea has been employed for the synthesis of ion-imprinted polymers.

This chapter gives an overview about the synthesis of different ion-imprinted polymers for different types of divalent metal ions. Their selective detection with accordance to their respective sensor response has been emphasized in this work. First section of the chapter deals with alkaline earth metals and in second section different synthetic methods are followed for Ni^{+2} ions.

Section 1

4.2 Synthesis of Mg^{+2} Imprinted Polymer

Ion-imprinted polymer for Mg^{+2} has been synthesized by addition polymerization reaction. Polyurethane based on di-isocyanate monomer was

chosen for this purpose due to its various advantages over other polymer systems. N-methyl-D-glucamine was used as additional cross linker along with the bis phenol A (BPA) and phloroglucinol to bind selectively Mg^{+2} ions. The detailed procedure for imprinted and non-imprinted polymer is as below.

For imprinted polymer, 197 mg of BPA and 22.2 mg of phloroglucinol were dissolved in 300 µL of pyridine. 50 mg of $MgCl_2.6H_2O$ was dissolved in 100 µL of methanol and mixed with above cross linker solution to make a homogenous mixture avoiding any phase separation, name this solution **A**. 100 mg of diphenyl di-isocyanate (DPDI) along with 19.5 mg of N-methyl-D-glucamine was heated at 60 ℃ in 2 mL sample vial just for 20 seconds. After heating, 200 µL of pyridine was added immediately to sample vial to prevent gel formation. It was now mixed with the solution **A** to prepare final pre-polymer matrix which was heated at 70 ℃ for 1hour in water bath to complete the polymerization reaction.

Non-imprinted polymer was prepared by excluding the addition of Mg^{+2} ions in matrix **A** while rests of the steps are similar to those of imprinted polymer. After polymerization the imprinted and non-imprinted polymers are diluted appropriately with pyridine to prepare coating solutions.

4.3 Preparation of QCM

10 MHz QCM have been prepared following the same method as described in previous chapter section 3.4.1. Imprinted and non-imprinted polymer layers have been coated by spin coating methods at a speed of 3000 rpm. The coated QCM have been heated at 120 ℃ for at least 2 hours to dry layers. The layer heights of both channels have been noted by calculating the difference of frequencies before and after coating.
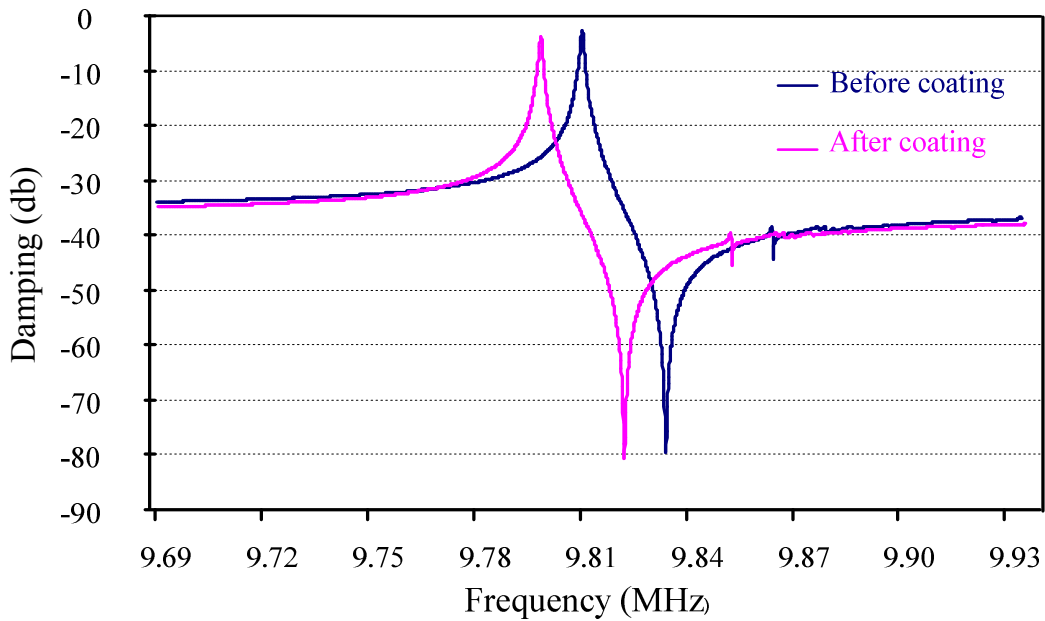
Figure 38: Damping spectra of QCM before and after coating the layers.

4.4 Cell Design

A special flow cell is designed for mass sensitive measurements as shown in the figure. In this cell QCM is exposed to water only from one side while other side remains in air. The cell has inlet and outlet for continuous flow of water which is maintained by ISMATEC MCP V5.21 pump at flow rate of 2 mL/min during measurement.
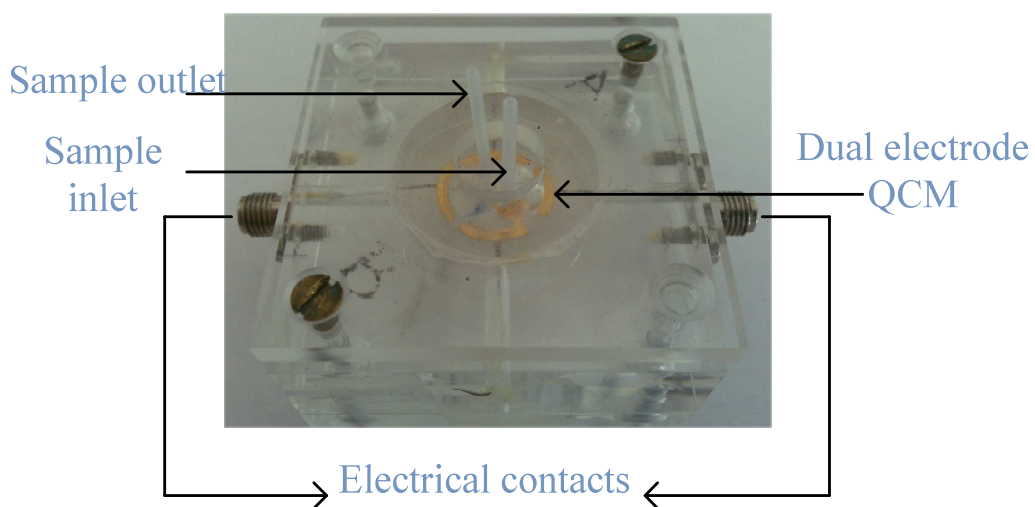

Figure 39: Flow cell used for metal ions detection in liquid phase.

4.5 Results and Discussion

4.5.1 Mass Sensitive Measurements

For mass sensitive measurements, a stock solution of 1.0 mM concentration was prepared by dissolving specific amount of $MgCl_2.6H_2O$ in de-ionized water. Further lower concentrations can be prepared by making suitable dilutions from stock solution. The coated QCM was placed in the cell and de-ionized water was passed through it at flow rate of 2mL per minute. It removes template ions from imprinted electrode generating very fine recognition sites which causes in frequency enhancement of this channel while for non-imprinted electrode there is not an appreciable frequency shift. The process is continued for a while unless equilibrium is developed between the flowing de-ionized water and electrode surface. As a result a stable base line is obtained. At this point 0.1 mM concentration of Mg^{+2} ions was passed through the cell that starts the accumulation of ions into the surface of imprinted channel which results a frequency shift from base line value. The non-imprinted channel does not show any significant change in its base line frequency. After running 0.1 mM concentration of Mg^{+2} ions for a while, cell is shifting again on de-ionized water. The frequency goes back to its original value that shows the reversible nature of the imprinted layer. The difference of frequencies between imprinted and non-imprinted channel appears to be the net sensor response.

Further higher concentrations have been passed through the cell to examine the linearity of the designed sensor as shown in the figure. The temperature is maintained at 25 ºC during the whole measurement. The sensor response Δf (Hz) is recorded as a function of time (min.) for all concentrations of Mg^{+2} ions. As from figure it was noticed that when system is shifted from water to metal ion solution, frequency immediately goes down which is due to the rapid inclusion of reactive metal ions into the layer material and conversely same is true when

69
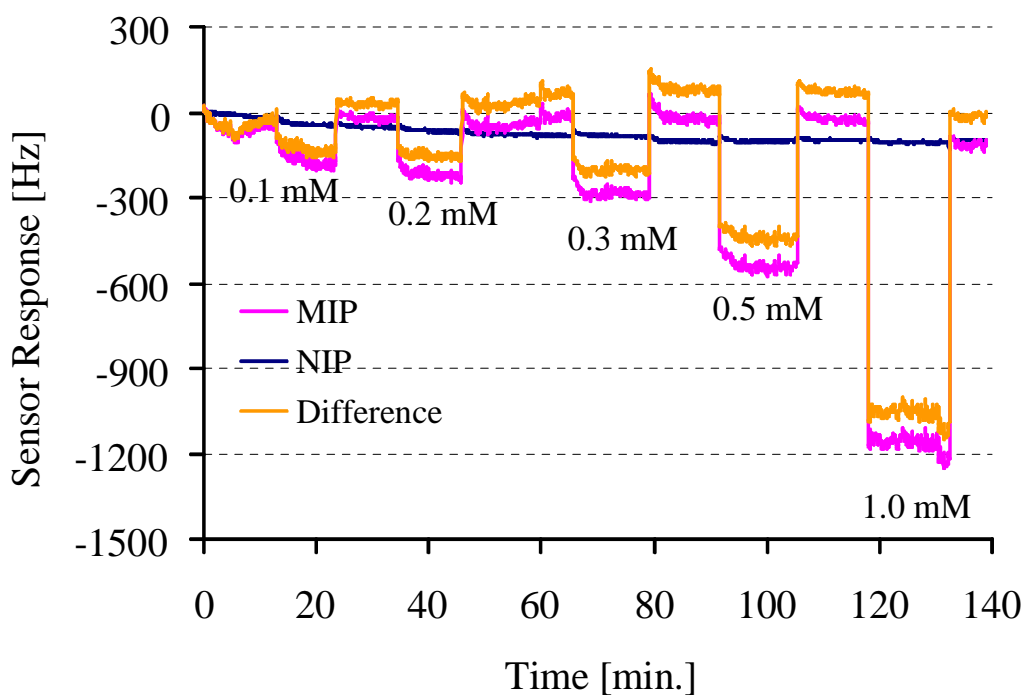
Figure 401: Sensor response of Mg^{+2} imprinted polyurethane layer to different concentrations of Mg^{+2} ions.

system was shifted on water again. It is obvious that each time from metal ions solution frequency comes back to its original value which shows two important features of the polyurethane layer. First is that it is fully reversible for higher and lower concentrations of metal ions and second is that the layer material is not washed away due to continuous flow of water. These are very important aspects while designing a commercial sensor because it provides long term stability.

4.5.2 Cross Sensitivity Measurements for other Alkaline Earth Metal Ions

The Mg^{+2} imprinted polyurethane layer had been expose to other alkaline earth metal ions such as Ca^{+2}, Sr^{+2} and Ba^{+2} ions in same molar quantities. The stock solutions for these ions were prepared from their hydrated chlorides salts. Mass sensitive measurements performed with different concentrations of Ca^{+2}, Sr^{+2} and Ba^{+2} ions are shown in figures given below.
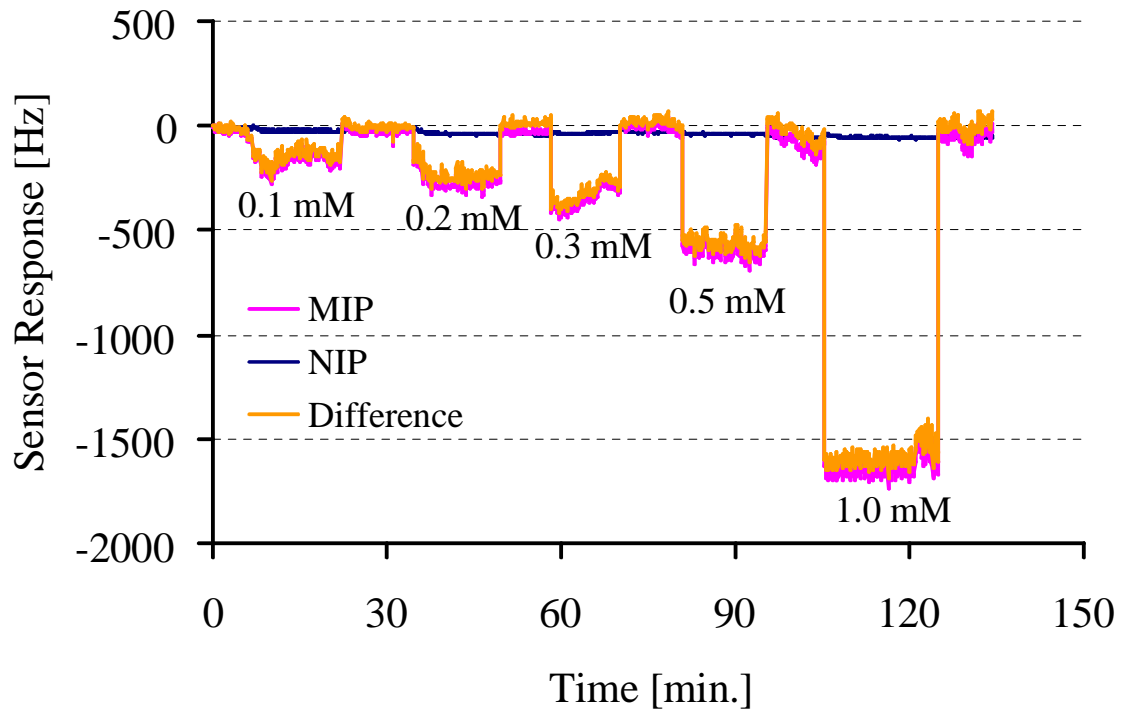
Figure 41: Sensor response of Mg^{+2} imprinted polyurethane layer to different concentrations of Ca^{+2} ions.
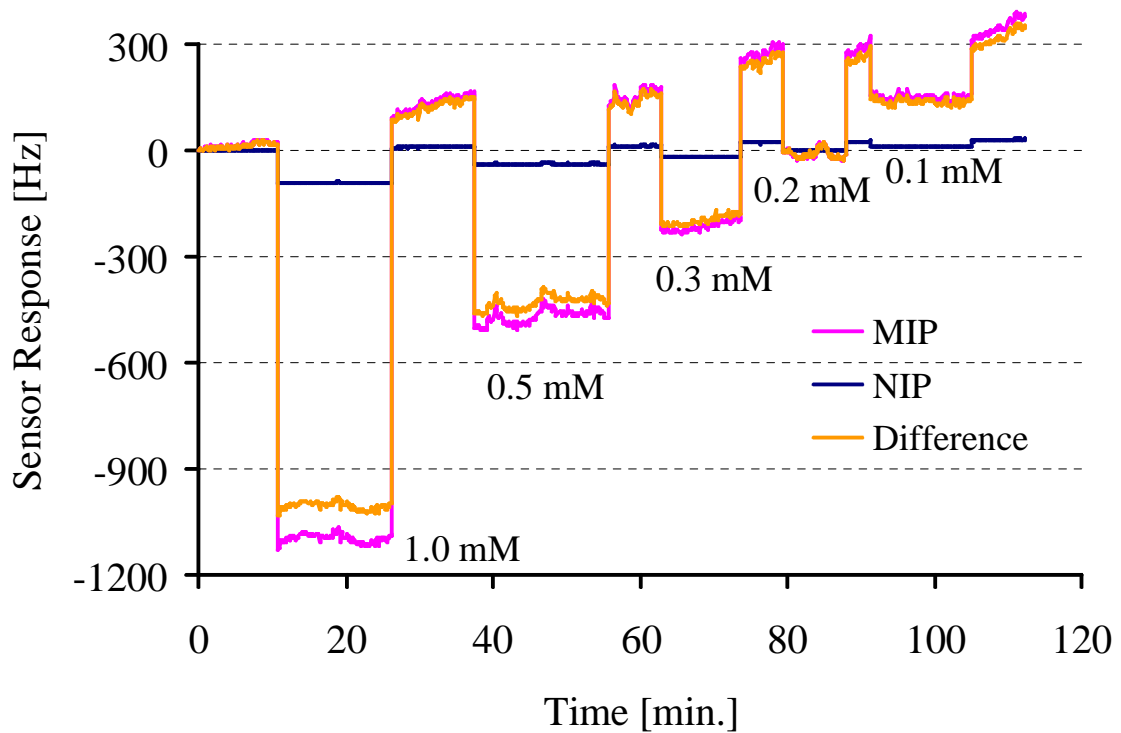

Figure 42: Sensor response Mg^{+2} imprinted polyurethane layer to different concentrations of Sr^{+2} ions.
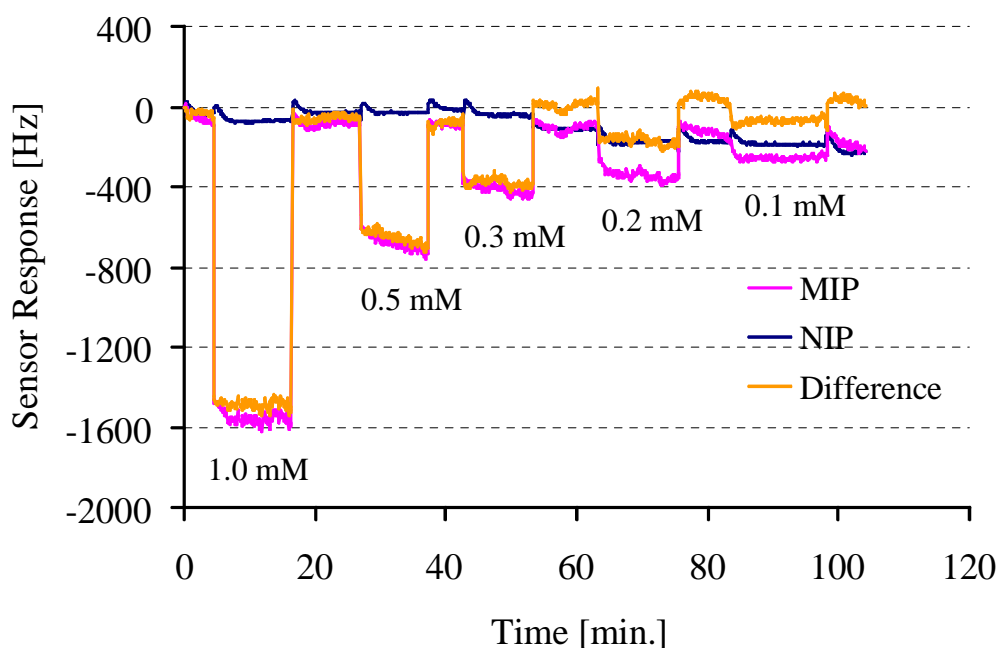
Figure 43: Sensor response Mg^{+2} imprinted polyurethane layer to different concentrations of Ba^{+2} ions.

The signal to noise ratio is very good in all mass sensitive measurements even for 0.1mM concentration. The sensor response of each metal ion is corresponding to their respective mM concentrations. Different metal ions possess different atomic weights, for example the solution of 1.0mM of Mg^{+2} ions contains less weight as compare to 1.0mM of Ba^{+2} ions although they have same molar concentrations. On the other hand transducer principal of QCM devices is based on mass loading of analyte on their surface. So, their respective sensor responses are not suitable for their cross sensitivity assessment. The problem can be overcome by dividing the sensor response of each metal ion on all concentrations to their respective atomic weights which is a better way to represent cross sensitivity comparison as shown in figure. The figure shows an excellent cross sensitivity pattern for Mg^{+2} imprinted polyurethane over other alkaline earth metal ions starting from 0.1mM to 1.0mM concentration levels. Cross sensitivity is one important aspect, while the other outstanding feature is linearity in sensor signal of this polymer system. This can be illustrated in the following figure.
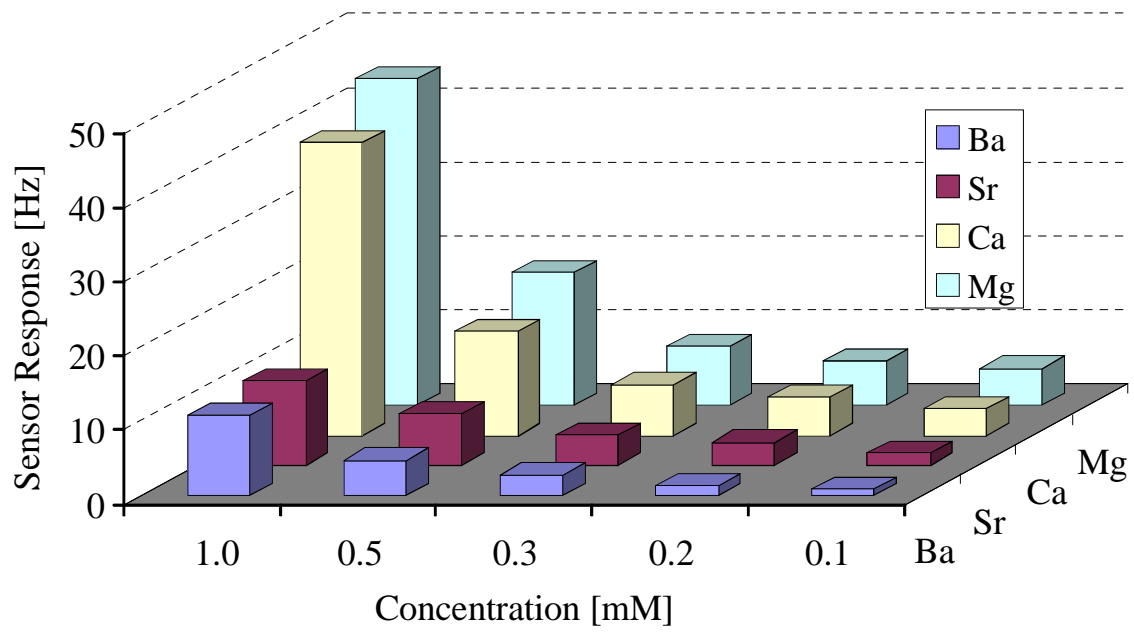
Figure 44: Comparison of sensor responses of Mg^{+2} imprinted polyurethane over other metal ions.
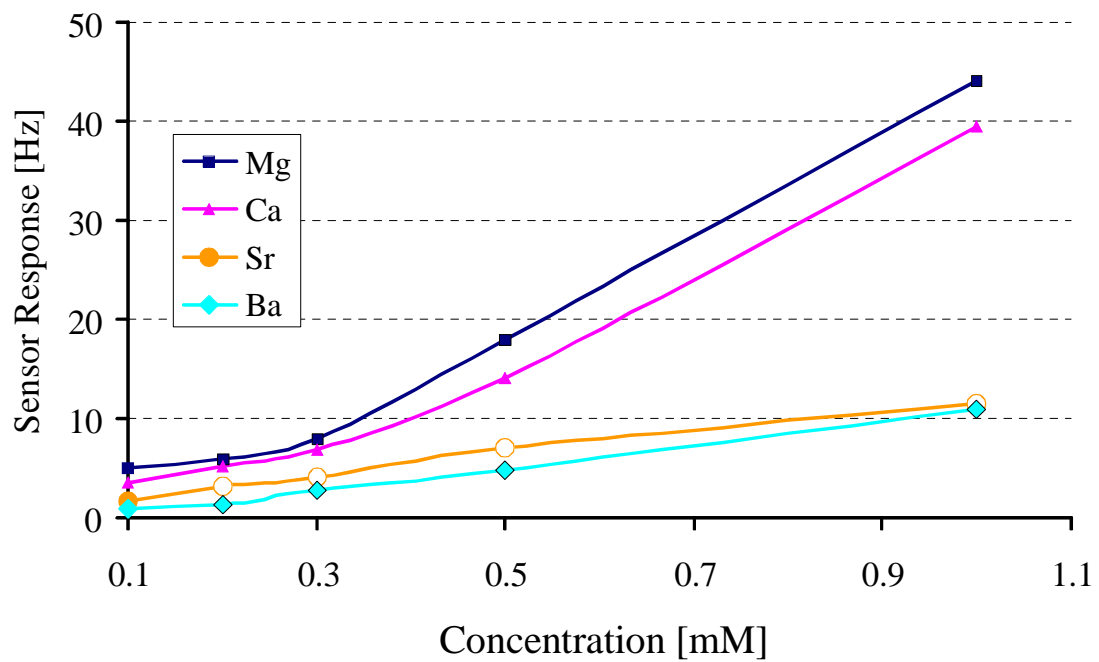
Figure 45: Sensor response of Mg^{+2} imprinted polyurethane layer showing the linearity at low concentrations.

The Mg^{+2} imprinted polyurethane layers have proven it highly competent

polymer system to design a sensitive and selective sensor. The only drawback is that this polymer scheme can not be extended for other alkaline earth metals such as Ca^{+2}, Sr^{+2} and Ba^{+2} due to certain reasons. For example, solubility of inorganic metal salts for ion imprinting is a serious issue because polyurethane system is based on pyridine which is purely an organic solvent that cannot dissolve larger metal ions. While in case of Mg^{+2} imprinting, the $MgCl_2.6H_2O$ is firstly dissolved in methanol and then brought to the rest of polymer system. This strategy is no more useful for imprinting the other alkaline earth metal salts. Even screening cannot be applied to these metal ions polymers because their salts are white in colour. A new polymer system is introduced starting from colored salts of metal ions preferably transition metals such as Ni^{+2}. It is based on vinyl pyrrolidone as monomer, N,N-Methylene-bis-Acrylamide as a cross linker and AIBN as an initiator. Different polymer schemes are proposed to design a selective system for Ni^{+2}ions that will be described in section 2.

Section 2

4.6 Synthesis of Ni^{+2} imprinted polymer

The Ni^{+2} imprinted polymers were synthesized by free radical polymerization reaction. For this purpose 10mg of N,N-Methylene-bis-Acrylamide (cross linker) was added in 90mg of vinyl pyrrolidone (monomer) in the presence of 1.2 mg of Azobisisobutyronitrile (AIBN) as an initiator in a vial, this matrix was named X1. 10 mg of $NiCl_2.6H_2O$ was dissolved in 50 µL of de-ionized water and then this template solution was added to matrix X1. The final mixture was heated at 70 ºC by constant stirring in a water bath until the gel formation started. This is very critical step because we have to stop the reaction at initial stage of gel formation otherwise the whole reaction mixture will be turned into a solid grains which are no more useful for coating the QCM. For synthesis of non-imprinted polymer, same process is followed as mentioned above simply excluding the template. The imprinted and non-imprinted polymer

layers have been coated on dual QCM following the same parameters including cell design, sensor setup and stock solution preparations as described in section 1 to proceed mass sensitive measurements.

4.7 Results and discussion

4.7.1 Mass sensitive measurements

Mass sensitive measurements were performed first with different concentrations of Ni^{+2} ions starting from highest concentration of 1.0 mM to lowest of 0.1 mM as shown in the figure.
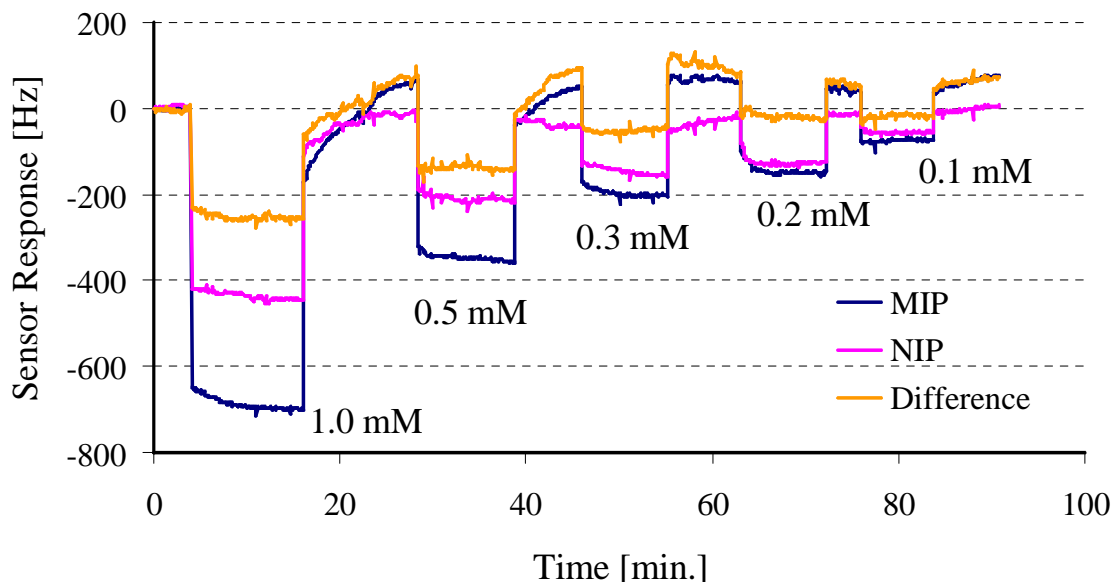
Figure 46: Sensor response of Ni^{+2} imprinted polymer layer to different concentrations of Ni^{+2} ions.

For cross sensitivity measurements, same set of concentrations of other heavy metal ions such as Co^{+2}, Cu^{+2} and Zn^{+2} have been passed through the cell. The stock solutions of these ions were prepared from $CoCl_2.6H_2O$, $CuSO_4.5H_2O$ and $ZnCl_2.2H_2O$ respectively. Their respective sensor responses have been shown in following figures.

75
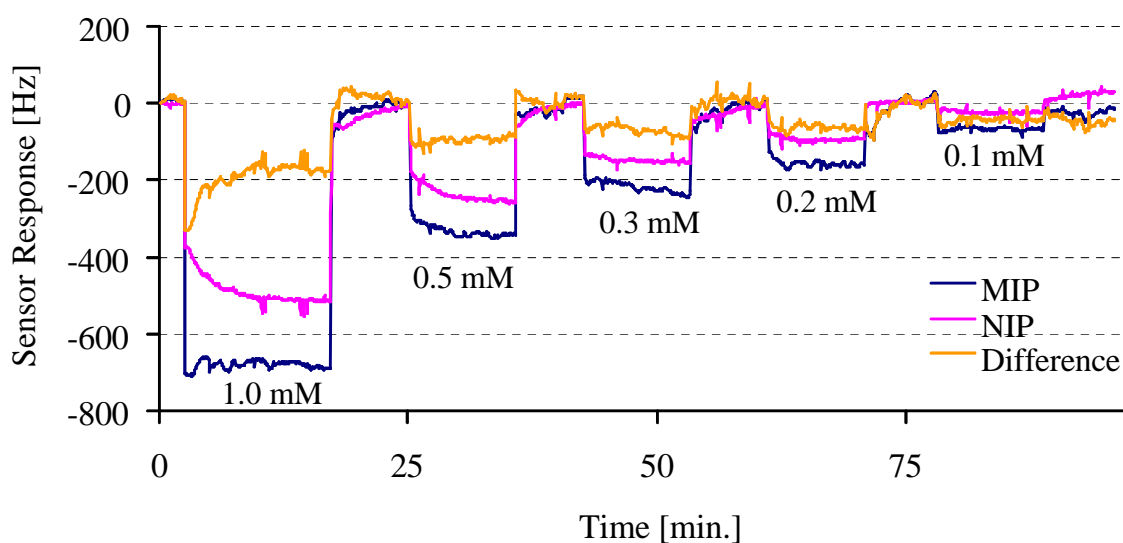
Figure 47: Sensor response of Ni^{+2} imprinted polymer layer to different concentrations of Co^{+2} ions.

In these entire curves, the measurement has been started from higher concentration because sometimes the base line is not stable at beginning and lower concentrations are not suitable to proceed. The selectivity trend can be demonstrated by plotting the sensor response for different concentrations of respective metal ions as shown in figure.
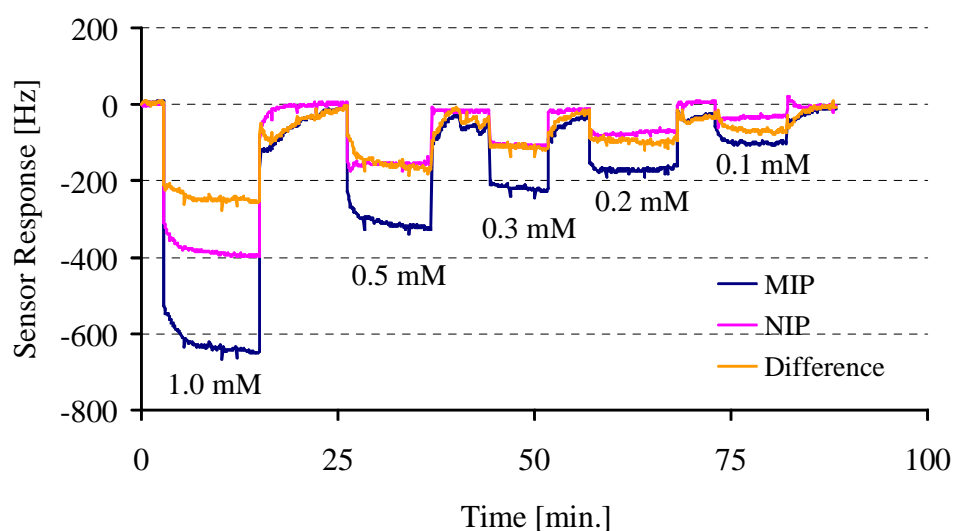

Figure 48: Sensor response of Ni^{+2} imprinted polymer layer to different concentrations of Cu^{+2} ions.
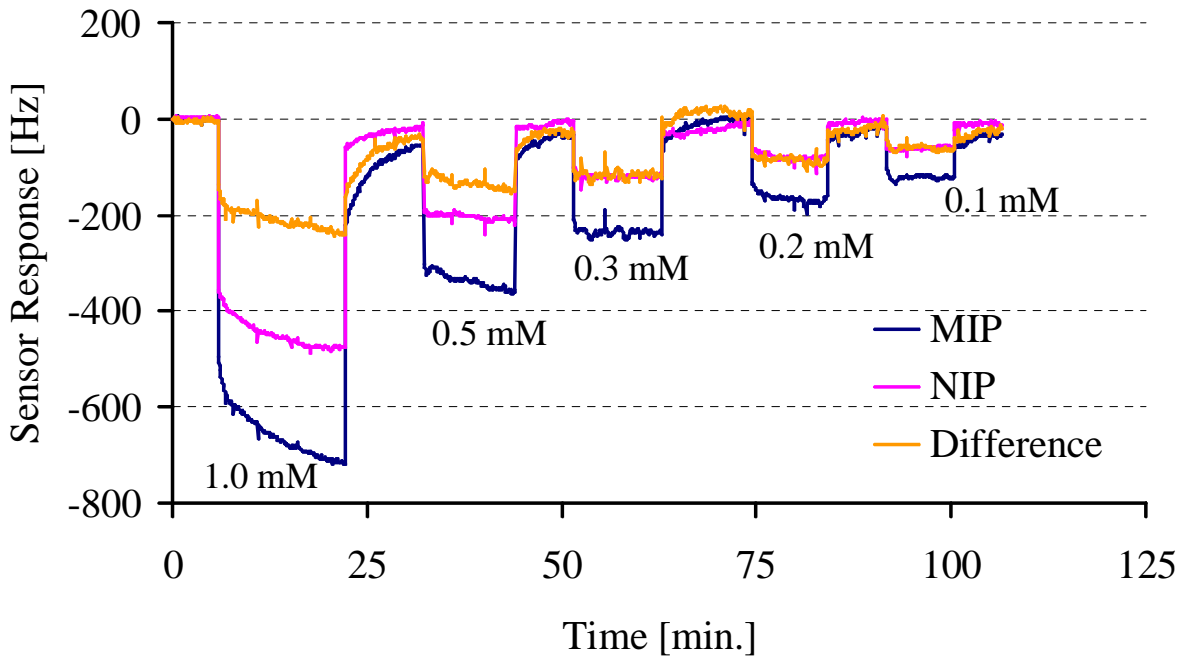
Figure 49: Sensor response of Ni^{+2} imprinted polymer layer to different concentrations of Zn^{+2} ions.
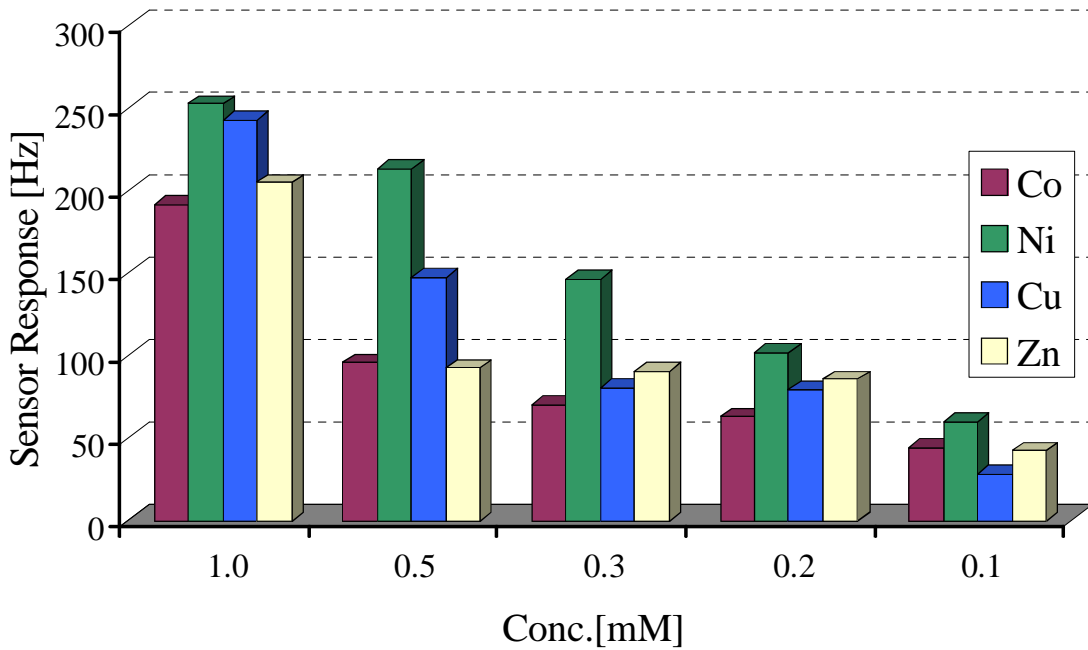

Figure 50: Comparison of sensor responses of Ni^{+2} imprinted polymer over other metal ions.

The graph shows relatively high cross sensitivity pattern for other heavy metal ions solutions but however it is selective for Ni^{+2} ions. It has been noticed that the selectivity trend is more pronounced at 0.1mM which is a remarkable feature of the sensor system to respond at extremely low concentration levels. Ni^{+2} has approximately similar molar mass as that of Co^{+2} but is about 8 and 11% lighter to Cu^{+2} and Zn^{+2} respectively. Considering the molar masses of these heavy metal ions, selectivity can be tuned by dividing the sensor response of each metal ion to their respective atomic weights. In this way the selectivity is further improved.

The successful polymer system is put under observation to improve further selectivity pattern. For this purpose the synthetic strategy is modified by varying the monomer template ratios keeping other parameters and reaction conditions constant. In the first experiment the monomer (vinyl pyrrollidone) and the cross linker (N,N-Methylene-bis-Acrylamide) ratio was [90:10] which is modified now by introducing new ratios as [85:15] and [95:5] respectively.
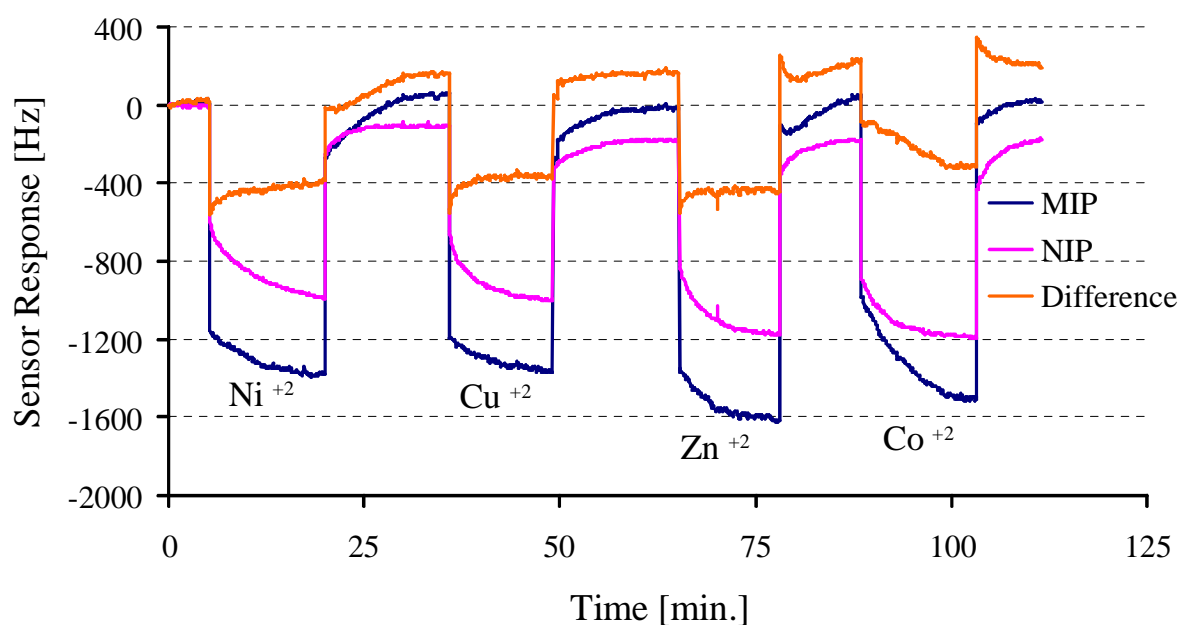

Figure 51: Sensor response of Ni^{+2} imprinted polymer [85:15] layer to 1.0mM concentrations of Ni^{+2}, Cu^{+2}, Zn^{+2} and Co^{+2} ions.

The first modified polymer recipe [85:15] was synthesized keeping all the experimental conditions identical. QCM have been prepared following same protocol as mentioned above to proceed the mass sensitive measurements. 1.0mM solution of all metal ions, Ni^{+2}, Cu^{+2}, Zn^{+2} and Co^{+2} have been passed through the flow cell and their respective sensor responses are presented in figure 52.

It is evident from above result that the net sensor response of Ni^{+2} is almost similar to rest of the metal ions which suggest that selectivity is vanished. The measurement was not stopped at this concentration but it was extended to further lower concentration from 0.5mM to 0.1mM level to confirm this effect. The results of all measurements can be summarized in the following graph. This graph clearly indicates distortion in selectivity pattern of Ni^{+2} ions over other metals.
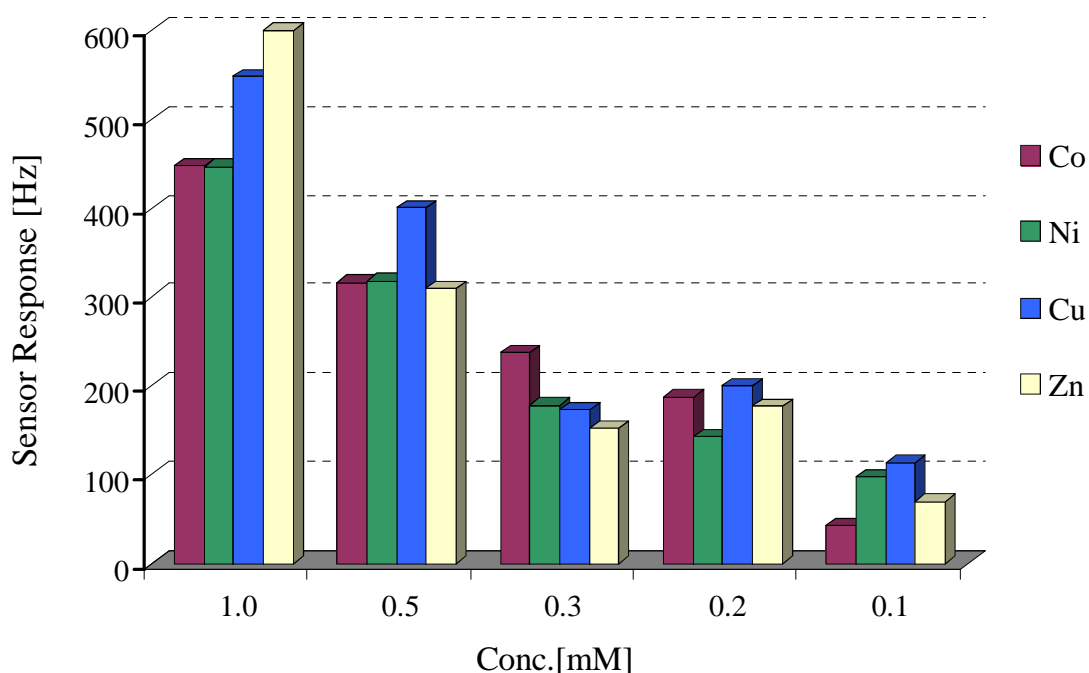
Figure 522: Comparison of sensor responses of Ni^{+2} imprinted polymer [85:15] layer over other metal ions.

The one obvious reason for this distortion is that these metal ions have very close ionic radii in picometer range e.g. Ni^{+2} ,Cu^{+2}, Co^{+2} and Zn^{+2} have ionic

radius of 69, 73,74.5 and 74pm respectively. Keeping in mind the closeness in the size of metal ions, any change in polymer composition makes serious impact on selectivity of the system. Similarly the selectivity pattern is also destroyed when [95:5] is tested under the same conditions.

Molecular Recognition of Anthracene through double Imprinting

5.1 Introduction

The class of hydrocarbons which composed of two or more fused aromatic rings resulting from incomplete combustion of organic matter is called polycyclic aromatic hydrocarbons (PAHs[45]). Additionally, these complex compounds do not have any hetero atom or substituent. In environment, the major sources of PAHs are burning of carbon containing substances such as wood, fuel oil, coal tar and road asphalt etc. The emissions from various chemical industrial plants exhaust from automobile vehicles and smoke of burning tobacco contain considerable high level of PAHs. The combustion of engine oil also produces a series of different PAHs which are exhausted into air. Production of these hydrocarbons depends upon the burning temperature of organic substances; low temperature burning produces more PAHs while fewer PAHs are produced at higher temperature. The exposure of PAHs to human body takes place in different ways like, breathing, drinking and skin contacting. The most dangerous source of exposing PAHs through breathing is smoking, and working in polluted environment of petrochemical industrial exhaust. Ash particles also contain some traces of PAHs which can reach to lungs causing cancer through breathing. They may absorb in skin causing allergy during handling of contaminated samples of soil and usage of certain medicated creams containing these compounds. Contamination of PAHs in drinking water is really a serious problem. Improper disposal of industrial waste water to crops and fields is very dangerous, because it can directly reach to ground water. The maximum contaminant level (MCLs) of public drinking water for total PAHs concentration is 0.2 ppb[46] to minimize the risk of adverse health effects.

Once the PAHs entered in the human body, their extraction becomes really difficult as they are highly hydrophobic in nature and on the other hand possesses great affinity towards lipids. This typical behavior of PAHs makes them to interact with DNA[47] structure influencing on its smooth functioning which can lead to serious damage ultimately causing cancer. Some of the PAHs have been shown in the following figure 53.
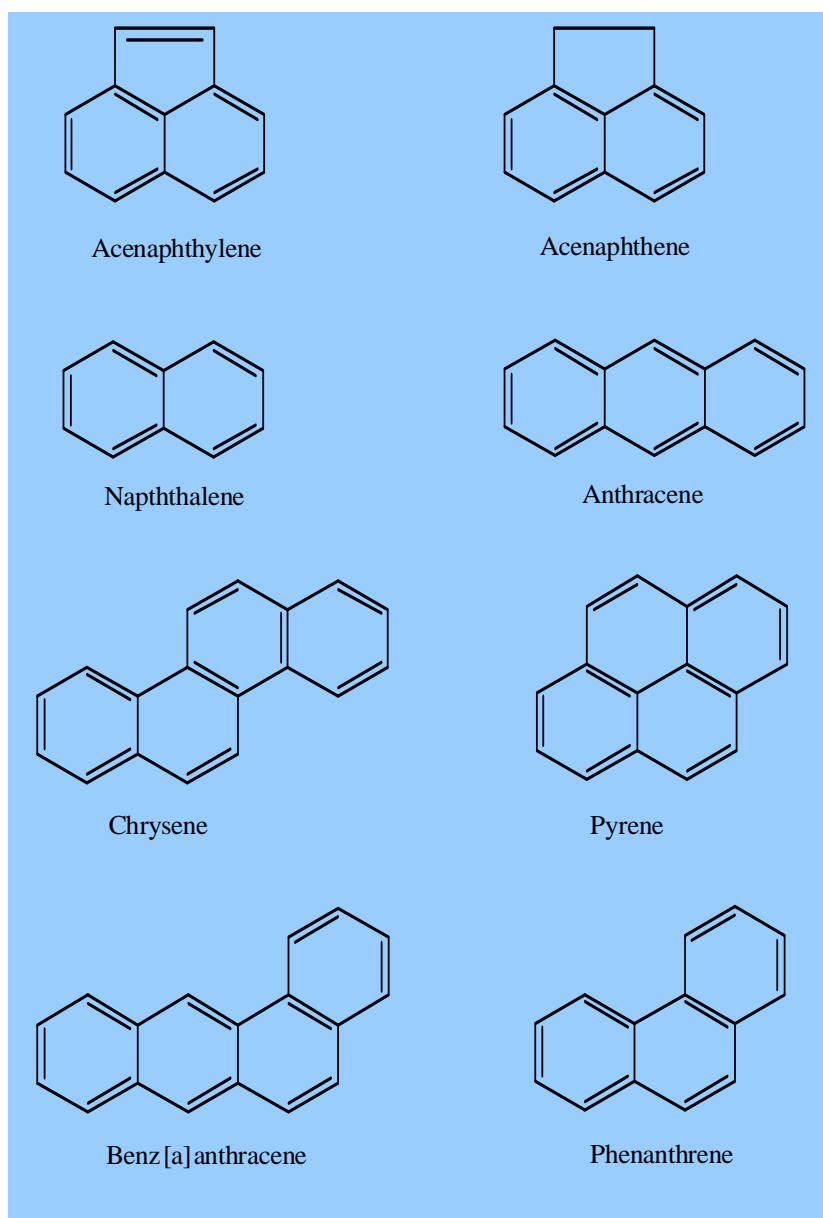

Figure 53: Structure of Different PAHs.

5.2 Literature Review

Monitoring of toxic and carcinogenic PAHs[48] is very important in environmental analysis especially in liquid media concerning drinking water. With the help of fluorescence spectroscopy[49,50] they can easily detected in visible range. But the fluorescence intensity is reduced in aqueous solutions due to the presence of quenchers such as humic acid, often present on surface water samples. This problem has been overcome by introducing some sensitive layers which selectively take up the specific analyte from water sample. For continuous monitoring of PAHs concentration in water, now it has become possible to perform the fluorescence measurements with high sensitivity and selectivity.

These sensitive layers can be combined with some other transducer like mass sensitive devices or fiber optics leading to development of powerful sensor systems. Molecular Imprinted Polymers (MIPs)[51] are very promising materials in design of chemical sensors of high selectivity and sensitivity. Molecular Imprinting is a very straight forward technique by which one can efficiently extract the analyte molecules even from complex matrices. In this way we can generate synthetic antibodies that have specific characteristics towards a certain analyte.

In imprinting the analyte molecules are directly added along with monomers in a solution and polymerized under certain conditions. As in case of PAHs, they do not possesses high functionality so the imprinting process is carried out considering all non-covalent interactions like Van der Waals forces[52]. It is very advantageous to use non-covalent imprinting method, because then it is not necessary to develop any sort of linkage between template and monomer. During polymerization monomer units combine with the cross linker and adjust their orientation around the added template molecules. After polymerization the template molecule is removed by heating or washing from the polymer layer which has been immobilized on transducer surface. The removal of template

leaves behind specific cavity structures which are analogous to shape of a distinct analyte. Now these synthetically designed materials act as a recognition element for selective re-inclusion of the target analyte.

In the case of PAHs, polyurethane has proven itself highly efficient for the imprinting procedures, as these polymers are rigid, robust and stable which cannot be dissolved by both organic and inorganic solvents. Furthermore, by varying the polymerization conditions like monomer cross linker ratio, amount of template, temperature and solvent, an optimized polymer of desired application can be achieved.

The sensitivity and selectivity of PAHs can be enhanced by introducing mixture of templates comprising of one larger and one smaller molecule, which is called double imprinting[59]. The idea of double imprinting introduces a new dimension in material design in more elegant way. It is a novel concept in sensor systems for improving the selectivity in detection of PAHs and off course the sensitivity has also been increased by a factor of five. In combination of two templates, imprinting procedures helps us to construct the highly suitable hollow cavities and provide excellent diffusion pathways for selective re-inclusion of analyte molecules.

In detection of PAHs, fluorescence technique is highly sensitive but the sensitivity is highly influenced by the quenchers present in aqueous media, where as the QCM devices gives a direct change in frequency corresponding change in mass of the layer due to analyte incorporation. In comparison of fluorescence spectrometer, quartz crystal microbalances combining with suitable layers are well suited transducers for the faster, cheaper and more sensitive and selective for environmental analysis[53].

Our focus in this work is the detection of anthracene at lower ppb range using fluorescence and QCM devices.

5.3 Experimental Section

In this section different imprinted polymers have been synthesized and put under fluorescence spectrometer to find out the suitable surface for the selective up take of anthracene from water. The designed optimal polymer layer for anthracene has been taken from fluorescence to quartz crystal microbalances and further tested. To perform fluorescence measurements, the basic characteristics of Anthracene along with some other PAHs have been listed below in table 2.

Table 2: Characteristics of different PAHs.

PAHs	Symbol	Excitation (nm)	Emission (nm)	Water Solubility (µg/L)
Acenpapthene	ACP	255	336	3470
Anthracene	ANT	250	380	70
Chrysene	CHR	320	418	2
Phenanthrene	PHE	255	365	1290
Pyrene	PYR	340	371	140
Naphthalene	NAP	275	356	31000

The scans for Anthracene have been recorded in both aqueous and organic solvent like cyclohexane on fluorescence spectrometer *Perkin Elmer LS-50B instrument*. From fluorescence spectra it is clear that the peaks are very sharp and distinct λ_{max} in cyclohexane while in water which is a more polar solvent the peaks are broadened as shown in figure 54 and 55 respectively. To design an optimal imprinted layer, the polymerization conditions like solvent, template ratio, selection of cross linker, solvent and temperature are varied and their corresponding results are compared.
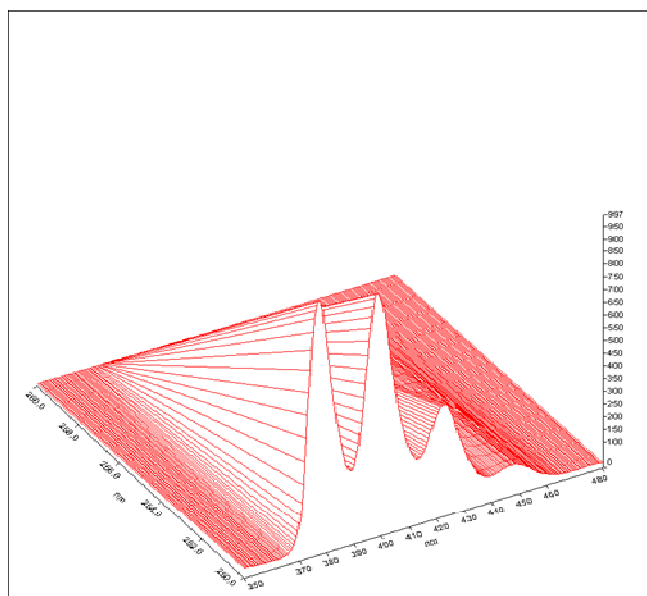
Figure 54: 2D fluorescence spectrum of anthracene in cyclohexane.
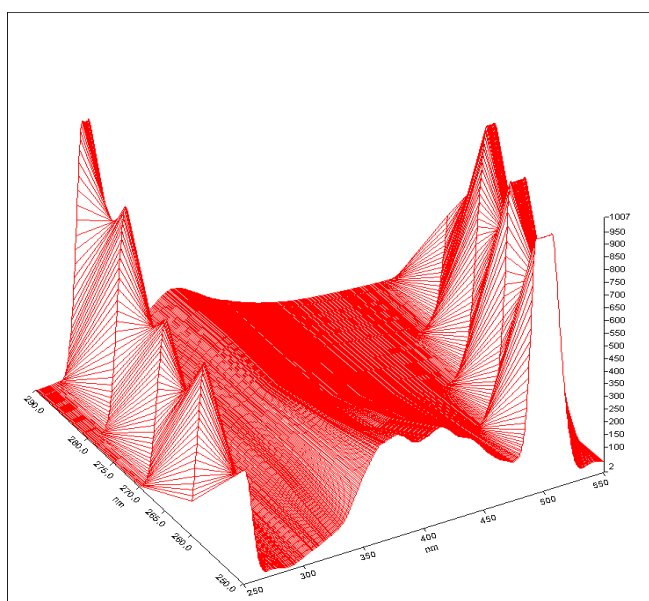
Figure 55: 2D fluorescence spectrum of anthracene in distilled water.

To prepare polyurethane, 100 mg of diphenyl methane diisocyanate (DPDI) as monomer and 100 mg of polyethylene glycol (PEG) [M.W. of 200 gm/mol] as a cross linker has been dissolved in 1000 µL of tetrahydrofuran (THF) separately.

For double Imprinting, different template ratios have been prepared comprising of Anthracene and Naphthalene. They all have been named from S1 to S5 and dissolved in 1000 μL of THF. Now 455 μL from monomer (DPDI) solution and 545 μL of cross linker (PEG) solution have been mixed in clean sample vial along with 50 μL of each template solution and have been polymerized at 70 °C for 30 minutes. For comparison a non imprinted sample has also been prepared in which template solution was not added, it is called SN. After polymerization, layers have been coated on glass slides of dimensions 1×2 cm and have been dried over night at room temperature. Template molecules were removed from the layer material by heating it at 90°C for 2 hours.

5.4 Results and Discussion

5.4.1 Temperature and Heating Time

To ensure the complete removal of template, fluorescence emission spectra of anthracene had been recorded in which no peaks were found in the mentioned range. These quartz slides were dipped over night in anthracene solution of conc. 10 μg/L to examine the re-inclusion effects. Under the same parameters fluorescence spectrum was obtained after drying the glass slides taken from anthracene solution at room temperature. A comparison of these two spectrums, after removing template and after re-inclusion has been compared in the following figure 56. The spectrum clearly shows that there is no appreciable up take of anthracene from the 10 μg/L solution by the polymer layer which was heated for only 30 minutes.

A similar protocol was followed for the synthesis of a new set of polyurethane layers keeping all the conditions same except the heating time which is changed from 30 minutes to 1 hour. Now the above mentioned procedure is repeated to monitor the removal and re-inclusion effects and the spectrum obtained is as follows in the figure 56.
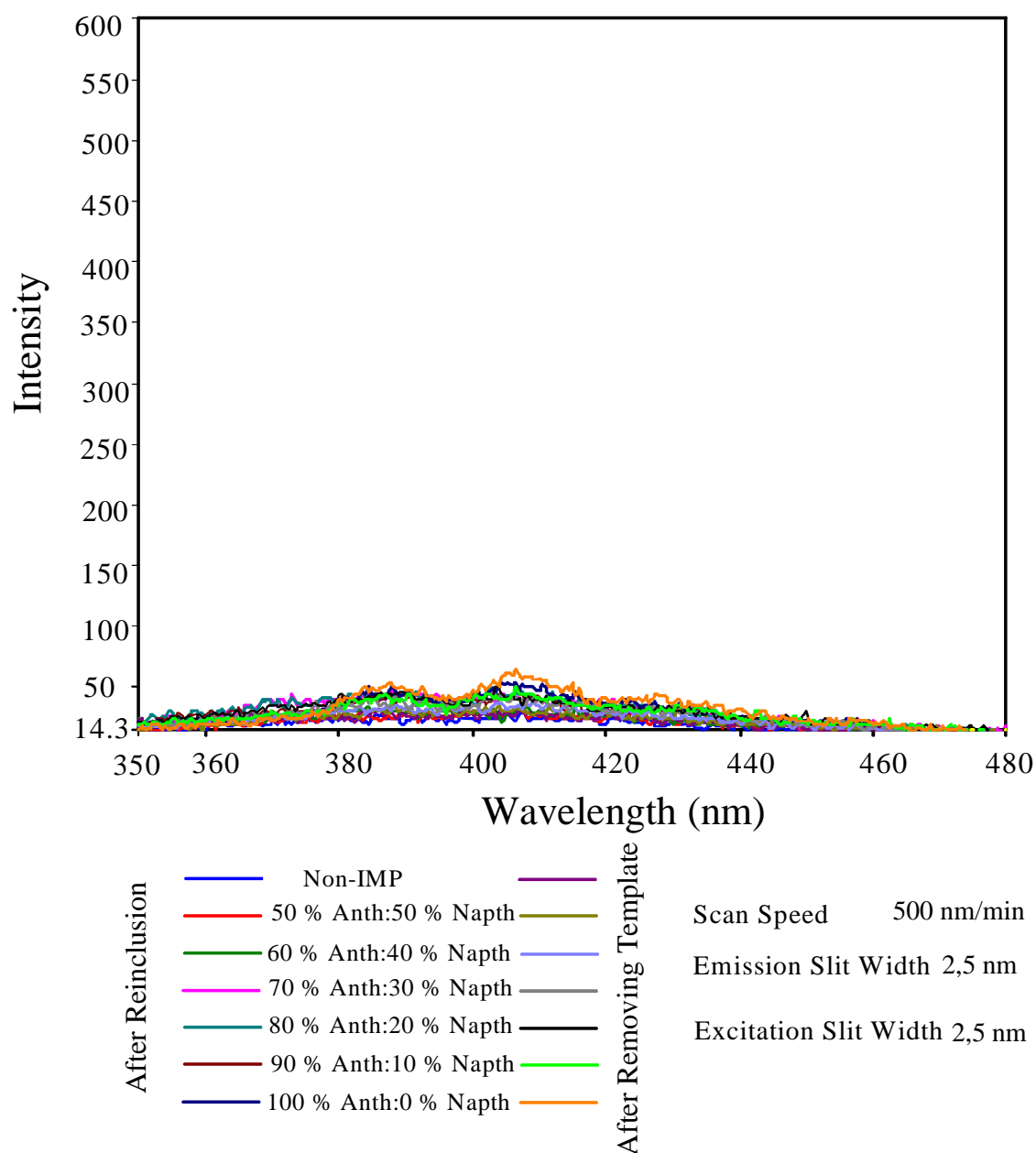
Figure 563: Fluorescence spectrum of polyurethane layer heated for 30 minutes for re-inclusion effects.

This clearly suggest that in the first case heating time of polyurethane was not enough to polymerize the matrix while when the heating time was changed from 30 minutes to 1hour then the extraction ability of layer material has been enhanced and it has been shown in the following graph.

After Reinclusion

- Non-IMP
- 50 % Anth:50 % Napth
- 60 % Anth:40 % Napth
- 70 % Anth:30 % Napth
- 80 % Anth:20 % Napth
- 90 % Anth:10 % Napth
- 100 % Anth:0 % Napth

After Removing Template

Scan Speed	500 nm/min
Emission Slit Width	5,0 nm
Excitation Slit Width	5,0 nm
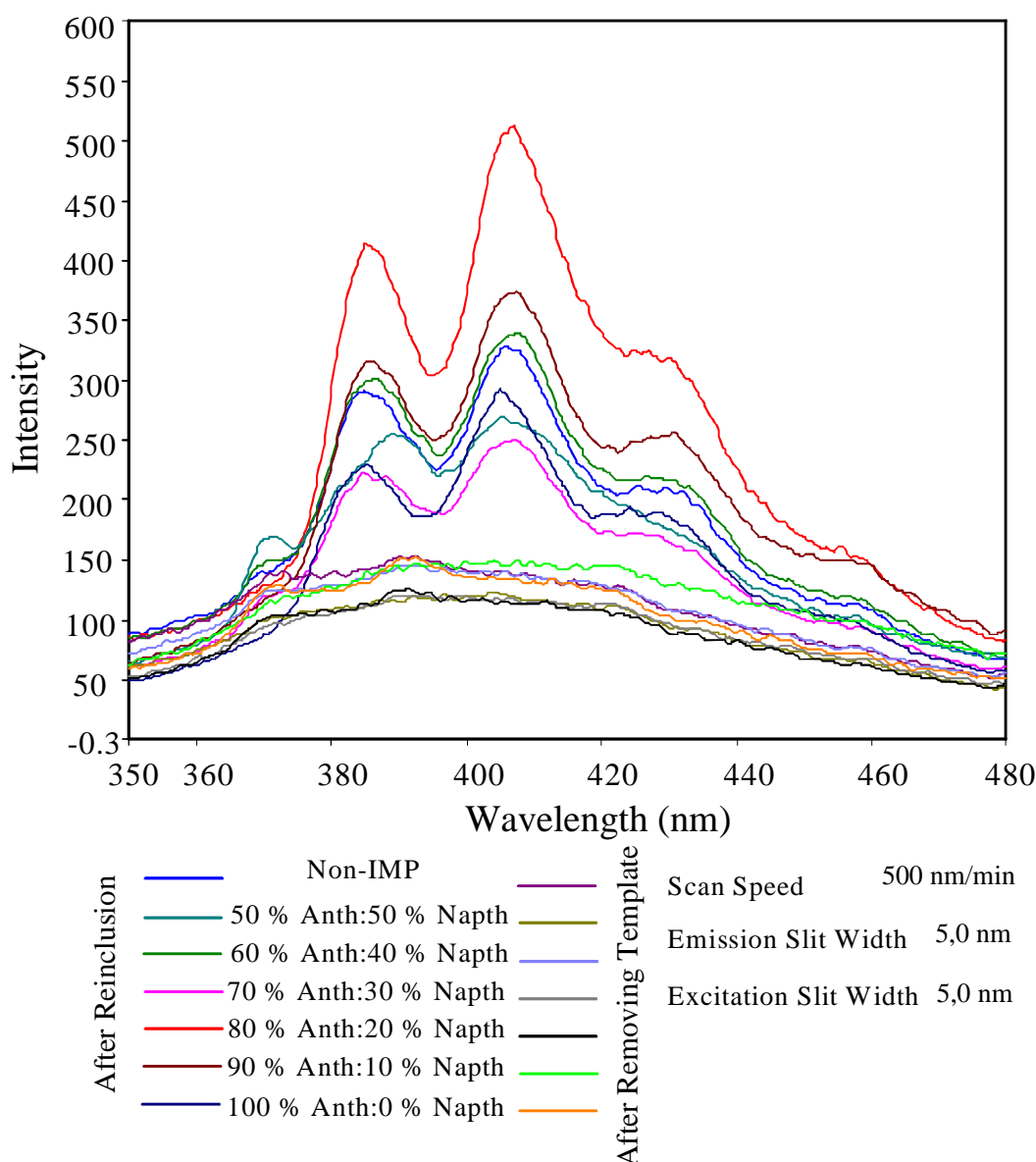
Figure 57: Fluorescence spectrum of polyurethane layer heated for 1 hour for re-inclusion effects.

5.4.2 Monomer and Cross Linker Ratio

In order to find out the optimal ratio of monomer (DPDI) to cross linker (PEG) in two different solvent such as pyridine and tetrahydrofuran, a series of different polymers have been synthesized which were named depending upon solvent systems mentioned in table 3. The results obtained are presented in the figure 58 and 5p for pyridine and THF respectively.

Table 3: Different compositions of monomer to cross linker ratios in two diff. solvents.

| Sr. no.	Solvent [Pyridine]	Solvent [THF]	DPDI (µL)	PEG (µL)
1	P1	T1	450	550
2	P2	T2	500	500
3	P3	T3	550	450
4	P4	T4	600	400
5	P5	T5	650	350
6	P6	T6	700	300
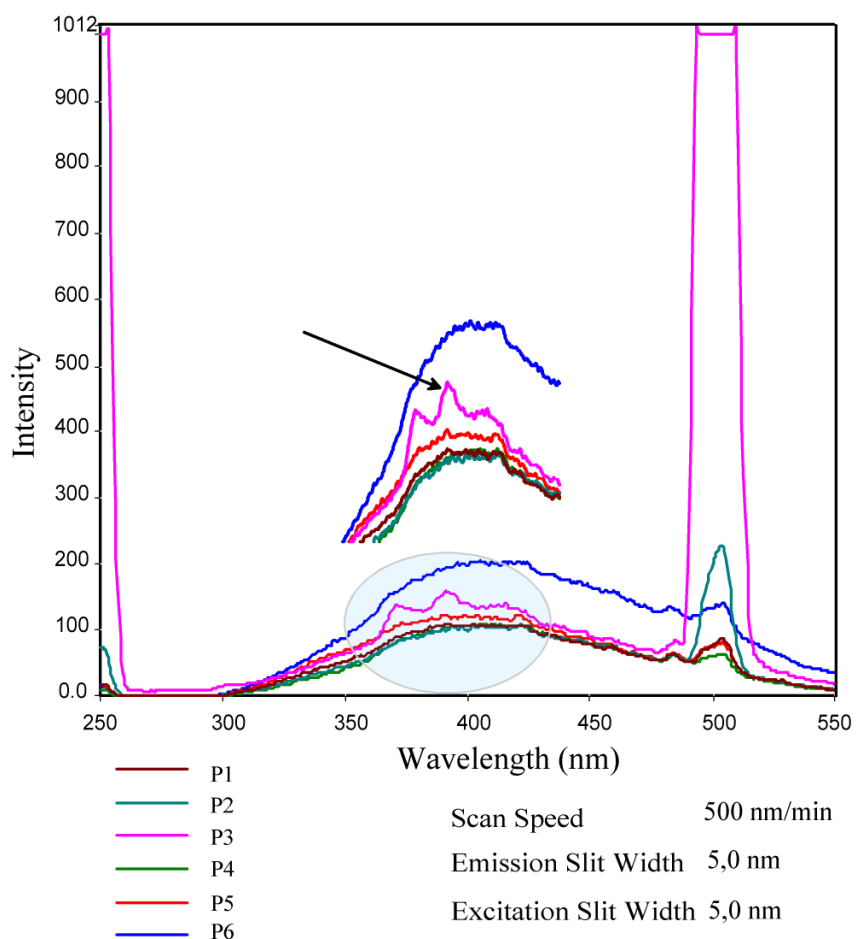
Figure 58: Fluorescence spectrum of polyurethane layer heated for 1hour for re-inclusion effects of Pyridine solvent system.
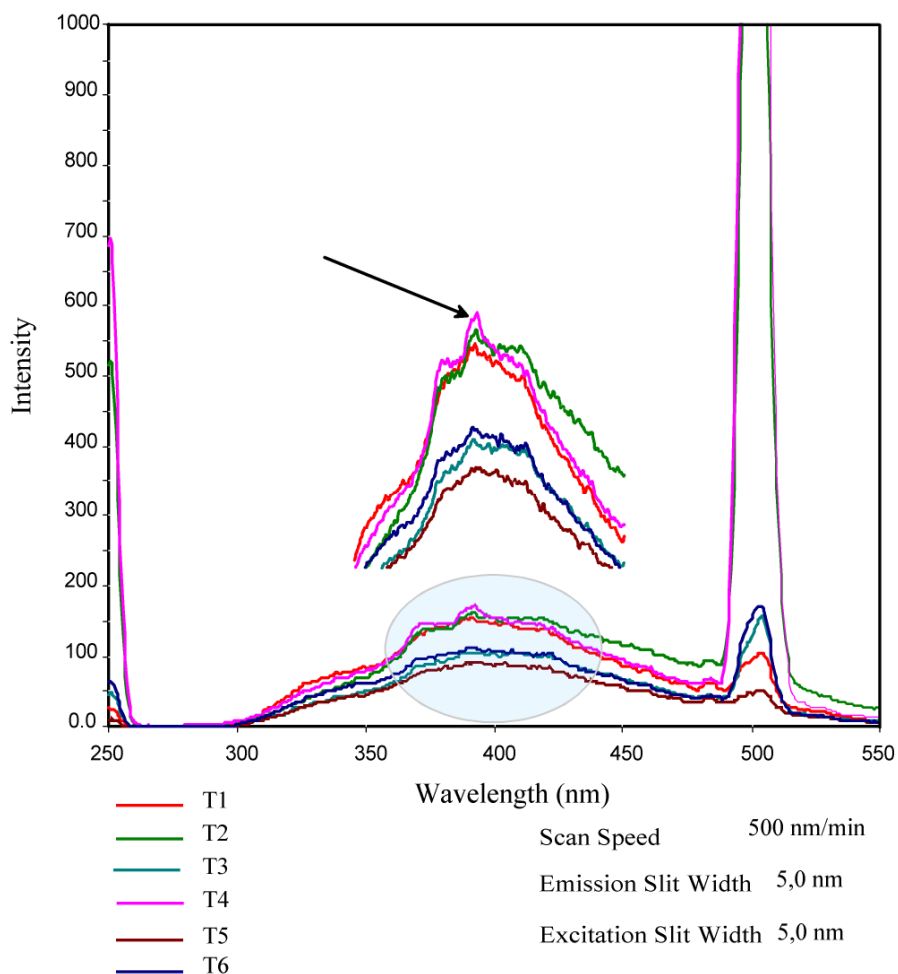
Figure 59: Fluorescence spectrum of polyurethane layer heated for 1 hour for re-inclusion effects of Tetrahydrofuran system.

From graph it is clear that the P3 and T4 solvent systems are best among others for re-inclusion of anthracene from water sample which help us to design optimal monomer to cross linker ratio. Furthermore comparing the results of P3 and T4, pyridine is slightly better solvent than tetrahydrofuran.

5.4.3 Selection of Template Mixture

The idea is to optimize the technique of double imprinted, for this purpose three different template mixture have been proposed for detection of anthracene. Already developed polymerization conditions concerning temperature, heating

time, monomer to cross linker ratio and suitable solvent system were followed. The three different templates along with anthracene are naphthalene, acenaphthene and pyrene respectively. For the selection of best template mixture the polymer layer is characterized by time drive fluorescence emission spectrum instead of simple scan.

In time drive spectrum, a fine polymer layer is exposed to fluorescence light and an analyte solution is run through it by continuous pumping, during this procedure the fluorescence intensity is monitored by the function of time. This gives us a better picture not only about the selective uptake of anthracene from water solution by the surface material but also concerning the reversibility of the polymer layer. A special Teflon cell was constructed for this purpose shown in figure 60.

The mechanism of these wave guides is very simple as an incident light falls on the sensitive layer immobilized on glass surface and sends the fluorescence information at an angle of 90° to the detector. So the glass slide on which the layer material is deposited actually acts as planner wave guide as shown in figure to which fluorescence emission is coupled and the data is transferred to detector.
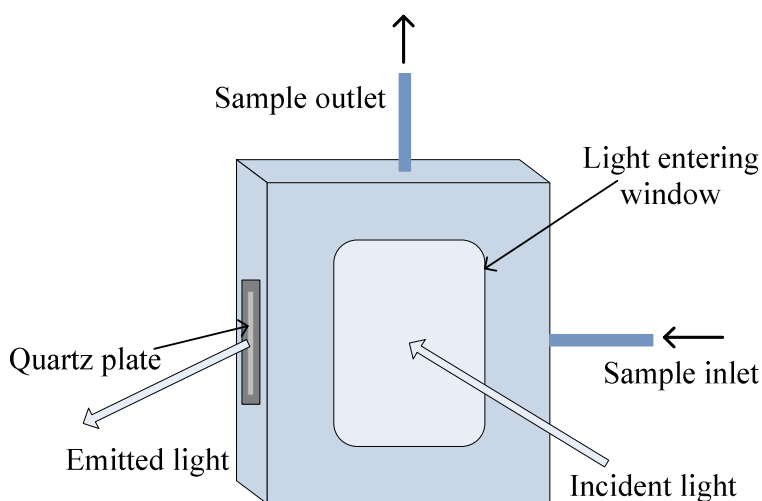

Figure 60: Picture of the fluorescence cell used for the measurements; illustrating the structure and working principle of a planar waveguide.

To get higher sensitive signal glass slide can be replaced with quartz sheet, but before performing the actual measurements, a normal emission scan of both glass and quartz slide were made just to check that there is not any glass or quartz material interference with the original fluorescence data. The scan was performed with empty flow cell, quartz, glass and the analyte solution; results obtained were compared in figure 61.
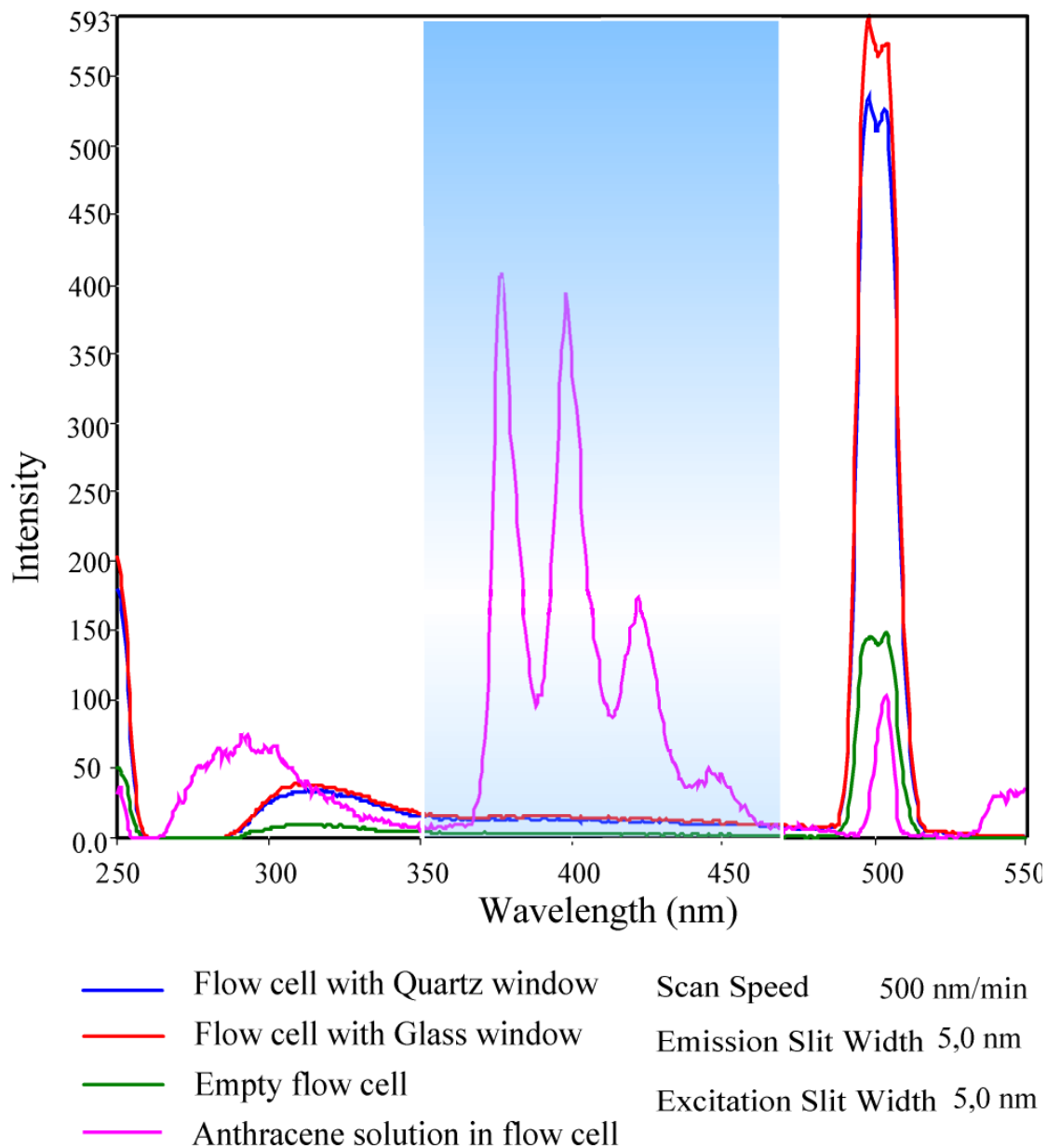

Figure 61: Comparison of fluorescence scans of glass, quartz and anthracene solution in flow cell.

The time drive measurements were performed with three different layers, are presented as follows starting from anthracene: naphthalene, anthracene: pyrene and finally anthracene: acenaphthene from figure 62 to 63 under different concentrations that were run through the cell.
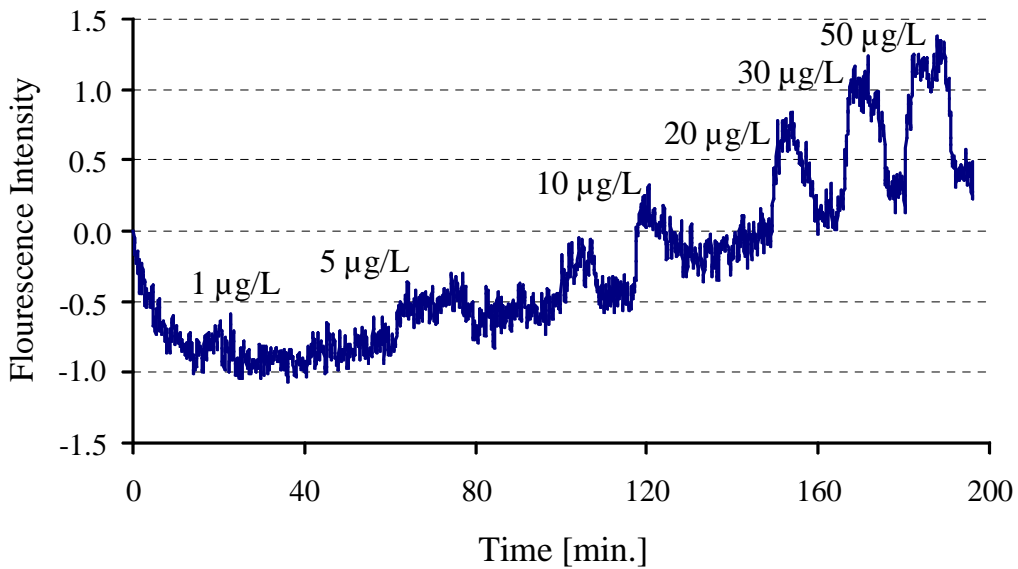
Figure 62: Fluorescence Time drive spectrum of polyurethane layer (Anthracene 80 %: Naphthalene 20 %)
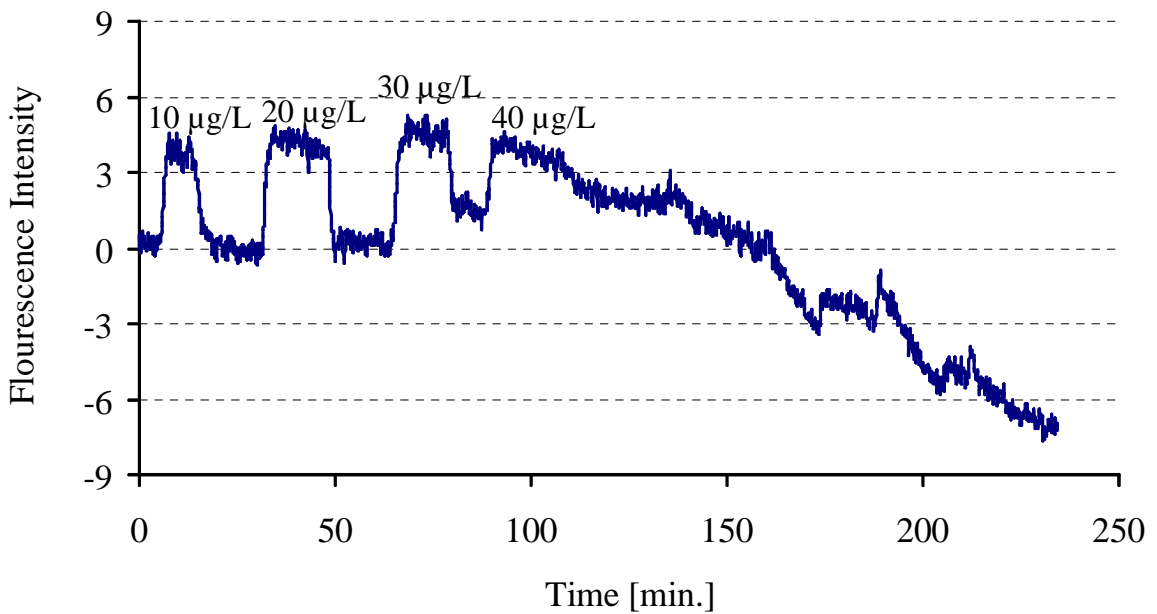
Figure 63: Fluorescence Time drive spectrum of polyurethane layer (Anthracene 80 %: Pyrene 20 %)
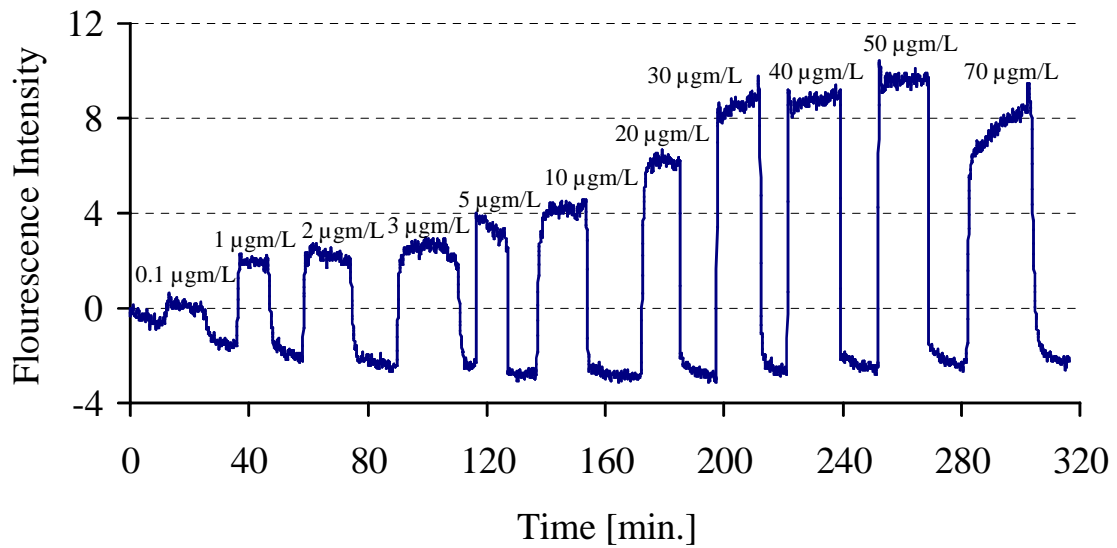
Figure 64: Fluorescence Time drive spectrum of polyurethane layer (Anthracene 80 %: Acenaphthene 20 %)

Among all the above spectrums, anthracene: acenaphthene template pair found to be best. A concentration dependant curve for this polymer layer in figure 5.9 has been drawn explaining the linearity of the fine film even at higher concentrations.
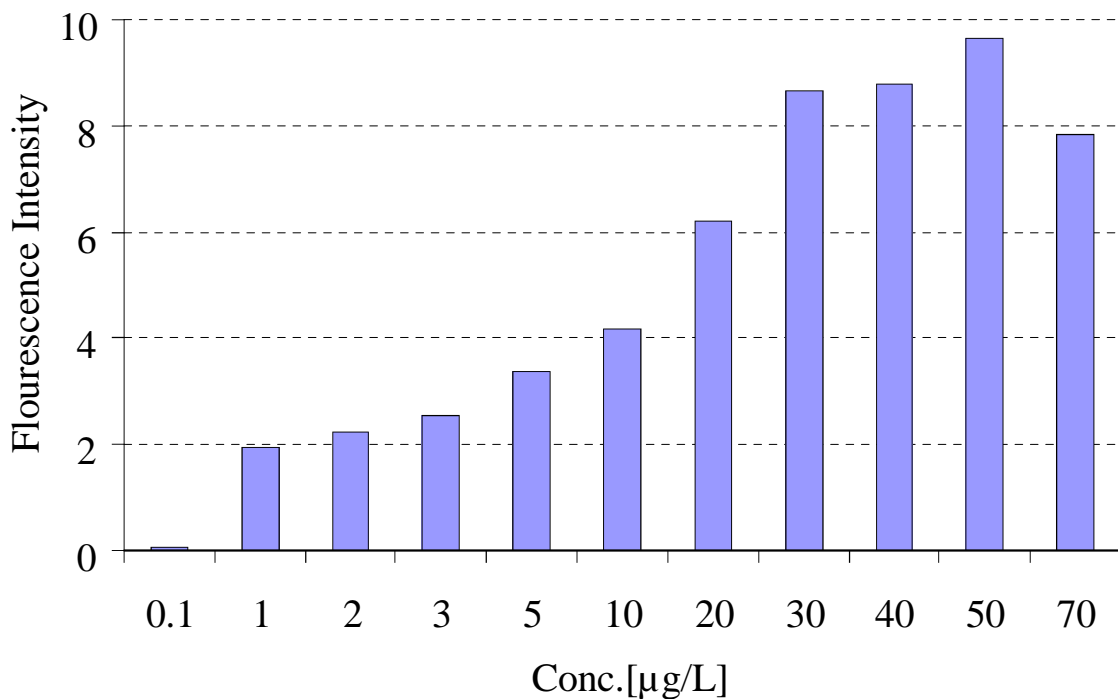
Figure 65: Concentration dependent bar graph for polyurethane layer (Anthracene 80 %: Acenaphthene 20 %)

To find out the maximum fluorescence intensities of different concentrations anthracene solution in water, following scans were made in figure 67. The respective intensities of different solutions of anthracene were plotted against function of concentration as shown following graph.
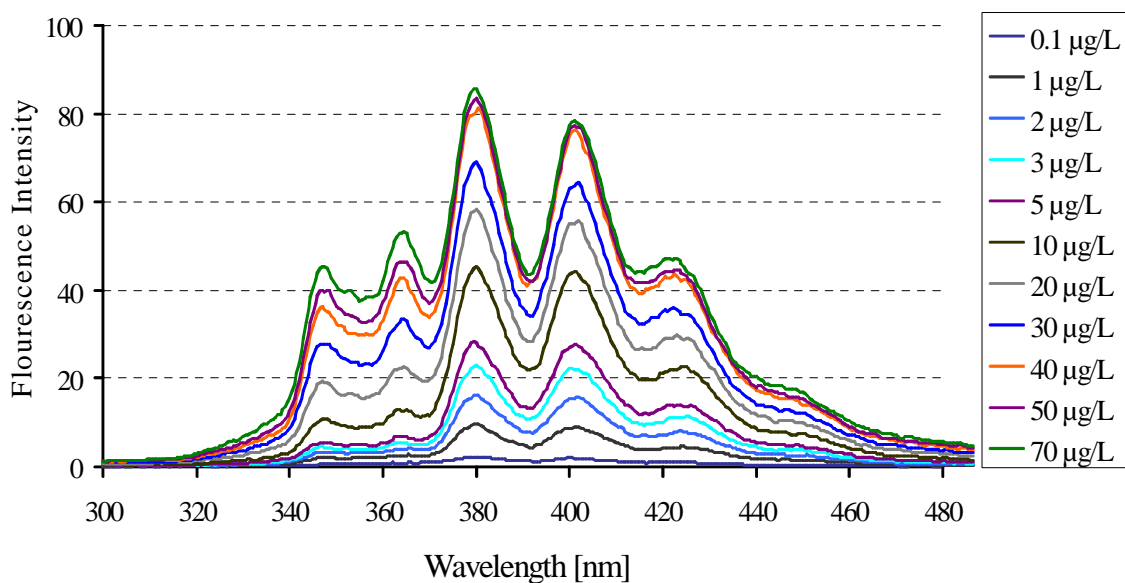
Figure 66: Fluorescence scan of freshly prepared solution of anthracene at different
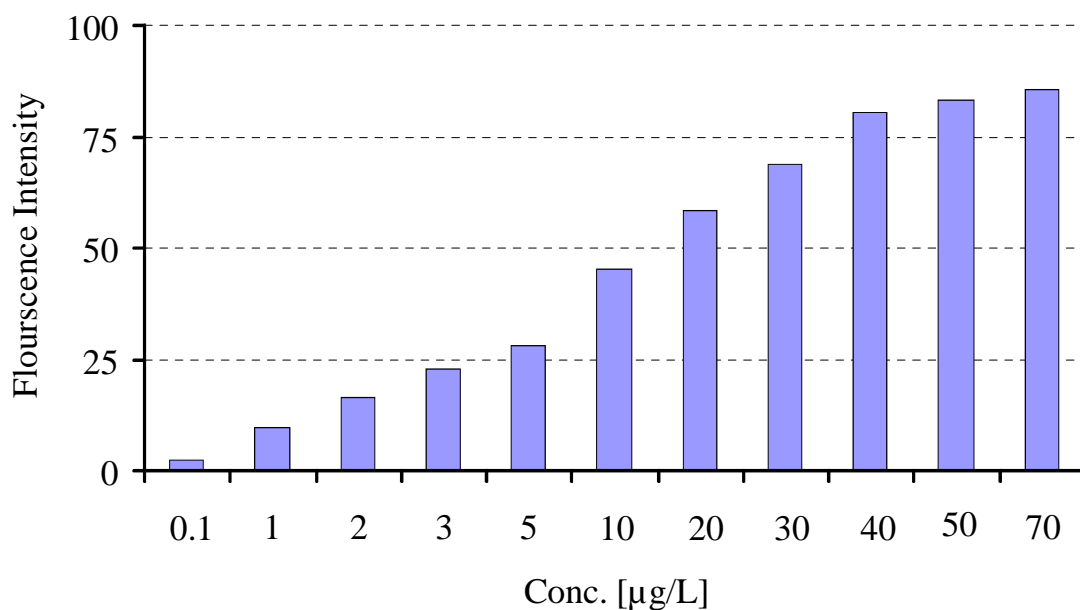
Figure 67: Concentration dependent bar graph of freshly prepared solution of anthracene.

5.4.4 Surface Studies

The surface of polyurethane film doubly imprinted with anthracene and acenaphthene was characterized on AFM in tapping mode. The AFM images obtained for deflection and height measurements are presented in figure 68.
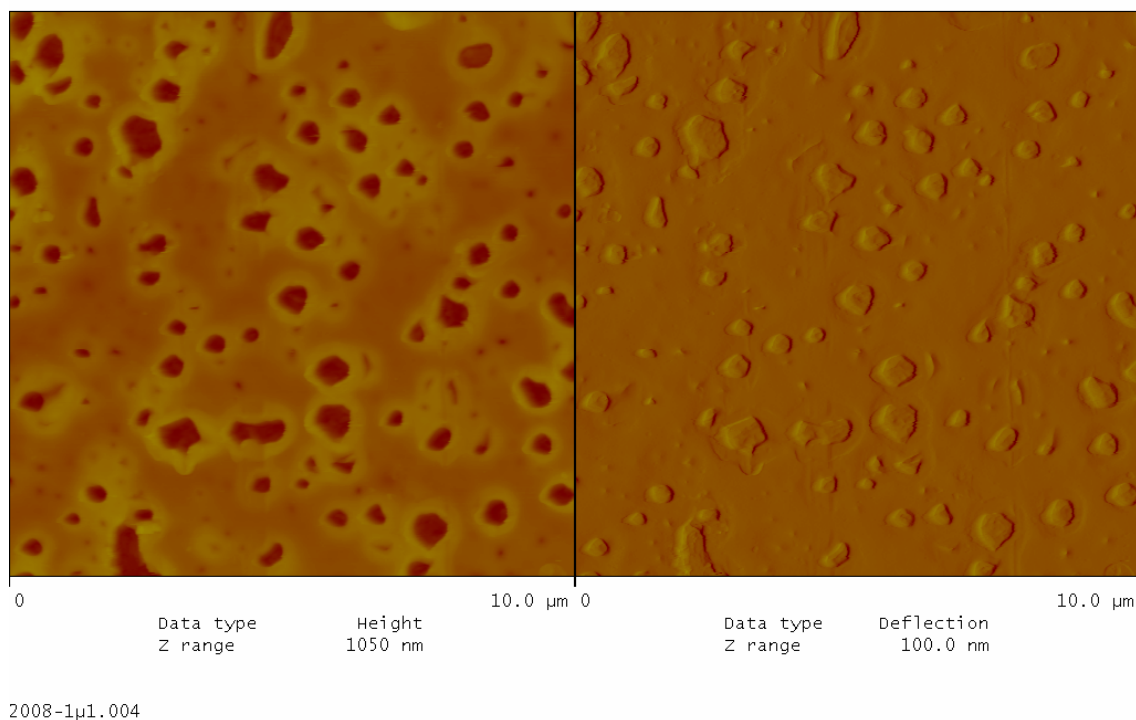
Figure 68: AFM image of double imprinted polyurethane film for surface studies.

A 3-D image of this polymer film has also been taken on a scale of 10 µm which help us to understand the generation of cavities and imprinting effects on surface. The 3-D images of double imprinted polyurethane film in figure 69 suggest that the cavities generated on the polymer surface provide suitable interaction sites for PAHs.
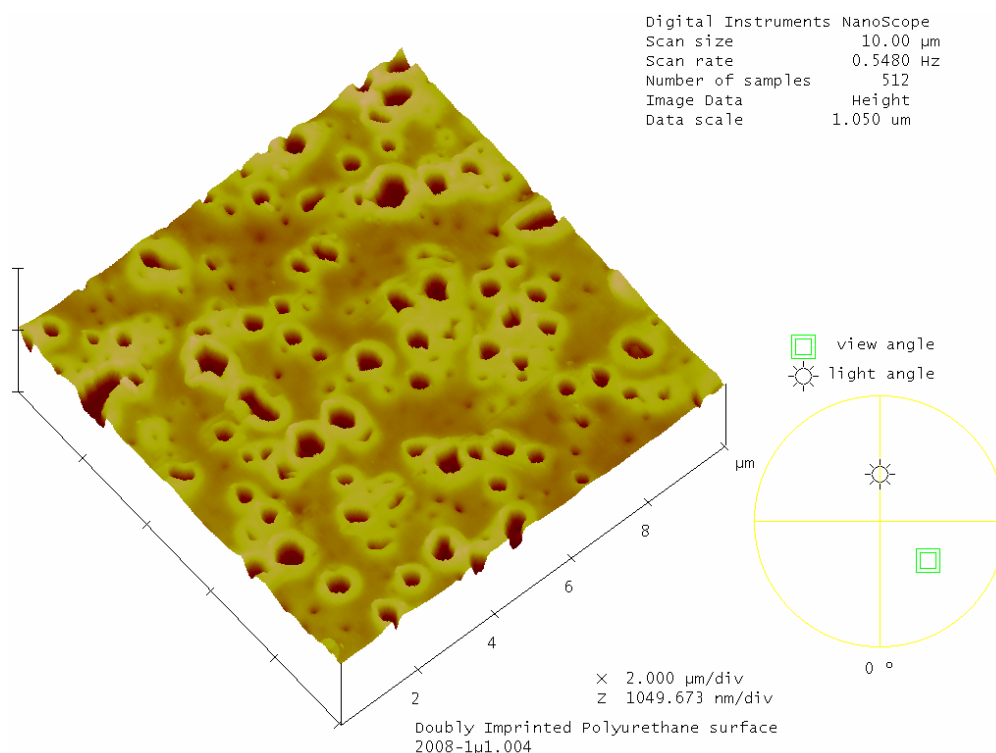
Figure 69: A 3D surface scan of double imprinted polyurethane layer.

5.4.5 Preparation of QCM

The QCMs were prepared in a similar manner as described in chapter 3 for the mass sensitive measurements. In this case the electrode design was identical to QCMs that were prepared for detection of metal ions in liquid phase keeping same flow cell. A thin layer of doubly imprinted layer was coated on of gold electrode while for reference other was coated with non-imprinted polymer layer. After that these QCMs were heated at 90°C for 2hours to remove the templates from the layer material and make it dry and rigid. The layer height is calculated from the difference of frequencies before and after the coating of QCM.

5.4.6 Mass Sensitive Measurements

Mass sensitive measurements were performed on this QCM in a flow cell at a flow rate of 2 mL/min. using pump. The temperature of the flow cell was kept at

25°C and maintained by water bath during the measurement. Anthracene stock solution was prepared by putting defined amount of anthracene in water on an ultrasonic water bath. The reported maximum solubility of anthracene in water is 70 µg/L. From this stock solution further standard solutions of different concentrations can be prepared. First the distill water was run through the cell until a stable base line is attained and then pumping system was shifted to known concentration of analyte solution. The curve obtained from this measurement for 0.1 µg/L concentration is as follows in the figure 70.
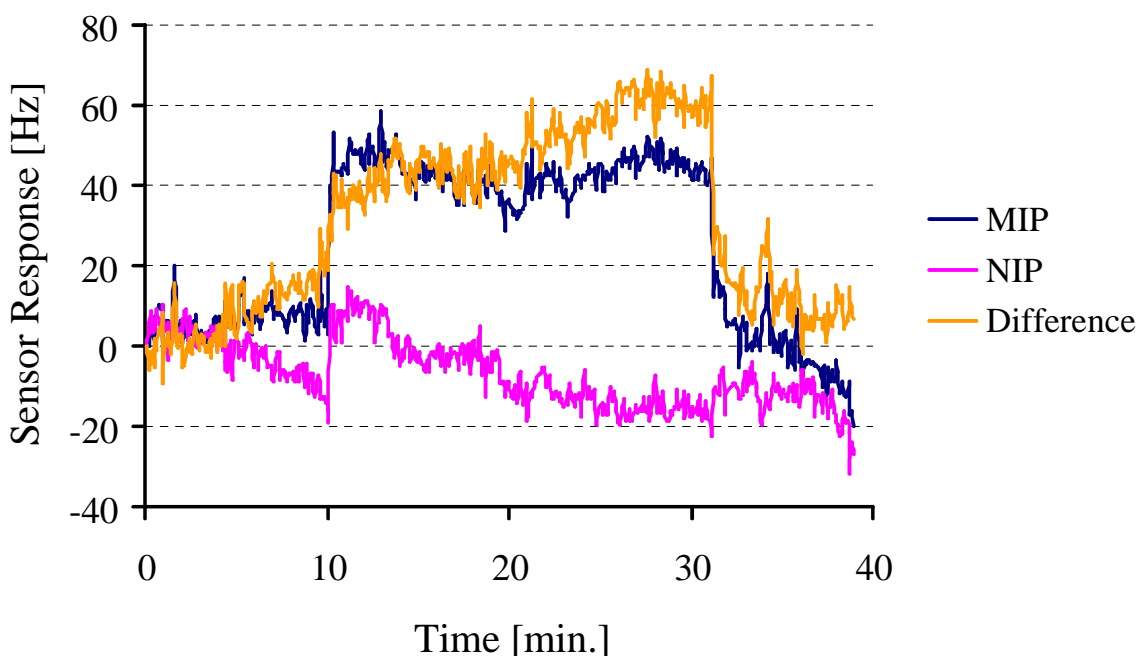
Figure 70: Sensor response of polyurethane layer for 0.1 µg/L concentration of anthracene.

For further higher concentrations, the mass sensitive measurements performed are as follows.

In these curves an anti Sauerbrey effect i.e. frequency enhancement has been observed when happens a splitting off some mass from the quartz surface. Continuous flow of distilled water over QCM surface develops equilibrium with polymer layer which is disturbed when analyte solution flows across it. The

interaction of anthracene with polyurethane layer is very interesting, water molecules present on polymer surface are more excluded due to the hydrophobic nature of PAHs causing a sudden increase in the frequency of the QCM. Considering same polymer recipe in case of florescence time drive spectrum the intensity was increased due to selective uptake of anthracene from water sample.
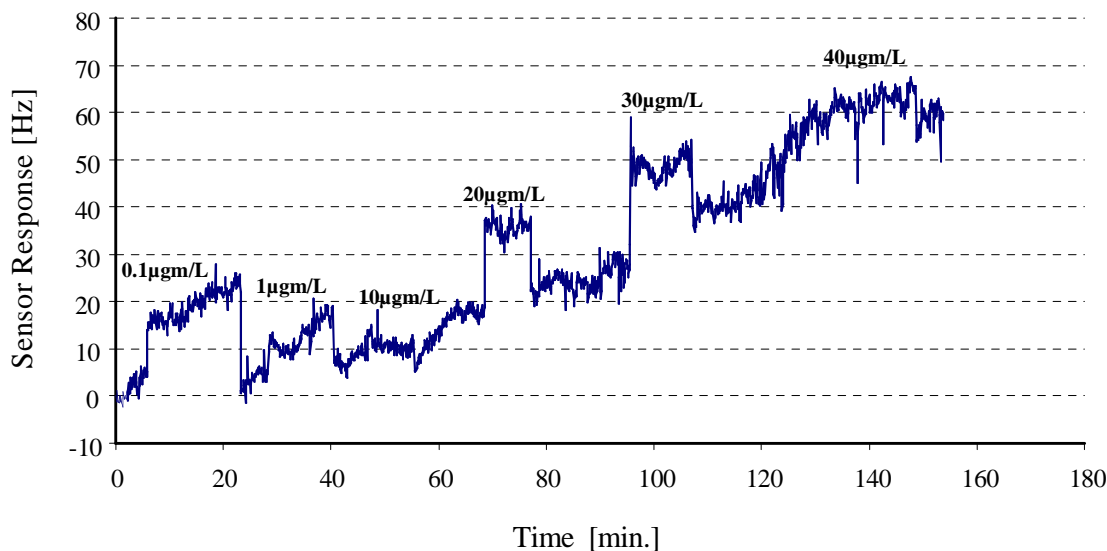
Figure 71: Sensor response for further higher concentrations.

In the case of QCM the analyte molecules are also extracted in same way from water but the loss of already present water molecules is much high in comparison of small gain of anthracene molecules which makes the net effect positive and the frequency of the quartz increases. One can observe that the shifting the system from analyte solution to distilled water, the frequency comes back to the base line indicating the reversibility of the sensor layer.

A modified polyurethane recipe mentioned* as under was introduced for mass sensitive measurements considering the nature of cross linker and the result obtained are as follows. As in this curve Sauerbrey law is followed and a decrease in the frequency of the QCM has been observed.

*DPDI 46 mg, phloroglucinol 8.8 mg, poly vinyl phenol 58mg, THF 800 µL, anthracene : acenaphthene [80:20] 5% in THF and at a temperature of 70 ºC for 1 hour.
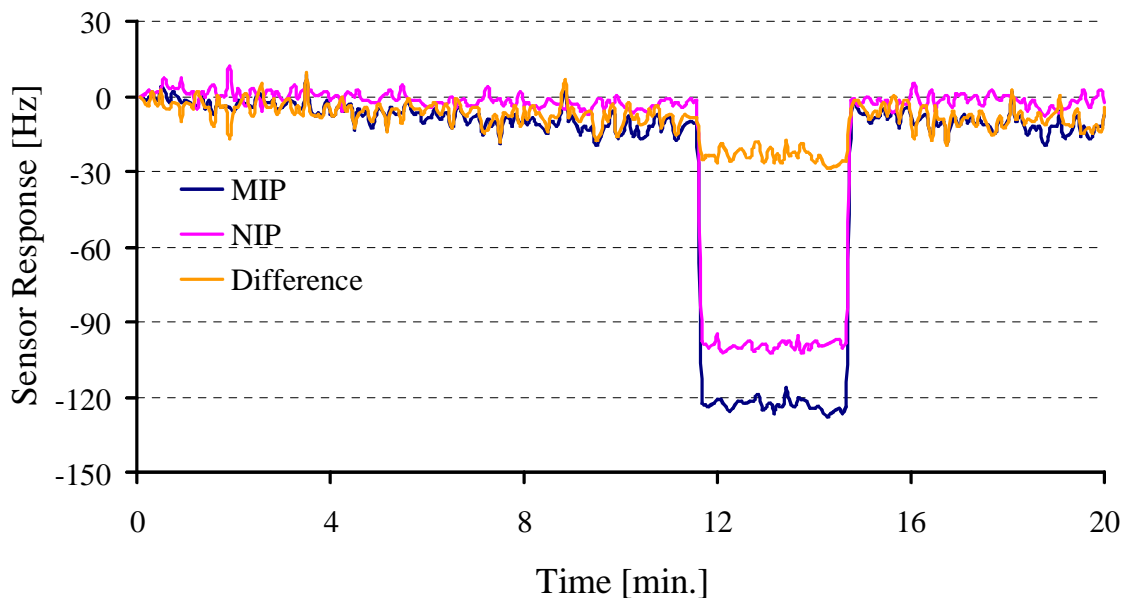
Figure 72: Sensor response of improved polyurethane layer for 0.1 µg/L concentration of anthracene.

This is the polymer recipe in which temperature, template mixture and the monomer used above all are same; the major difference is replacement of the cross linker. Some further measurements were made for other higher concentrations and the results obtained are in figure 73.
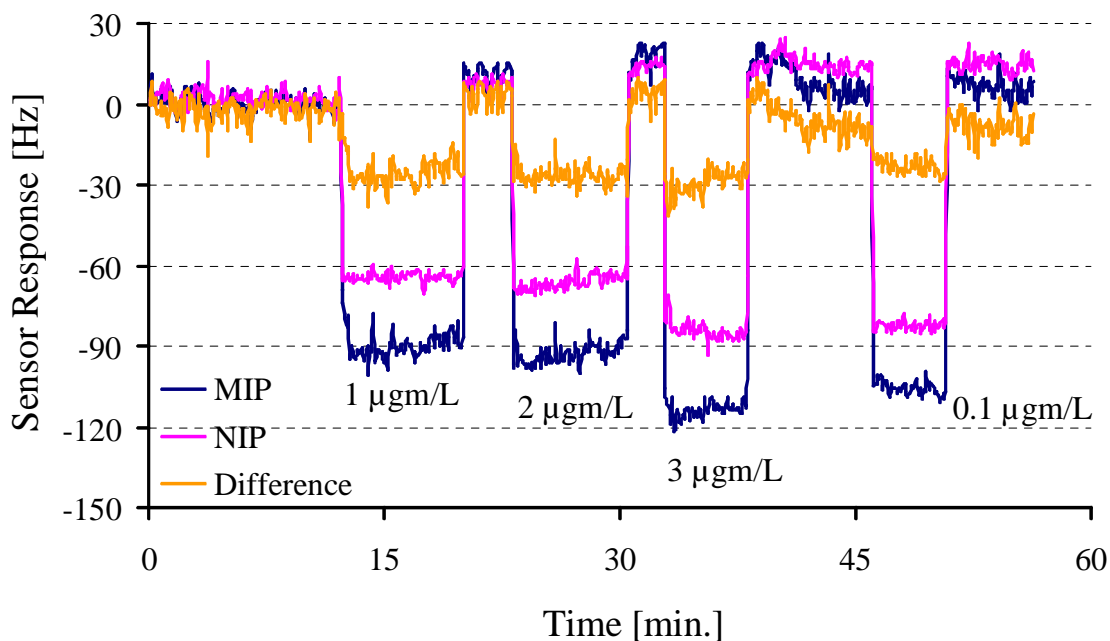
Figure 73: Sensor response of improved polyurethane layer for further higher concentrations of anthracene.

Phloroglucinol and bisphenol A (BPA) were used as cross linkers in polyurethane synthesis instead of Poly ethylene glycol (PEG). The reason of Sauerbrey and anti-Sauerbrey effect mainly depends upon the nature of cross linkers that were used in polyurethane. In mass sensitive detection of anthracene, PEG is more hydrophilic in nature and its interaction with water running over the surface of the polymer layer is higher as compared to that of PAHs are hydrophobic in their properties. This incompatibility of the cross linker with polymer and the analyte makes it to show anti Sauerbrey effect. On the other hand phloroglucinol and BPA are more hydrophobic in nature and suit best for the selective uptake of anthracene following Sauerbrey equation in liquids.
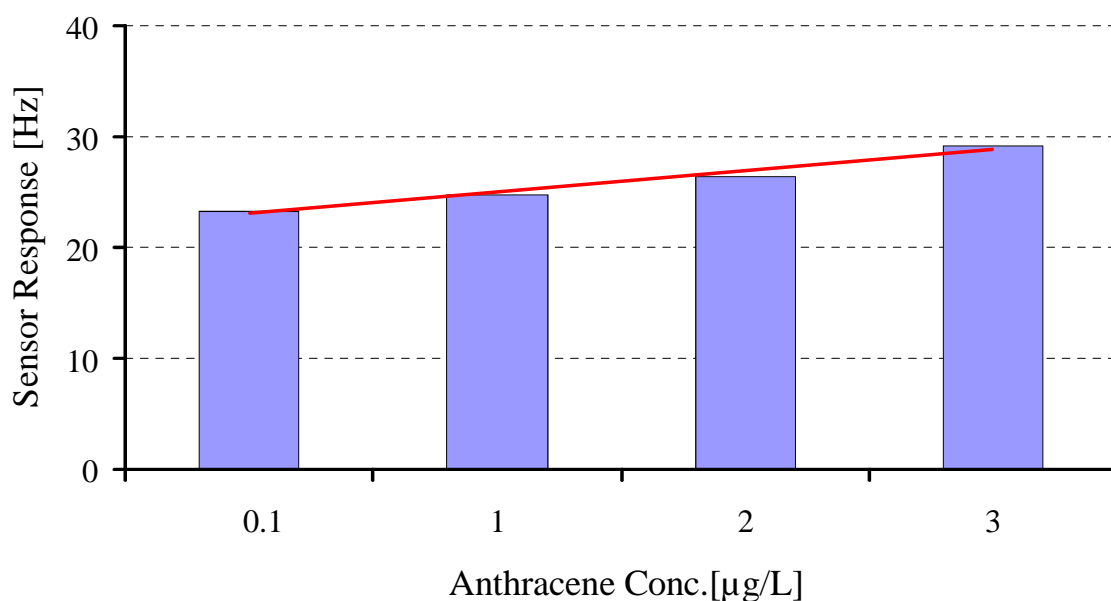
Figure 74: Concentration dependence curve for improved polyurethane recepie.

5.5 Conclusion

Extensive study has been done to design an optimal polyurethane composition by varying the different polymerization conditions like temperature, monomer cross linker ratio and template mixture etc for a highly sensitive detection of anthracene. Fluorescence time drive spectra of polyurethane layer provided an

excellent way to determine the minute concentrations of anthracene with significant sensitivity. Taking mass sensitive measurements in to account on QCM of 10 MHz considering both Sauerbrey and anti Sauerbrey effect an appreciable sensor response has been recorded for a concentration of 0.1 ppb in water which is even below the approved limit. This proves the sensitive nature of artificially designed polymer material which can be further improved for much higher sensor responses in the detection of PAHs.

A Novel Approach to Multi Sensor Array

6.1 Introduction

Monitoring the quality of natural and drinking water is one of the most important tasks of modern world due to a number of diseases that are caused environmental pollution. Currently more than half of world's population is suffering from serious water quality problems. If the quantity of any particular substance is over than the approved limit of WHO then it is considered as polluted water which is not suitable for drinking or for other defined purposes. Pollutants can be categorized into three different classes' namely organic, inorganic and biological pollutants. Presence of heavy metal ions[54], polycyclic aromatic hydrocarbons[55], pesticides, herbicides[56], contamination of hazardous viruses or bacteria are some of the major causes of water pollution. The nature of disease depends upon the type of contaminant in water sample. So a continuous and rapid determination of these pollutants is necessary to control the water quality and avoiding environmental damages.

There are several techniques for analyzing different components present in water which mostly includes normal laboratory methods for a very wide range of analytes but they are expensive, time consuming and some of them require high amount of samples as well. More over these analyses can only be done by highly trained personnel to ensure the quality of water sample. A relatively cheap, rapid and accurate analysis technique is required for the online monitoring of water quality which can be done even by a layman. For continuous monitoring, these sort of systems should not require some special maintenance and repair. QCM based multi sensor arrays had already shown their effectiveness for monitoring of different chemical compounds coming out from composting[57]. Different sensitive layers are coated on single QCM shows reasonable sensor response towards a particular analyte. The results obtained from these QCM sensor arrays are

comparable to those of GC-MS. The small size, re-usability, rapidity, accuracy, and robustness of QCM sensor arrays make them superior than other multi sensor systems in detection of different analytes.

6.2 Liquid Sensor Array[58]

In liquid phase a very similar approach was followed for monitoring of the quality of water by detecting several different analytes. A four channel QCM sensor array was designed for determination of three different analytes in water samples considering one electrode as a reference. Starting from very basic development of a liquid sensor array; three different analytes from three different classes were selected which give a true impression of multi sensor system. Atrazine, Pyrene and Nickel represent the three different classes i.e. herbicides, polycyclic aromatic hydrocarbons and metal ions respectively.

Atrazine is well known herbicide which is widely used to protect the crops from pre or post emergence of broad leaf and sometimes to stop the growth of grassy weeds. Moreover it also used in tillage processes to avoid soil erosion. Since 2004 it is banned in European Union due to its consistently increasing level in ground water that leads to serious contamination. Pyrene belongs to poly aromatic hydrocarbons which have already been discussed in previous chapter. It is a carcinogenic compound which has highly adverse health effects. Presence of Nickel or its salts in water samples above than the approved limit is not only harmful for the human beings but also toxic to aquatic life.

For monitoring of these analytes on a single QCM in liquid phase, a specially designed sieve is introduced to maintain the shape and the geometry of the electrodes which are very important while developing a multi sensor.

6.3 Experimental Section

6.3.1 Sieve Design for QCM Preparation

A four electrode sieve is prepared in a similar way as explained in previous section 3.3 by only changing the impression of two electrodes to four. The sieve design, shape of mass and electric end is shown in figure 75. The diameter of electrode is reduced to 4.5 mm from mass end while from electric end it is 3.0 mm. These are much smaller in comparison to the dual electrodes QCM.
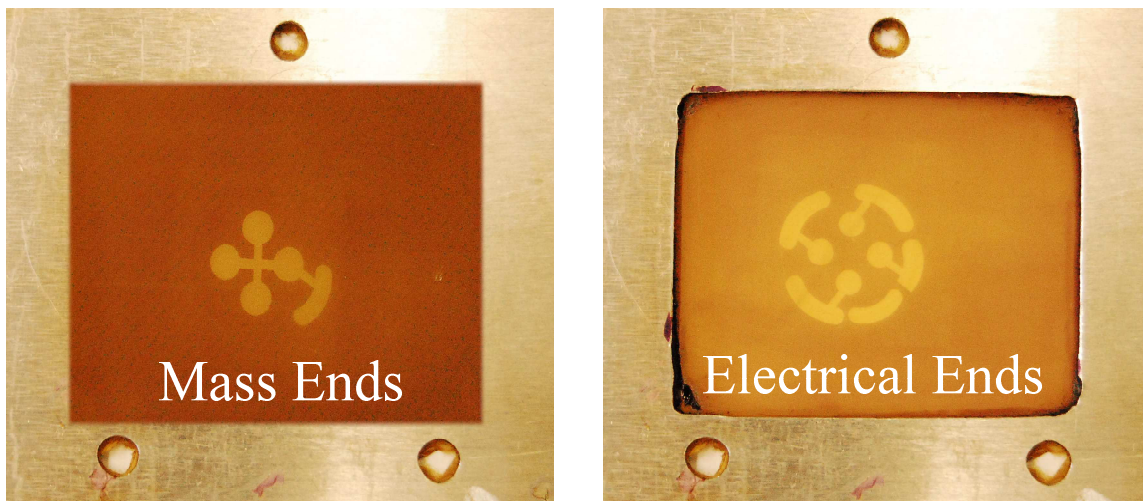
Figure 75: Printing sieve used for tetra electrode quartz preparation.

The layer height of the gold on quartz surface should not exceed than 150nm as more thick gold layers lead to high cross talk and damping as well. To make the gold layer thin dichloromethane was added to gold paste in appropriate amount which also reduces surface roughness. First gold paste is applied to a glass slide and it is kept in oven at 400 ℃ for 3 hours. A cut was made by a sharp blade to this gold layer coated on glass surface and was placed under the AFM tip which probed that surface and give layer height of gold as shown in figure 76.
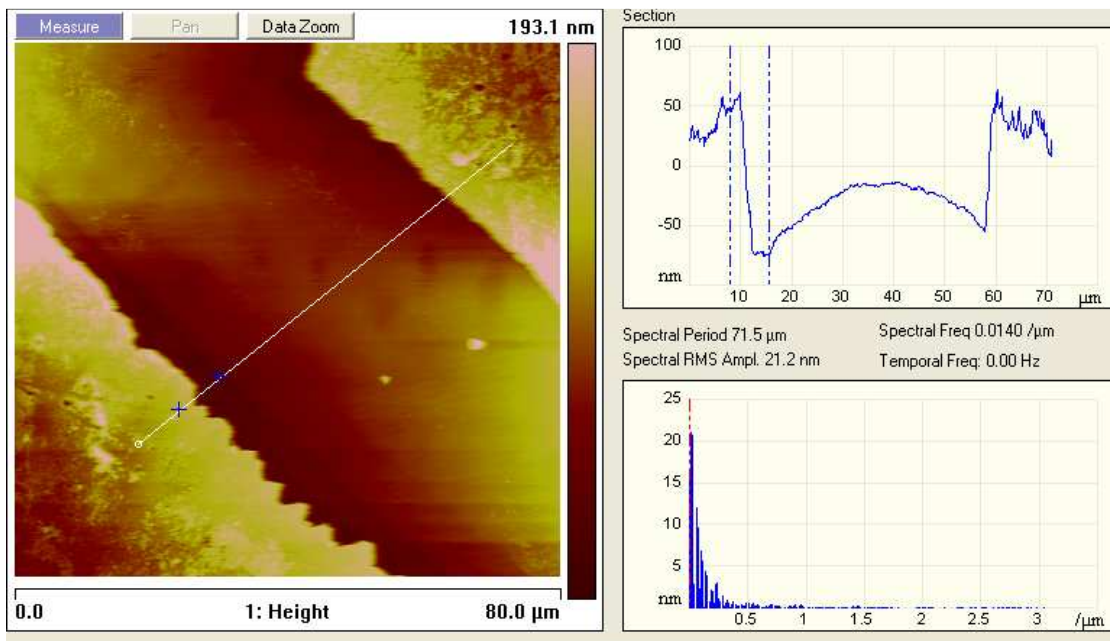
Figure 76: Section analysis of a gold layer coated on QCM. The layer height calculated for it is about 119.388nm.

6.3.2 Synthesis of Imprinted polymers

The synthesis of MIPs for atrazine, pyrene and Ni^{+2} ions is explained as follows.

> *Atrazine*

Methacrylic acid MAA as monomer 46 mg

EDMA 58 mg

AIBN 3.5 mg

DMF 100 µL

THF 1000 µL

In a mixture of 46mg methacrylic acid, 58 mg EDMA, 10 mg Atrazine as template, 100 µL of DMF and 800 µL of THF were taken and dissolved by stirring. After dissolution, 3.5 mg of AIBN as initiator was added and the solution was heated while stirring at 65 ºC for 45 minutes. Following the same

procedure another solution was also prepared excluding the template to be used as reference for sensor response.

➤ *Pyrene*

Diphenyl methane di-isocyanate DPDI as monomer   100 mg

Polyethylene glycol [PEG-200 gm/mol.] as cross linker   100 mg

Pyrene 80 mg, acenaphthene 20 mg as template mixture

Pyridine (solvent)

100 mg of both DPDI and PEG were dissolved in 1000 µL of water free pyridine separately. To prepare a template mixture for double imprinting, 80 mg of pyrene and 20 mg of acenaphthene were dissolved in 1000 µL of dry pyridine. Now 545 µL of DPDI, 455 µL of PEG and 50 µL from the template stock solution were mixed in a sample vial to form a homogenous mixture of pre-polymerized solution. Finally it was heated at 70 ℃ for 1 hour in a water bath.

➤ *Ni^{+2} ions*

Vinyl pyrolidone as monomer   90 mg

N,N methylene bis Acrylamide as cross linker   10 mg

AIBN (initiator)   2 mg

$NiCl_2.6H_2O$ (template)   10 mg

These above mentioned quantities were mixed together with 30 μL of deionised water and heated at 70°C until the gel point is reached.

6.3.3 Coating of the Layer Materials

Coating of the MIPs polymers on quartz surface requires intensive care because the four channels are so close to each other that during layer coating there is chance of spreading of polymer layer from one electrode to other. So

while coating one electrode others should be covered by some PDMS layer to avoid any cross interference. Atrazine layer was coated on first electrode as this layer require some post coating treatment which others not. A 50% dilution was made to above synthesized polymer, from this solution 5 µL of taken and coated on one channel at a speed of 3000brpm. This coated QCM was kept under UV light for overnight. In order to wash out template from the layer, QCM was kept in methanol for 2 hours. The frequency of electrodes was again recorded from network analyzer to confirm washing off template molecules. Molecularly imprinted layer of pyrene was coated on second electrode by applying 5 µL from a suitable dilution of above prepared polyurethane at a speed of 3000 rpm. The coated quartz was then put in a heating oven at a temperature of 110 ℃ for 2 hours; this will not only dry the layer but also removes template from layer.

The final layer was coated of Ni^{+2} ions on third electrode under same parameters. This layer does not require any template removal as when water flows across the surface, Ni^{+2} ions automatically goes in to the flowing liquid from surface leaving behind the recognition sites. The naked fourth electrode serves as a reference for others. After coating the layers, frequency of the tetra electrode QCM is also recorded to calculate layer heights and damping.

6.3.4 Cell Design

For measuring three different analytes on single quartz, a special flow cell with an inlet and outlet is constructed as shown in figure. This cell has four points outside for electrical contacts which are connected to two different circuit oscillators. In fact from inside it has a fifth point as well for grounding. The cell protects the QCM from external thermal and mechanical shocks. The positioning of coated QCM in cell and the tightening of screws is very critical. A slightly different position of quartz in cell and improper tightening will tends to increase the noise and might break QCM. In following figure the placement of coated QCM has been shown.
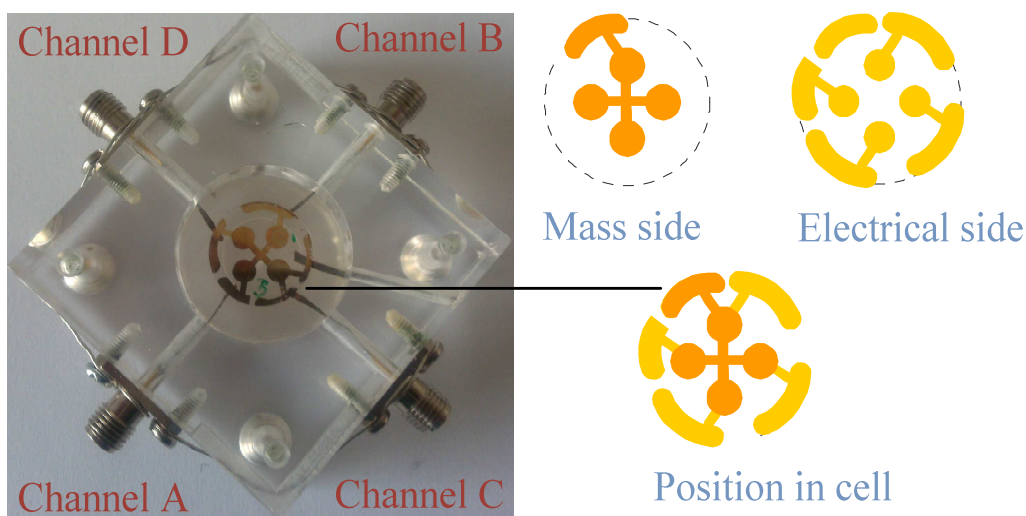
Figure 77: Position of the tetra electrode QCM in the four channel flow cell. The mass and electrical ends are also highlighted.

6.4 Results and Discussion

6.4.1 Mass Sensitive Measurements

Mass sensitive measurements were made by placing the coated QCM in the cell exactly at the designated places of electrical contacts; otherwise the frequencies will be disturbed. The screws should be tightened with delicacy because a slight increase in pressure during tightening could break quartz due to number of wires which are in contact from rear side.

First a test measurement was performed in which a 0.2 mM solution of Ni^{+2} metal ions was flow through the cell and corresponding change in frequency was calculated. This has been shown in the following curve. This curve shows an excellent separation of different sensor signals.

The pattern of sensor response is quite understandable as it is highest for Ni^{+2} ions to which it is imprinted and lowest for the un-coated channel. Atrazine imprinted layer showed less response than Ni^{+2} imprinted layer but more than the

110

pyrene imprinted layer. The reason is logical as acrylic acid layer is more polar
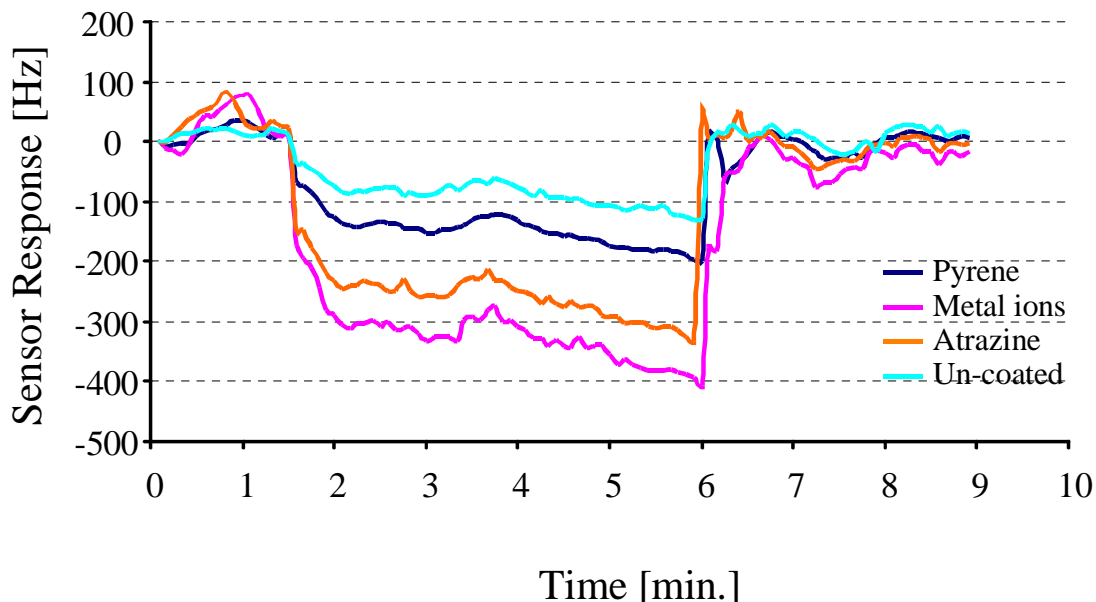
Figure 78: Separation of sensor signals of a tetra electrode QCM for 0.2 mM solution of Ni^{+2} ions.

than polyurethane layer which makes itself more attractive for Ni^{+2} ions.

To have a full picture of multi sensor array mass sensitive measurements were done with a series of different concentrations of three different analytes. The stock solution of first analyte was prepared by dissolving a particular amount of atrazine in water by sonication in ultrasonic bath for 1 hour. The un-dissolved amount of atrazine is filtered and further dilutions can be made from filtrate. Same procedure was followed for making the different dilutions of pyrene as this method is followed because of low solubilities of both these compounds. Atrazine has a maximum solubility of 7 ppm and pyrene has 0.134 ppm in water at 20°C. So that is why the dilutions cannot be made by direct weighing. On the other hand Nickel chloride hexahydrated salt is fairly soluble in water, so there is not any difficulty in making the dilutions of Ni^{+2} ions.

At least five different concentrations were taken for each analyte and run through the flow cell turn by turn. The first five concentrations that were run through the cell were of atrazine followed by pyrene and then Ni^{+2} ions respectively. So a total of fifteen different concentrations were passed through the cell and their corresponding sensor response of each layer was measured simultaneously to function of time as illustrated in figure.
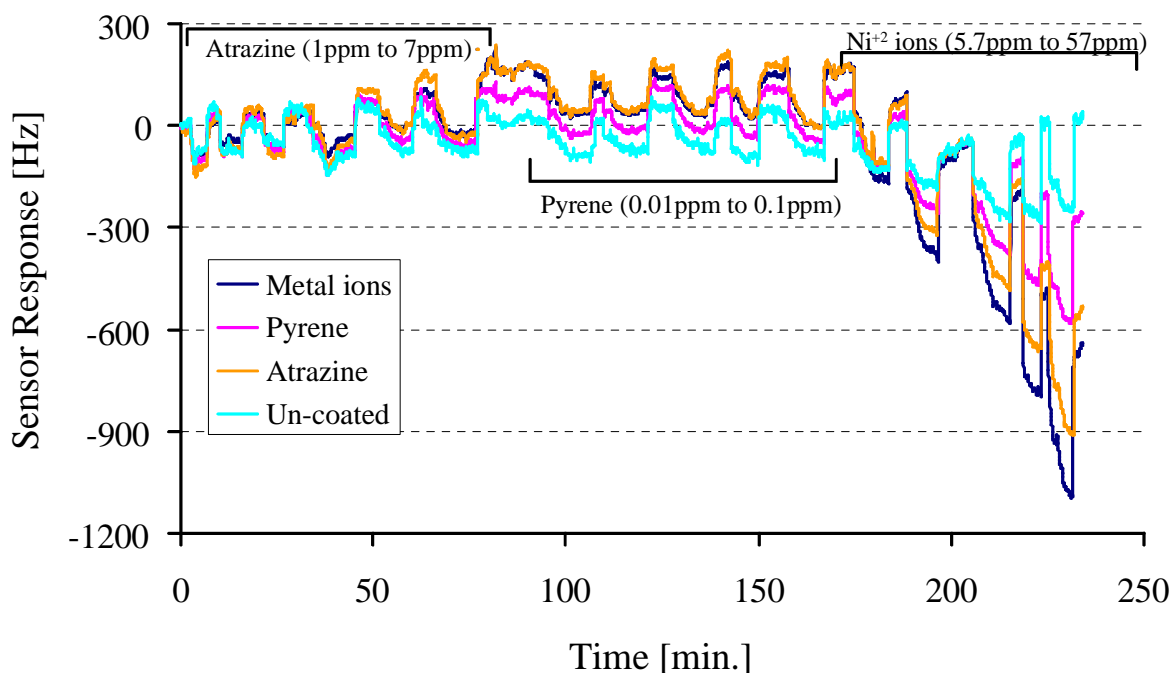
Figure 79: Sensor response of tetra electrode QCM with 5 different concentrations of Atrazine, Pyrene and Ni^{+2} respectively.

This curve can be splited into three parts where each part represents a series of a particular analyte as shown in following way. In In first part different concentrations ranging from 1ppm to 5ppm of atrazine were passed through while for pyrene and Ni^{+2} follow it. For the frequency change for all the four channels at different concentrations of atrazine can be represented in a following manner.
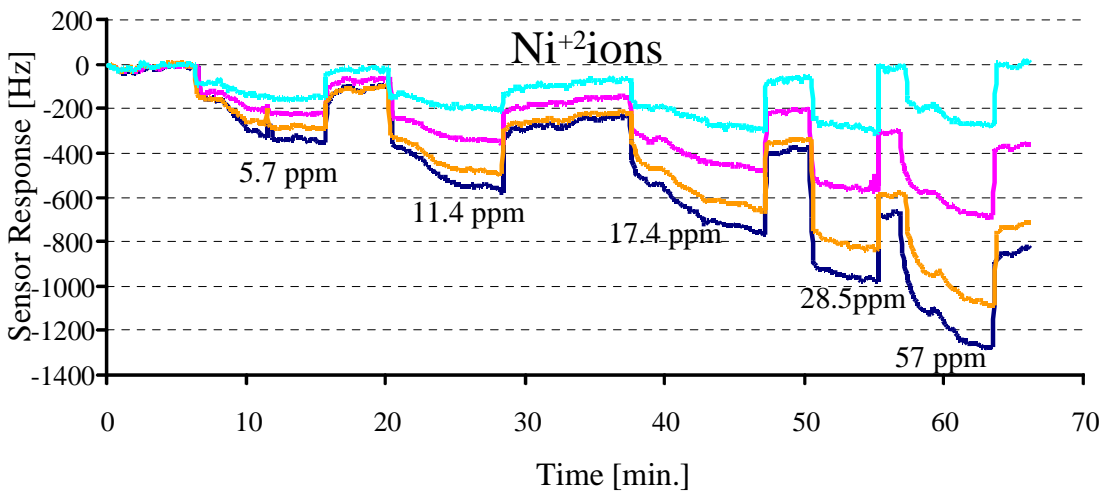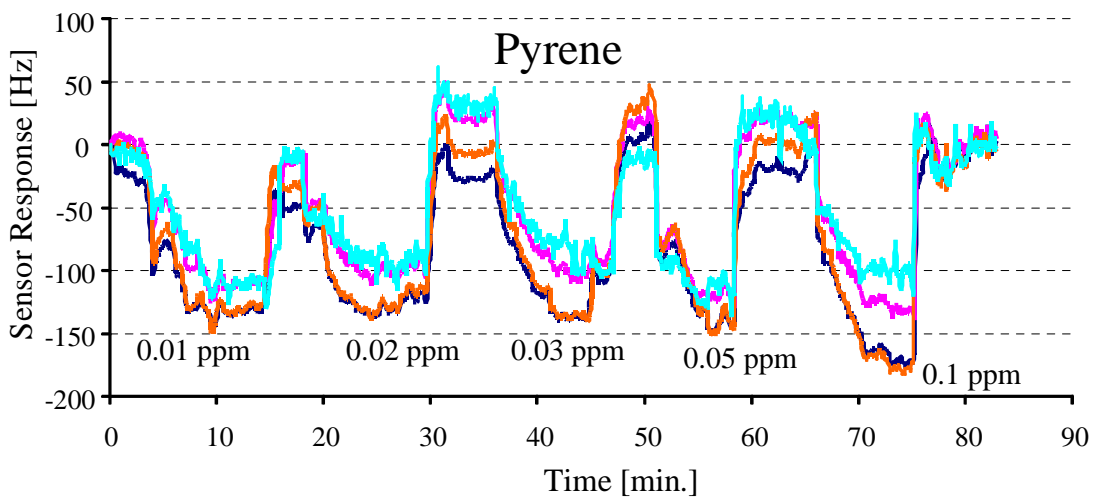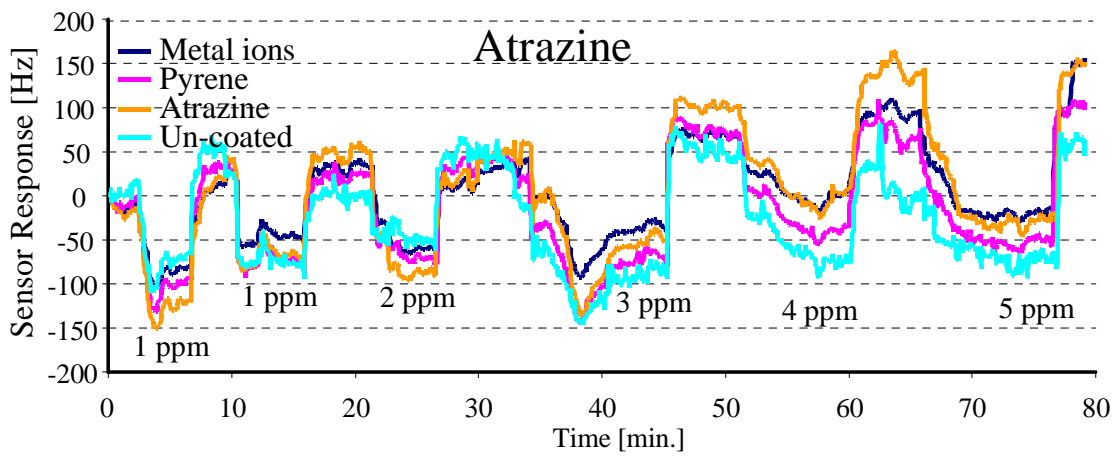
Figure 80: Separation of three different analytes according to their mass sensitive measurements.
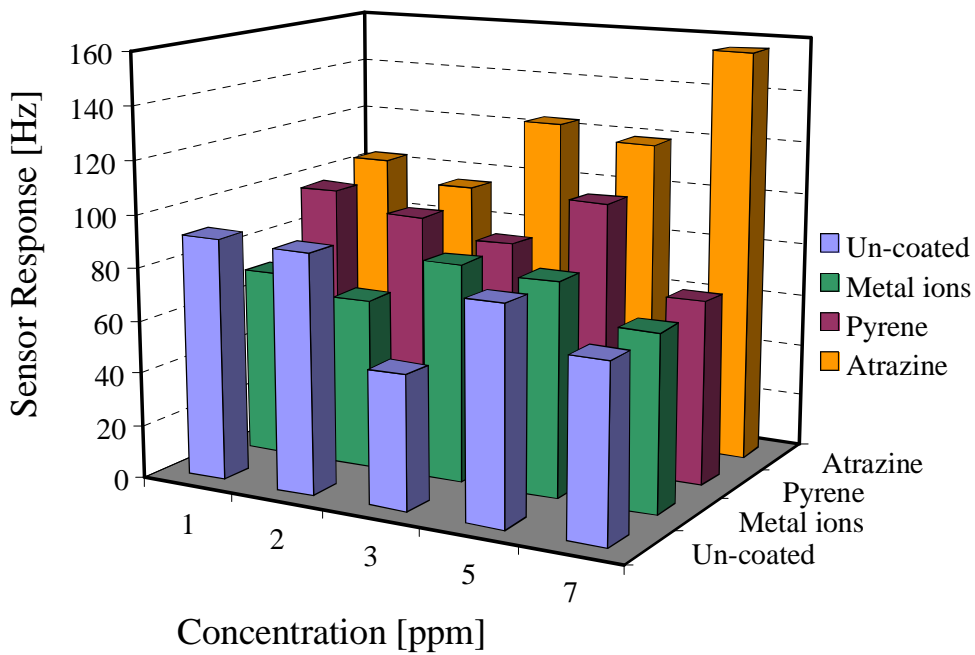
Figure 81: Cross sensitivity comparison of tetra electrode QCM on running different concentrations of Atrazine.
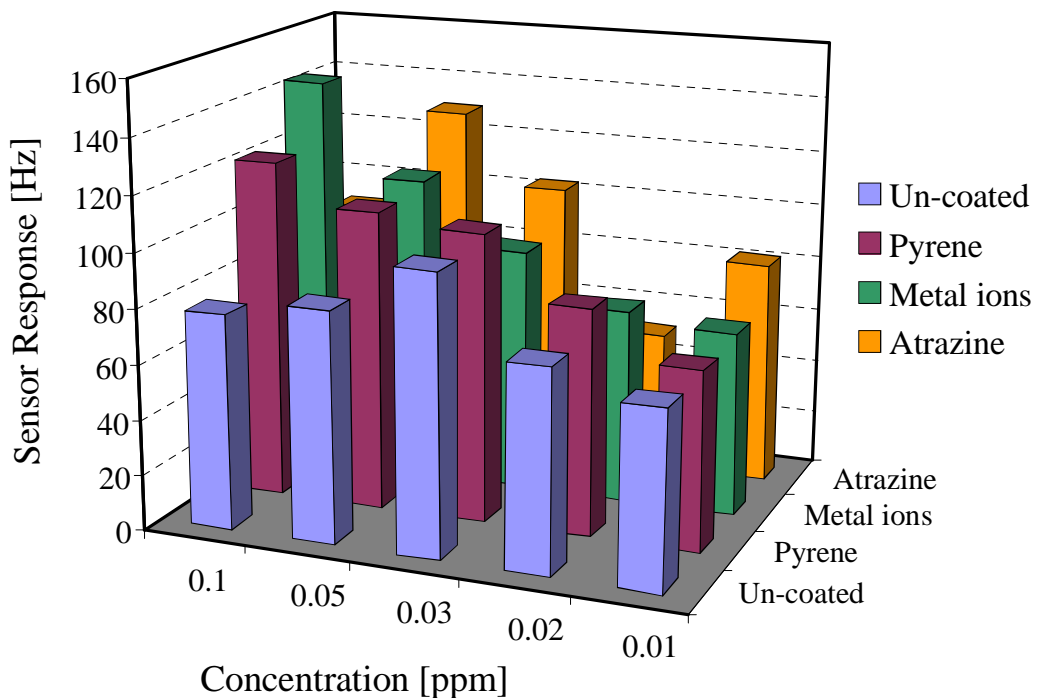
Figure 82: Cross sensitivity comparison of tetra electrode QCM on running different concentrations of Pyrene.
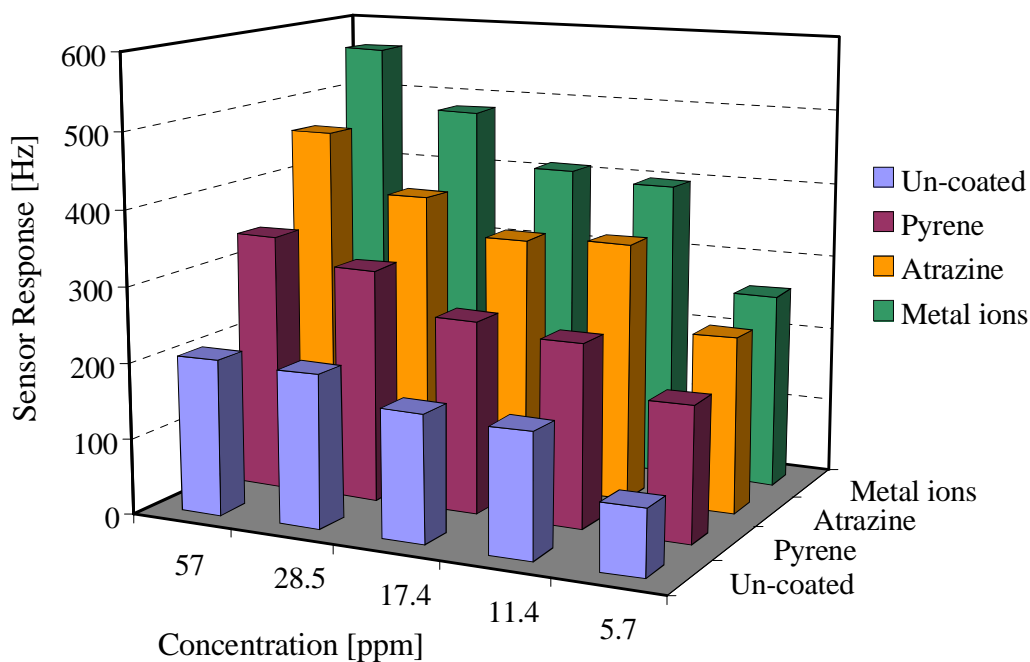
This three dimensional picture provides a complete view of all channels. Un-coated channel shows a minimum change in the frequency as compared to the other coated channels. Although the sensor response of atrazine imprinted polymer layer is not so linear but it is still higher than any other channel at any concentration. Similar bar graphs are plotted for different concentrations of pyrene and Ni^{+2} ions respectively as shown in following figures.80 to 83.

It is obvious that the sensitivity and selectivity pattern is not so appreciable in the case of pyrene and atrazine results in figure 81 and 82 which is probably due to lower concentrations passed through the cell. The problem concerned about the sensitivity is related to the maximum solubility of compound in a particular solvent and at particular temperature as well. In case of atrazine and pyrene it is 18mg/L and 0.134mg/L at 25 ºC respectively. While on the other hand the salt of Ni^{+2} is highly soluble in water so, the three different substances differ widely from each other regarding solubility. Due to extremely low solubility of two analytes it is very difficult to make more concentrated solution

for them. The size of the electrode is another factor as it is approximately half of the two channels quartz which strongly influences the interaction of analyte to the layer material because at reduced surface area the sensor response will also be reduced.

The chemical interaction of different layers towards different analytes is also a serious issue regarding cross selectivity of the sensor. As Ni^{+2} imprinted polymer layer is more polar than atrazine layer offering more attraction to atrazine molecules which becomes more favorable at extremely low concentrations. Some other nonspecific interactions could have impact on selectivity.

In spite of all other problems, the behavior of QCM in liquids is entirely different. Unlike in gases, the analysis becomes more tedious in liquid phase due to the visco-elastic properties of medium. This will not only increase the damping loss of QCM but also influences fundamental resonating frequency. In comparison to the previous work where two electrode QCM was used for analysis, the cross talk becomes more pronounced in the case of multi electrode QCM. This high cross talk can shift different frequencies of different channels to a single value which makes the measurement impossible.

Abstracts

English:

The idea of combining mass sensitive devices along with synthetic polymers has proven an effective strategy for designing chemical sensors. Quartz crystal microbalance QCM coated with molecularly imprinted MIP layers are very useful for selective detection of various analytes from complex mixtures. This work is an important contribution to realize the applications of chemical sensors based on mass sensitive devices using artificial receptors.

In the first part of the thesis, capric acid imprinted zirconia nanoparticles have been synthesized and tested for degradation analysis of waste engine oil products i.e. acidic components. Mass sensitive measurements were performed by coating imprinted nanoparticles on 10 MHz AT-cut quartz crystal. The morphology of nanoparticles was studied by atomic force microscopy (AFM). The sintering or temperature effect on sensor response was observed as the degradation processes normally undergo at higher temperatures. These particles were also tested with different aged oil samples and corresponding sensor signal was monitored. The correlation between Infra red (IR) absorbance and the sensor signal of different waste oil samples was also made and found in accordance. The combined effect of imprinted titania and zirconia nanoparticles as next generation was also studied by designing composite material of titania and zirconia in 1:1. The size and distribution of this composite sensing material was also characterized by AFM and relationship between size of particles and sensor response was also evaluated.

Imprinted polyurethane was used for the detection of alkaline earth metal ions. Mg-imprinted polyurethane layers have shown substantial sensitivity and selectivity over other metal ions such as Ca^{+2}, Sr^{+2} and Ba^{+2}. The study was

extended for transition divalent metal ions and new polymer system was developed i.e. poly vinyl pyrrolidone. The sensor response of Ni^{+2} imprinted polymer was compared to other test metal ions solutions i.e. Cu^{+2}, Co^{+2} and Zn^{+2} and significant selectivity pattern was observed.

Rigid and robust polyurethane layers were synthesized for detection of poly aromatic hydrocarbons (PAHs) i.e. anthracene in water. The anthracene was introduced in polyurethane matrix by following double imprinting approach where a large and a relatively small molecule are added in appropriate ratios. The designed sensitive layers have shown sensitivity up to 0.1 µg/L of anthracene in water both on fluorescence and QCM system.

In the final part of thesis, a multi sensor QCM system was developed for the detection of three different analytes i.e. PAHs, herbicides and metal ions. A tetra electrode QCM was designed for this purpose and a special Teflon cell was constructed for measurements. A set of different concentrations of each analyte was run on the cell and corresponding sensor response of all four channels was determined.

German:

Die Kombination von massensensitiver Instrumentierung mit synthetischen Polymeren ist eine effektive Strategie, um chemische Sensoren zu entwerfen. Schwingquarze (QCM) mit molekular geprägter Schicht MIP sind für die selektive Detektion von unterschiedlichen Analyten in komplexer Mischungen sehr geeignet. Diese Arbeit stellt einen Beitrag zur Anwendung von chemischen Sensoren basierend auf QCM unter Verwendung von synthetischen Rezeptoren dar.

In ersten Teil dieser Dissertation wurden Zirkonium-Nanopartikel mit Kaprinsäure geprägt und der Alterungsprozessen von Ölen über die Detektion von azidischer Degradationsprodukten charakterisiert. Massensensitive Messungen wurden mit geprägten Nanopartikeln mit 10 MHz AT-cut Schwingquarzen durchgeführt. Die Beschaffenheit der Nanopartikel wurde mit Hilfe von Atomkraftmikroskopie AFM überprüft. Der Effekt der Temperatur auf den Sinterprozess des Materials wurde über die Sensorantworten verfolgt. Diese Nanopartikel wurden ebenfalls mit unterschiedlich alten Oelproben getestet und das dazugehörige Sensorsignal aufgezeichnet. Es konnte ein Zusammenhang zwischen der IR-Absorption und dem Sensorsignal von unterschiedlichen Ölproben ermittelt werden. Durch die Kombination von Titan und Zirkonium im Verhaeltnis 1:1 wurde eine neue Variante von Titan und Zirkonium gepraegten Nanopartikeln geschaffen. Die Groesse und Verteilung von diesem gemischten sensitiven Material wurde mittels AFM charakterisiert, und eine Beziehung zwischen der Partikelgroesse und der Sensorantwort hergestellt.

Für die Detektion von Erdalkalimetallionen wurden geprägte Polyurethane verwendet. Magnesium-gepraegte Polyurethanschichten zeigten substantielle Selektivität und Sensitivität gegenüber anderen Metallionen wie Ca^{2+}, Sr^{2+} und Ba^{2+}. Die Untersuchung wurde auf zweiwertigen Übergangsmetallionen erweitert, und ein neues Polymersystem, wie z.B. Polyvinylpyrrolidone, entwickelt. Die Sensorantworten vom Ni^{2+}-gepraegten Polymer wurde mit

anderen Metallionenprobeloesungen verglichen, z.B. Cu^{2+}, Co^{2+} und Zn^{2+}, und es wurden zufriedenstellende Selektivitaetsmuster beobachtet.

Fuer die Detektion von polyaromatischen Kohlenwasserstoffen PAHs, z.B. Anthracen in Wasser, wurden rigide und robuste Polyurethanschichten synthetisiert. Die Anthracene wurden in die Polyurethanmatrix durch doppelte Prägung eingefügt, wobei ein großes und ein relativ kleines Molekuel in geeigneten Verhältnissen zusammengefügt wurden. Die entworfenen sensitiven Schichten zeigten Sensitivität bis zu 0.1 µg/L Anthracen in Wasser, sowohl bei der Fluoreszenzmessung als auch bei Schwingquarzmessung.

Im letzten Teil der Dissertation wurde ein multidimensionales QCM Sensorsystem für die Detektion von drei unterschiedlichen Analyten, z.B. PAHs, Herbizide und Metallionen, entwickelt. Es wurde ein 4-Elektroden QCM fuer diesen Zweck entworfen, und eine spezielle Teflonzelle fuer die Messungen konstruiert. Die Messzelle wurde mit einer Reihe von unterschiedlichen Konzetrationen von jedem Analyten gefüllt und die entsprechenden Sensorantworten von allen vier Kanälen wurden aufgezeichnet.

Abbreviations

AFM	Atomic Force Microscope
AIBN	Azobisisobutyronitrile
BAW	Bulk Acoustic Wave devices
DPDI	Diisocyanato Diphenylmethane
FT-IR	Fourier Transformation Infra Red
FET	Field Effect Transistor
GCMS	Gas Chromatography Mass Spectrometry
HPLC	High Performance Liquid Chromatography
ICP	Inductively Coupled Plasma
IDT	Inter-digital Transducer
LED	Light Emitting Diode
MIP	Molecularly Imprinted Polymer
MOSFET	Metal Oxide Semiconductor Field Effect Transistor
MS	Mass Spectrometry
NIR	Near Infra Red
PAH	Polycyclic Aromatic Hydrocarbons
PEG	Polyethylene Glycol
QCM	Quartz Crystal Microbalance
QMB	Quartz Microbalance
SAW	Surface Acoustic Wave devices
SPR	Surface Plasmon Resonance

TAN	Total Acid Number
TBN	Total Base Number
THF	Tetrahydrofuran
TSM	Thickness Shear Mode
UV	Ultra-Violet
WHO	World Health Organization

References

[1]   W. GoPel, J. Hesse, J. N. Zemel, *Sensors, Wiley-VCH, Weinheim,* Vol. 2, **1989**

[2]   U. E. Spichiger-Keller, *Chemical Sensors and Biosensors for Medical and biological Applications, Wiley-VCH, Weinheim,* **1998**

[3]   *Encyclopedia of Analytical Chemistry* R.A. Meyers (Ed.) pp. 3831–3855 Ó John Wiley & Sons Ltd, Chichester, **2000**

[4]   Springer Series on Chemical Sensors and Biosensors Volume 5(2007)pp. 173-210 Springer-Verlag Berlin Heidelberg **2006**

[5]   *Chemical Sensors and Biosensors* (Analytical Techniques in the sciences (AnTs) Brain R.Eggins. John Wiley & Sons Ltd, Chichester, **2002**

[6]   (a) H. Dueker, K.H. Friese, W.D. Friese, 'Ceramic Aspects of the Bosch Lambda Sensor', SAE Paper 750223, SAE Automotive Engineering Congress, Detroit, February **1975**, 807–824, **1975**; (b) G.V. Velasco, J.P. Schnell, 'Gas Sensors and Their Applications in the Automotive Industry', *J. Phys. E (Sci. Instrum.)*, **16**, 973–977 (1983).

[7]   A. Chiba, 'Development of the TGS Gas Sensor', in *Chemical Sensor Technology*, ed. S. Yamauchi, Kodansha,Tokyo and Elsevier,Amsterdam, 1–18, Vol. 4, **1992**.

8   G. Sauerbrey, 'Verwendung von Schwingquarzen zur Wägung dünner Schichten und zur Mikrowa¨gung', *Z. Phys.*, **155**, 206–222 (**1959**).

9   P. Curie, J. Curie; Développement, par pression, de l'électricité polaire dans les cristaux hémièdres à faces inclinées; C.R. T.91 (**1880**) 294-295.

10   Lord Rayleigh "On Waves Propagated along the Plane Surface of an Elastic Solid", "Proc. London Math. Soc. s1-17 (**1885**), p. 4-11"

11   (a) J.B. Briot, S. Ballandras, E. Bigler, G. Martin, 'Gravimetric Sensitivity of Transverse Waves Trapped by Metal Gratings on Thin Quartz Plates', in *Proceedings of* **1997** *IEEE International Frequency Control Symposium, Orlando, Florida*, IEEE Cat. No. 97CH36016,IEEE, Piscataway, NJ, 207–212, 1997; (b) M. Tom-Moy,R.L. Baer, D. Spira-Solomon, T.P. Doherty, 'Atrazine Measurements Using Surface Transverse Wave Devices', *Anal. Chem.*, **67**, 1510–1516 (**1995**).

12   O'Sullivan, C. K.; Guilbault, G. G. Commercial quartz crystal microbalances - theory and applications.   Biosensors & Bioelectronics (**1999**), 14(8-9), 663-670

13   Sauerbrey, G.Z., **1959**. Use of quartz vibration for weighing thin films on a micro balance. *J. Physik* **155**, pp. 206–212.

14   Marx, Kenneth A. Quartz crystal microbalance: a useful tool for studying thin polymer films and complex bimolecular systems at the solution- surface interface. Bio macro molecules (**2003**), 4(5), 1099-1120

[15]   King, W. H., Jr. *Anal. Chem.* **1964**, *36*, 1735-1741

[16]   Guilbault, G. G. *Anal. Chem.* **1983**, *55*, 1682-1684.

[17]   Konash, P. L.; Bastiaans, G. J. *Anal. Chem.* **1980**, *52*, 1929-1935.

[18]   K Jyonosono, T Imato, N Imazumi, M Nakanishi, Spectrophotometric flow-injection analysis of the total base number in lubricants by using acid–base buffers Analytica Chimica Acta 438 (**2001**) 83–92

[19]   K. Cammann, U. Lemke, A. Rohen, J. Sander, H. Wilken, B. Winter, *Angew. Chem. Int. Ed. Engl.* **1991**: 30, 516

[20]   H. S. Lee, S. S. Wang, D. J. Smolenski, *Lubr. Eng.* **1993**: 50, 605

[21]   S. S. Wang, H. S. Lee, D. J. Smolenski, *Sensors and Actuators B,* **1994**: 17, 179

[22]   M. Tomita, H. Kamo, Y. Nomura, M. Nozawa, S. Yamaguti, *JSAE Review,***1995**: 16, 283

[23]   Su, Bin; Su, Hai-ding. Comparison of two methods for monitoring the degradation of engine oil in service. Runhuayou (**2007**), 22(3), 52-55

[24]   S. S. Wang, *Sensors and Actuators B,* **2001**: 73, 106

[25]   R. Hoss, F. Vögtle, *Angew. Chem. Int. Ed. Engl.* **1994**: 33, 357

[26]   T. Wesa, W. Göpel, *Fresenius J. Anal. Chem.* **1998**: 361, 239

[27]   Peter A. Lieberzeit, A. Afzal, G. Glanzing & Franz L. Dickert, Molecularly imprinted sol–gel nanoparticles for mass-sensitive engine oil degradation sensing Anal Bioanal Chem (**2007**) 389:441–446

[28]   C. J. Brinker, G. W. Scherer, *Sol-Gel Science: The Physics and Chemistry*

of Sol-Gel Processing, Academic, Boston, MA. **1990**

29   Peter A. Lieberzeit , A. Afzal, A. Rehman, Franz L. Dickert Nanoparticles for detecting pollutants and degradation processes with mass-sensitive sensors Sensors and Actuators B 127 (**2007**) 132–136

30   D. Vollath, F. D. Fischer, M. Hagelstein Phases and phase transformation in nanocrystalline ZrO_2, *Journal of Nanoparticle Research* (**2006**) 8: 1003-1016

31   (a) Biot, C.; Wintjens, R.; Rooman, *M. J. Am. Chem. Soc.* **2004**, 126, 6220. (b) McFail-Isom, L.; Shui, X.; Williams, L. D *Biochemistry* **1998**, 37, 17105. (c) DeVos, A. M.; Ultsch, M.; Kosssiakoff, *A. A. Science* **1992**, 255, 306.

32   (a) Zakian, V.A. Science **1995**, 270, 1601. (b) Rooman, M.; Lievin, J.; Bulsine, E.; Wintjens, R. J. Mol. Biol. **2002**, 319,67.

33   H. Prestel · A. Gahr · R. Niessner Detection of heavy metals in water by fluorescence spectroscopy: On the way to a suitable sensor system. Fresenius J Anal Chem. (**2000**) 368 :182–191

34   ES Forzani, H Zhang, W Chen, N Tao, Detection of Heavy Metal Ions in Drinking Water Using a High-Resolution Differential Surface Plasmon Resonance Sensor *Environ. Sci. Technol.* **2005**, 39, 1257-1262

35   Bannon, D. I.; Chisolm, J. J. Anodic stripping voltammetry compared with graphite furnace atomic absorption spectrophotometry for blood lead analysis. *Clin. Chem.* **2001**, *47* (9), 1703-1704.

36   Liu, H. W.; Jiang, S. J.; Liu, S. H. Determination of cadmium, mercury and lead in seawater by electro thermal vaporization isotope dilution inductively coupled plasma mass spectrometry. *Spectrochim. Acta*, *Part B* **1999**, *54* (9), 1367-1375.

37   Yang, W. R.; Chow, E.; Willett, G. D.; Hibbert, D. B.; Gooding, J. J. Exploring the use of the tripeptide Gly-Gly-His as a selective recognition element for the fabrication of electrochemical copper sensors. *Analyst* **2003**, *128* (6), 712-718.

38   Baldo, M. A.; Daniele, S.; Ciani, I.; Bragato, C.; Wang, J. Remote stripping analysis of lead and copper by a mercury-coated platinum microelectrode. *Electro analysis* **2004**, *16* (5), 360-

366.

39   Eksperiandova, L. P.; Blank, A. B.; Makarovskaya, Y. N. Analysis of waste water by X-ray fluorescence spectrometry. *X-ray Spectrom.* **2002**, *31* (3), 259-263.

40   Arai, Y.; Lanzirotti, A.; Sutton, S.; Davis, J. A.; Sparks, D. L. Arsenic speciation and reactivity in poultry litter. *Environ. Sci. Technol.* **2003**, *37* (18), 4083-4090.

41   Das-Ak Chakraborty, R., Cervera, M.L., Delaguardia, M., **1996.** Mikrochim. Acta 122 (3–4), 209.

42   F. Dickert Molecular imprinting Editorial Anal Bioanal Chem (**2007**) 389:353–354

[43]   G, Wulff, A. Sarhan, Angew. Chem. Int. Ed. 11 (**1972**) 341.

[44]   R. Arshady, K. Mosbach, Makromol. Chem. 182 (**1981**) 687.

[45]   Peter A. Lieberzeit & Franz L. Dickert *Anal Bioanal Chem* **2007**, 387, 237-247

[46]   S. Stanley, C. J. Percival, *Anal. Chem.* **2003,** 75, 1573-1577

[47]   Hoffman, D. J.; Rattner, B. A.; Burton, G. A. Jr.; Cairns, J. Jr. *Handbook of Ecotoxicology*; Lewis Publishers: London, **1995.**

[48]   M. Cichna, D. Knopp, R. Niessner, *Anal. Chim. Acta* **1996**, 339, 241.

[49]   R. Niessner, *Trends Anal. Chem.* **1991**, 10, 310.

[50]   P. Canizares, M. D. Luque de Castro, *Fresenius J. Anal. Chem*. **1996**, 354, 291.

[51]   Dickert FL, Besenböck H, Tortschanoff M, *Adv. Mater.* **1998**, 10, No. 2, 149-151

[52]   Dickert FL, Tortschanoff M, *Anal. Chem.* **1999**, 71, 4559-4563

[53]   Dickert FL, Achatz P , Halikias K *Fresenius J Anal Chem* (**2001**) 371 :11–15

[54]   P. W. W. Kirk and J. N. Lester Significance and behaviour of heavy metals in wastewater treatment processes IV. Water quality standards and criteria, The Science of the Total Environment, Volume 40, Issue 1, December **1984**, Pages 1-44

[55]   Huiyong Wang and Andres D. Campiglia, Determination of Polycyclic Aromatic Hydrocarbons in Drinking Water Samples by Solid-Phase Nano extraction and High-Performance Liquid Chromatography *Anal. Chem.*, **2008**, 80 (21), pp 8202–8209

[56]   T. S. Thompson and B. D. Mille, Use of solid phase extraction disks for the GC-MS analysis of acidic and neutral herbicides in drinking water. *Chemosphere* Volume 36, Issue 14, June **1998**, Pages 2867-2878

[57]   Franz L. Dickert, Peter A. Lieberzeit, Paul Achatz QCM array for on-line-monitoring of composting procedures. *Analyst* , **2004**, 129, 432 – 4 37

[58]   Patrycja Ciosek, Wojciech Wro´ blewski Sensor arrays for liquid sensing – electronic tongue systems *Analyst*, **2007**, 132, 963–978

RESUME

Adnan Mujahid

Profile

Born: 02th January, 1982

Nationality: Pakistani

Residence: Currently residing in Austria for Ph.D studies since February 2007.

Status: Presently pursuing Doctoral studies at the University of Vienna, Austria

Degrees

Doctor of the Natural Sciences **(Continued)**

Institute of Analytical Chemistry, University of Vienna, Austria

Master of Science (MSc) in Chemistry **(2004)**

Department of Chemistry, University of Punjab, Lahore, Pakistan (1st division)

Distinction:

Chief Minister Scholarship holder in 2004

University Scholarship holder in 2003

Bachelor of Science (BSc) in Chemistry, Physics and Math **(2002)**

Government Waris Shah Degree College, Jandiala Sher Khan, Pakistan in affiliation with the University of Punjab, Lahore, Pakistan

Distinction: 1st position in college, (1st division)

Higher Secondary School Certificate (HSSC) Examination in Chemistry, Physics and Math **(1999)**

Government College of Science Wahdat Road Lahore, Pakistan in affiliation with the Board of Intermediate and Secondary Education Lahore, Pakistan

Distinction: (1st division)

Secondary School Certificate (SSC) Examination in Sciences **(1997)**

Govt. High School Kotlakhpat, Lahore in affiliation with the Board of Intermediate and secondary Education Lahore, Pakistan

Distinction: (1st division)

Research Work

Since February 2007 on PhD Dissertation with title

Synthetic Materials Designed by Molecular Imprinting for Developing Chemical Sensors for Oil Degradation, Metals Ions and PAHs

Institute of Analytical and Food Chemistry, University of Vienna Austria
December 2003-October 2004 on MSc thesis with title

> **Synthesis and characterization of some Poly vinyl alcohol metal based composite**

Institute of Chemistry, University of Punjab, Lahore, Pakistan

Professional Experience

Worked as an *Analyst* in **Highnoon Laboratories Limited** in Quality Control department from 2004 to 2007

Scholarships

- Doctoral scholarship from the Higher Education Commission of Pakistan to pursue PhD studies in Austria

Contact Information

Office

Institute of Analytical Chemistry, University of Vienna

Waehringerstrasse 38, 1090-Vienna, Austria

Phone: +43 1 4277 52341

Fax: +43 1 4277 9523

Email: adnan.mujahid@univie.ac.at

Cell: +43 650 5824395